



Book of abstracts

18TH INTERNATIONAL CONFERENCE ON LASER APPLICATIONS IN LIFE SCIENCES

<https://lals.sciencesconf.org>



11-14 October 2024
Muğla, Turkey

Dear Participants,

On behalf of the Organizing Committee, we invite you to attend the “18th International Conference on Laser Applications in Life Science” (LALS-2024).



The conference is held from October 11-14, 2024, at the Convention Centre of the Liberty Hotels Lykia/Oludeniz in Muğla, Turkey.

The aim of LALS-2024 is to provide a global platform for researchers, engineers, and physicians to present and discuss recent optical techniques and innovations aimed at applications in life science. We hope to bring together professionals and scientists from various areas of life sciences to introduce novel biophotonics methods to healthcare professionals, encourage knowledge exchange, and promote the establishment of cooperation ventures. The scientific program will include plenary and invited talks, and we will also offer a wide range of social programs such as boat cruises and visits to historical places.

We welcome companies and institutions to showcase their state-of-the-art products and equipment in the conference area.

We look forward to your participation in LALS-2024 and meeting you at the conference.

Best regards,

Conference chair,

Prof., Dr. Kirill Larin (University of Houston, USA)





**18th International conference
on Laser Applications in Life Sciences**
11-14 October 2024, Muğla (Turkey)

Conference Chair

Kirill Larin (University of Houston, USA)

International Advisory Board

Name	Affiliation	Countries
Bizheva Kostadinka	University of Waterloo	Canada
Blondel Walter	University of Lorraine / CRAN, Nancy	France
Bykov Alexander	University of Oulu	Finland
Chikishev Andrey	M.V. Lomonosov Moscow State University, Moscow	Russia
Conde Olga	Universidad de Cantabria	Spain
Darvin Maxim	Fraunhofer Institute for Photonic Microsystems IPMS, Cottbus	Germany
Dunaev Andrey	Orel State University	Russia
Kano Hideaki	University of Tsukuba	Japan
Kirillin Michail	Institute of Applied Physics RAS, Nizhny Novgorod	Russia
Koenig Karsten	Saarland University	Germany
Larin Kirill (chair)	University of Houston	USA
Larina Irina	Baylor College of Medicine, Houston	USA
Lugovtsov Andrei	M.V. Lomonosov Moscow State University, Moscow	Russia
Meglinski Igor	Aston University	UK
Novikova Tatiana	Ecole Polytechnique / LPICM, Palaiseau	France
Oliveira Luis	Polytechnic of Porto – School of Engineering (ISEP)	Portugal
Popov Alexey	VTT Technical Research Centre of Finland, Oulu	Finland
Popp Juergen	Institute of Physical Chemistry	Germany
Priezzhev Alexander	M.V. Lomonosov Moscow State University, Moscow	Russia
Rueck Angelika	Ulm University	Germany
Schneckenburger Herbert	Aalen University	Germany
Shirshin Evgeny	M.V. Lomonosov Moscow State University, Moscow	Russia
Tuchin Valery	Saratov State University, Saratov	Russia
Zalevsky Zeev	Bar-Ilan University / Faculty of Engineering	Israel
Zhu Dan	Huazhong University of Science and Technology, Wuhan	China



*The official sponsor of the
"18th International Conference on Laser Applications in Life Science" (LALS-
2024)*



<https://artphotonics.com>

[art photonics GmbH](https://artphotonics.com), founded in Berlin in September 1998, is one of the worldwide leaders in development and production of specialty fiber products for a broad spectrum from 300 nm to 16 μm . Unique technologies of Polycrystalline Mid InfraRed (PIR-) fibers and Metal coated Silica fibers are used for assembly of various spectroscopy probes for medical diagnostics and industrial process control, in volume production of fiber for medical and industrial lasers, for different fiber bundles, etc.

Contact art photonics GmbH directly

<https://artphotonics.com/contact/>

Rudower Chaussee 46

12489 Berlin, Germany

+49 (0) 30-6779 887-0




+49 (0) 30-6779 887-99

+49 (0) 30-6779 887-40

sales@artphotonics.com



Contents

 Abstracts	1
 Table of contents by talk name and first author	92
 Author Index	100

Ultrafast optoacoustic imaging in biology and the clinics

Daniel RAZANSKY^{1,2}

¹ *Institute for Biomedical Engineering and Institute of Pharmacology and Toxicology, Faculty of Medicine, University of Zurich, Switzerland*

² *Institute for Biomedical Engineering, Department of Information Technology and Electrical Engineering, ETH Zurich, Switzerland*

daniel.razansky@uzh.ch

ABSTRACT

Optoacoustic imaging is increasingly attracting the attention of the biomedical research community due to its excellent spatial and temporal resolution, centimeter scale penetration into living tissues, versatile endogenous and exogenous optical absorption contrast. State-of-the-art implementations of multi-spectral optoacoustic tomography (MSOT) are based on multi-wavelength excitation of tissues to visualize specific molecules within opaque tissues [1]. As a result, the technology can noninvasively deliver structural, functional, metabolic, and molecular information from living tissues [2]. The talk covers most recent advances pertaining ultrafast imaging instrumentation, intelligent reconstruction algorithms, smart optoacoustic contrast approaches, as well as multi-modal combinations with ultrasound, optical microscopy, magnetic resonance imaging and more [3-5]. Our current efforts are also geared toward exploring potential of the technique in studying multi-scale dynamics of the brain and heart, monitoring of therapies, fast tracking of cells and microrobots as well as targeted molecular imaging applications [6-10]. MSOT further allows for a handheld operation thus offers new level of precision for clinical diagnostics of patients in a number of indications, such as breast and skin lesions, inflammatory diseases and cardiovascular diagnostics [11-13].

REFERENCES

- [1] V. Ntziachristos, D. Razansky, *Chem. Rev.* 110, 2783-2794, 2010.
- [2] X. L. Deán-Ben et al, *Chem. Soc. Rev.* 46, 2158-2198, 2017.
- [3] S. K. Kalva et al, *Nature Prot.* 18, 2124–2142, 2023.
- [4] N. Davoudi, X. L. Deán-Ben, D. Razansky, *Nature Mach. Intell.* 1, 453–460, 2019.
- [5] Z. Chen et al, *Chem. Soc. Rev.* <https://doi.org/10.1039/D3CS00565H>, 2024.
- [6] S. Gottschalk et al, *Nature Biomed. Eng.* 3, 392-401, 2019.
- [7] C. Özsoy et al, *Proc. Nat. Acad. Sci. USA* 118, e2103979118, 2021.
- [8] X. L. Deán-Ben et al, *Nature Comm.* 14, 3584, 2023.
- [9] P. Wrede et al, *Science Adv.* 8, eabm9132, 2022.
- [10] R. Ni et al, *Nature Biomed. Eng.* 6, 1031-1044, 2022.
- [11] F. Knieling et al, *N. Engl. J. Med.* 376, 1292-1294, 2017.
- [12] I. Ivankovic et al, *Radiology* 291, 45–50, 2019.
- [13] A. Karlas et al, *Nature Biomed. Eng* 7, 1667–1682, 2023.

Multimodal optical endoscopy

Wolfgang Drexler

(on behalf of the MIB, ESOTRAC, PROSCOPE and PHAST consortium)

Most recent advances of multimodal optical endoscopy will be presented including *in vivo* OCT cystoscopy in the human bladder, OCT/Raman cystoscopy, OCT/Raman colonoscopy, OCT/multiphoton endoscopy as well as an OCT/photoacoustic imaging based tethered capsule for esophageal screening. These endoscopes have been developed in 4 different European projects.

Fluorescence Lifetime Imaging in Clinical Interventions

Laura Marcu

¹*Department, Neurological Surgery and Biomedical Engineering, University of California Davis, USA*

lmarcu@ucdavis.edu

ABSTRACT

This presentation overviews fluorescence lifetime spectroscopy and imaging techniques for label-free in vivo characterization of biological tissues. Numerous studies have shown that tissue autofluorescence properties have the potential to assess biochemical features associated with distinct pathologies in tissue and to distinguish various cancers from normal tissues. However, despite these promising reports, autofluorescence techniques have been sparsely adopted in clinical settings. This presentation overviews clinically-compatible multispectral fluorescence lifetime imaging (FLIM) techniques developed in our laboratory and their ability to operate as stand-alone tools, integrated with a biopsy needle and intravascular catheters and in conjunction with surgical robots. We present clinical studies in patients undergoing surgery that demonstrate the potential of label-free FLIM for intraoperative delineation of brain as well as head and neck cancer including image-guided augmented reality during trans-oral robotic surgery (TORS). Our findings suggest that label-free FLIM-based tissue assessment, characterized by simple, fast and flexible data acquisition and display, could find applications in a variety of interventional procedures.

Axial Tomography in Live Cell Microscopy

Herbert SCHNECKENBURGER¹ and Christoph CREMER^{2,3,4}

¹Institute of Applied Research, Aalen University, Germany

²Kirchhoff-institute for Physics, University Heidelberg, Germany

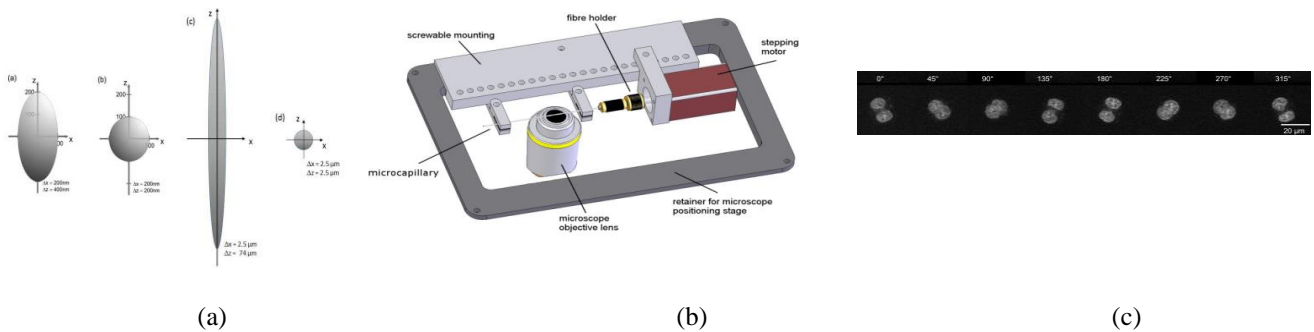
³Max-Planck-Institute for Polymer Research, Mainz, Germany

⁴Institute of Molecular Biology (IMB), Mainz, Germany

herbert.schneckenburger@hs-aalen.de

ABSTRACT

For many biomedical applications, laser-assisted methods are essential to enhance the three-dimensional resolution of an optical microscope. Axial Tomography allows for rotation of an object into the best perspective required for optical imaging, thus permitting a 3D resolution, which corresponds to the best resolution of the system (usually that of the object plane) [1,2]. Furthermore, images recorded under variable angles can be combined to one image with isotropic resolution [3,4]. As demonstrated in Fig. (a), this concept is not only applicable to objective lenses with high numerical aperture, but should be even more effective for low aperture lenses with working distances up to the mm–cm range. For an improvement of 3D image contrast, Axial Tomography can be combined with light sheet or laser scanning microscopy; for an enhancement of resolution down to 100 nm or less, Structured Illumination (SIM) or even 3D Single Molecule Localization Microscopy (SMLM) methods may be used. The potential of Axial Tomography includes Deep View Microscopy, e.g. of 3D cell cultures or organoids, as well as Molecular Imaging, e.g. for the analysis of functional genome structures in multicellular aggregates (for an overview see [5]).



Figures: (a) Point spread functions for conventional microscopy and axial tomography at high (left) and low (right) numerical aperture, (b) axial tomograph, (c) doxorubicin within 2 cell nuclei observed under various angles.

REFERENCES

- [1] Staier, F.; Eipel, H.; Matula, P.; Evsikov, A.V.; Kozubek, M.; Cremer, C.; Hausmann, M. Micro axial tomography: a miniaturized, versatile stage device to overcome resolution anisotropy in fluorescence light microscopy. *Rev Sci Instrum* 2011, 82, 093701.
- [2] Richter, V.; Bruns, S.; Bruns, T.; Weber, P.; Wagner, M.; Cremer, C.; Schneckenburger H. Axial tomography in live cell laser microscopy. *J Biomed Opt* 2017, 22, 91505.
- [3] Heintzmann, R.; Cremer, C. Axial tomographic confocal fluorescence microscopy. *J Microsc* 2002, 206, 7–23.
- [4] Herzog, E.; Richter, V.; Schneckenburger, H. Axial Tomography of Living Cells – an Update, *Int. Conf. Focus on Microscopy*, Porto, April 02-05, 2023.
- [5] Schneckenburger, H.; Cremer C. Axial tomography in live cell microscopy, *Biophysica* 2024, 4, 142–157.

Combined Photodynamic/Photothermal Therapy of Model Cholangiocarcinoma Using Indocyanine Green and Gold Nanorods

Elina GENINA^{1,2,3}, Alla BUCHARSKAYA^{2,3,4}, Vadim GENIN^{1,2,3}, Nikita NAVOLOKIN⁴, Dmitry MUDRAK⁴, Boris KHLEBTSOV⁵, Galina MASLYAKOVA⁴, Nikolai KHLEBTSOV⁵, Valery TUCHIN^{1,2,3,6}

¹*Optics and Biophotonics Department, Saratov State University, Russia*

²*Laboratory of laser molecular imaging and machine learning, National Research Tomsk State University, Russia*

³*Science Medical Center, Saratov State University, Russia*

⁴*Department of Pathological Anatomy, Saratov State Medical University named after V.I. Razumovsky, Russia*

⁵*Institute of Biochemistry and Physiology of Plants and Microorganisms, FRC "Saratov Scientific Centre of the Russian Academy of Sciences" (IBPPM RAS), Russia*

⁶*Institute of Precision Mechanics and Control, FRC "Saratov Scientific Centre of the Russian Academy of Sciences", Russia*

eagenina@yandex.ru

ABSTRACT

The relevance of existing combined therapy technologies in oncology is due to the insufficient effectiveness of standard treatment methods for tumors of hard-to-reach localizations. In recent years, technologies for combined laser plasmon photothermal therapy (PPT) have been actively developing, including in combination with methods of photodynamic therapy (PDT), based on the interaction of laser radiation with a photosensitizer. Important advantages of this combination of methods are the coupling of both methods using optical radiation, acceleration of photochemical reactions with increasing temperature, use of lower power densities for laser irradiation, synergistic effects on tumor blood vessels, separation of the maximum therapeutic effects of both procedures in time, increased thermal sensitivity of cells in conditions of hypoxia caused by a photochemical reaction, etc. [1,2].

The study aimed to develop a combined technology of PPT and PDT in rats with transplanted cholangiocarcinoma PC-1. For PDT, indocyanine green was diluted in polyethylene glycol (PEG) at a ratio of 1:100 and intratumorally injected at a dose of 2 mg/kg. The maximum absorption wavelength of the ICG solution was 790 nm. For PPT, a suspension of PEG-coated gold nanorods (GNR) at a concentration of 400 µg/ml was injected intratumorally into 30% of the tumor volume. The aspect ratio of the GNR was about 4:1, so the plasmon resonance was observed in the spectral range of 800–820 nm. One hour after injections, the tumor was irradiated percutaneously with an 808 nm diode infrared laser at a power density of 2.3 W/cm² for 15 min. Animals were removed from the experiment 72 hours and 21 days after therapy. Morphological studies of the tumor were performed on sections stained with standard and immunohistochemical methods.

Inhibition of tumor growth 72 hours after therapy was not significantly different in all experimental groups. After 21 days, the greatest inhibition of tumor growth was noted after combined PPT/PDT therapy; the tumor growth inhibition index by weight was 77.4%.

The similarity of the absorption spectra of the photosensitizer and thermosensitizer makes it possible to use one infrared laser (808 nm) for combined PPT/PDT therapy, which can be considered an advantage of the proposed approach.

The developed combined technology of PPT/PDT therapy causes significant damage of grafted cholangiocarcinoma in rats due to sharp local heating during PPT and the cytotoxic effect of PDT on tumor cells. The antitumor effect of the proposed combined technology is superior to the results obtained when using only PPT or PDT. This synergistic effect can be associated with enhanced diffusion of the dye into cells at elevated temperature and more efficient generation of singlet oxygen and radicals by ICG in the strong local field of GNR. However, further research is needed both on the biophysical mechanisms of the complex interaction of photo- and thermosensitizers, and on the safety and long-term effects of the proposed therapy.

The work was supported by RSF grant 23-14-00287.

REFERENCES

[1] M.R. Younis, C. Wang, R. An, ACS Nano, 13, 2544, 2019.

[2] C. Kong, X. Chen, Int. J. Nanomedicine, 17, 6427, 2022.

Application of NIR microsecond laser pulses for tissue coagulation and resection. Current results and perspectives

Irina Dolganova¹, Arsen Zotov², Polina Aleksandrova², Anna Alekseeva³, Egor Yakovlev⁴,
Kirill Zaytsev², David Kichiev² and Vladimir Kurlov¹

¹*Osipyan Institute of Solid State Physics RAS, Russia*

²*Prokhorov General Physics Institute RAS, Russia*

³*Avtsyn Research Institute of Human Morphology, Russia*

⁴*Bauman Moscow State Technical University, Russia*

dolganova@issp.ac.ru

IN THIS TALK, THE MEDICAL APPLICATION OF LASER SYSTEM, WHICH ENABLES GENERATION OF MICROSECOND PULSES OF 1.08 MICRONS WAVELENGTH AND AVERAGED OUTPUT POWER NEAR 10 W, FOR TISSUE ABLATION AND DISSECTION IS DISCUSSED. THE POSSIBLE PROPAGATION OF ACOUSTIC WAVES IN TISSUES AFTER EXPOSURE WAS STUDIED EXPERIMENTALLY AND NUMERICALLY. THE COMBINATION OF THIS SYSTEM WITH COMPACT SAPPHIRE INSTRUMENTS FOR SUCH PULSES DELIVERING TO TISSUES WAS CONSIDERED. THE CURRENT RESULTS AND PERSPECTIVES ARE COVERED IN THIS TALK.

Recently, in clinical practice, the development of minimally invasive methods for therapy and resection of tissues have received significant attention. They are associated with both lower risks during manipulation and shorter recovery time for patients. Laser therapy and tissue resection are among such methods; they are based on tissue exposure to optical radiation, leading to their coagulation or ablation. Laser treatment methods are widely used in ophthalmology, urology, gynecology and other fields.

In this work, we have studied the application of microsecond pulsed laser system for medical purposes. It is characterized by the ability to deliver pulse train of 250 μ s duration, the wavelength 1.08 μ m, and average power near 10 W. The exposure of tissues to this radiation was studied numerically and experimentally; and the corresponding acoustic wave propagation in the medium was assumed and noticed. Next, the effects of using this laser system for tissue coagulation and resection were studied experimentally. The remarkable results were achieved, including an ability to perform marginal liver resection without blood loss.

Finally, the combination of this laser system with sapphire capillary needles for laser therapy was considered. Due to relatively high output power and acoustic exposure, the damage of quartz fiber for light delivering is a significant problem, especially in clinical applications. To address this issue, sapphire needles can be applied for the protection of tissues from the products of possible fiber damaging [1,2]. Due to biocompatibility, ability to withstand multiple sterilizations and high transparency in visible and near infrared ranges [3,4], sapphire needles, produced by means of edge-defined film-fed growth technique of crystal growth from melt [5], can be used for cutaneous or interstitial laser applications. The radiation patterns, formed by the combination of the sapphire needles with laser system were studied along with the effects of tissue exposure by them.

The recent results obtained in this work demonstrated the perspectives of the proposed laser system and its regimes for medical applications.

REFERENCES

- [1] I. Dolganova et al., J. Biophotonics 13, e202000164, 2020.
- [2] I. Dolganova et al., J. Biomed. Opt. 24 (12), 128001, 2019.
- [3] V.N. Kurlov, Sapphire: Properties, Growth, and Applications, in *Encyclopedia of Materials: Science and Technology*, Elsevier, Oxford, 8259–8264, 2001.
- [4] G. Katyba et al., Prog. Cryst. Growth Charact. Mater., 64, 133-151, 2018.
- [5] V.N. Kurlov et al, Shaped Crystal Growth, in *Crystal Growth Processes Based on Capillarity*, John Wiley & Sons, Ltd, 277–354, 2010.

Terahertz-wave – turbid tissue interactions

Kirill I. Zaytsev¹, Anna S. Kucheryavenko², Nikita V. Chernomyrdin¹, Irina N. Dolganova², Valery V. Tuchin^{3,4,5}

¹*Prokhorov General Physics Institute of the Russian Academy of Sciences, Russia*

²*Osipyan Institute of Solid State Physics of the Russian Academy of Sciences, Russia*

³*Institute of Physics and Science Medical Center, Saratov State University, Russia*

⁴*Institute of Precision Mechanics and Control, FRC “Saratov Scientific Centre of the Russian Academy of Sciences”, Russia*

⁵*Laboratory of Laser Molecular Imaging and Machine Learning, Tomsk State University, Russia*

kirzay@gmail.com

TERAHERTZ (THZ) TECHNOLOGY OFFERS A VARIETY OF APPLICATIONS IN MEDICAL SPECTROSCOPY AND IMAGING, WHERE TISSUES ARE COMMONLY ASSUMED TO BE OPTICALLY HOMOGENEOUS (AT THE THZ-WAVELENGTH SCALE) AND, THUS, DESCRIBED WITHIN THE EFFECTIVE MEDIUM THEORY (EMT). RECENT STUDIES OF TISSUES BY SUPERRESOLUTION THZ MICROSCOPY HAVE UNCOVERED THEIR INHOMOGENEITIES WITH DIMENSIONS COMPARABLE TO THE THZ WAVELENGTH. THEY CAN LEAD TO THZ-WAVE SCATTERING. IN OUR RESEARCH, WE COMBINE THE THZ PULSED SPECTROSCOPY (TPS), SUPERRESOLUTION THZ SOLID IMMERSION MICROSCOPY (THZ-SIM) WITH THE METHODS OF THE LORENTZ-MIE SCATTERING THEORY AND THE RADIATIVE TRANSFER THEORY (RTT) TO SHINE THE LIGHT ON THE THZ-WAVE – TURBID TISSUE INTERACTIONS.

THz spectroscopy and imaging [1–3] offer a variety of applications in medical diagnosis and therapy [4–7]. In such applications, tissues are commonly assumed to be optically homogeneous at the THz-wavelength scale, while the THz-wave–tissue interactions are described within EMT. Meanwhile, recent studies of tissues from human, animal, and plants involving emerging modalities of superresolution (beyond the Abbe limit) THz microscopy, have found tissue inhomogeneities with dimensions comparable to the THz wavelength ($\sim\lambda$). Such inhomogeneities can lead to THz-wave scattering effects [4,8–11], which poses a problem of studying an interplay between the absorption and scattering of the THz waves in soft turbid tissues. To address this problem, in our research, we combine the in-house polarization-sensitive TPS and different THz-SIM modalities [2,8–13], method of the Lorentz-Mie scattering theory, and RTT in order to shine the light on the THz-wave – turbid tissue interactions.

First, in Ref. [14], a tissue-mimicking phantom is developed that has the form of a gelatin slab (as a highly absorbing hydrated matrix), into which subwavelength or mesoscale amorphous silicon dioxide (SiO_2) microparticles are embedded (as scatterers with lower refractive index and loss). The Lorenz-Mie scattering theory have predicted a non-isotropic (non-scalar) differential extinction cross section for such scatterers, which results in the non-Rayleigh scattering regime and casts doubt on the EMT applicability for such tissues. Surprisingly, we have found theoretically (using RTT) and confirmed experimentally (using TPS) that the effective optical properties of the proposed phantom are still determined by EMT over wide ranges of the diameters ($d \leq 0.47\lambda$) and volume fractions ($f \leq 0.2$) of scatterers. This broadens the EMT applicability in THz biophotonics and medical imaging.

Next, in Ref. [15], quantitative polarization-sensitive THz-SIM is developed, which makes possible the study of local polarization-dependent THz response of mesoscale tissue elements with the resolution as high as 0.15λ . It is applied to retrieve the refractive index distributions over the freshly-excised rat brain for the two orthogonal linear polarizations, aimed at uncovering the THz birefringence of tissues. The most pronounced birefringence is observed for the Corpus callosum, formed by well-oriented and densely-packed axons bridging the cerebral hemispheres. The observed results are verified by TPS of the porcine brain. This is the first observation of the tissue birefringence in the THz range.

REFERENCES

- [1] H. Guerboukha et al., *Advances in Optics & Photonics* 10, 843–938, 2018.
- [2] N.V. Chernomyrdin et al., *Applied Physics Letters* 120, 110501, 2022.
- [3] D.S. Ponomarev et al., *Physics-Uspekhi* 67, 3–21, 2024
- [4] K.I. Zaytsev et al., *Journal of Optics* 22, 013001, 2020.
- [5] O.P. Cherkasova et al., *Journal of Biomedical Optics* 26, 090902, 2021.
- [6] H. Lindley-Hatcher et al., *Applied Physics Letters* 118, 230501, 2021.
- [7] N.V. Chernomyrdin et al., *Opto-Electronics Advances* 6, 220071, 2023.
- [8] N.V. Chernomyrdin et al., *Applied Physics Letters* 113, 111102, 2018.
- [9] N.V. Chernomyrdin et al., *Optics & Spectroscopy* 126, 560–567, 2019.
- [10] N.V. Chernomyrdin et al., *Optica* 8, 1471–1480, 2021.
- [11] A.S. Kucheryavenko et al., *Biomedical Optics Express* 12, 5272–5289, 2021.
- [12] A.S. Kucheryavenko et al., *Optics Express* 31, 13366–13373, 2023.
- [13] V.A. Zhelnov et al., *Advanced Optical Materials* 12, 2300927, 2024.
- [14] A.S. Kucheryavenko et al., *Physical Review Applied* 20, 054050, 2023
- [15] N.V. Chernomyrdin et al., *Scientific Reports* 13, 16596, 2023.

Characterization of UV transparency windows in tissues as a function of glycerol osmolarity

Luís OLIVEIRA^{1,2}, Maria PINHEIRO², Maria CARVALHO^{2,3} and Valery TUCHIN^{4,5,6}

¹Physics Department, Polytechnic of Porto – School of Engineering, Portugal

²Centre of Telecommunications and Multimedia, Institute for Systems and Computer Engineering, Technology and Science, Porto, Portugal

³Department of Electrical and Computer Engineering, Faculty of Engineering of Porto University, Porto, Portugal

⁴Institute of Physics and Science Medical Center, Saratov State University, Saratov, Russian Federation

⁵Laboratory of Laser Diagnostics of Technical and Living Systems, Institute of Precision Mechanics and Control of the FRC “Saratov Scientific Centre of the Russian Academy of Sciences”, Saratov, Russian Federation

⁶Laboratory of Laser Molecular Imaging and Machine Learning, Tomsk State University, Tomsk, Russian Federation

lmo@isep.ipp.pt

ABSTRACT

The tissue optical clearing method allows to increase tissue transparency through three main mechanisms – the tissue dehydration, the refractive index matching and the protein dissociation mechanisms [1]. These mechanisms are all reversible and various kinetic studies have previously been made to characterize both the dehydration and the refractive index matching mechanisms [2]. The protein dissociation mechanism is not easy to study or to characterize due to various factors, such as the protein content in the tissue under study, or the osmotic strength of the agent used to increase tissue transparency. An additional drawback for the study of this clearing mechanism is that proteins present their strongest absorption bands in the deep-ultraviolet, for wavelengths lower than 240 nm [3].

Recent studies have demonstrated that the application of clearing treatments to certain tissues lead to the creation of transparency windows in the ultraviolet range [4,5]. Depending on the tissue chromophores, the central wavelengths of those transparency windows may vary, but in some cases they occur at 230 nm and 300 nm [4,5].

With the objective of evaluating the effect of the protein dissociation mechanism in the magnitude of the induced transparency windows, kinetic collimated transmittance measurements were performed from rabbit pancreas and from pig heart muscle samples during immersion in glycerol solutions with different osmolarities.

After processing the measured kinetic spectra for the various treatments, it was observed that two transparency windows occur at 230 and 300 nm, both for the pancreas and for the heart muscle tissues. In the case of the pancreas, as the osmolarity of the glycerol solution increases, the magnitude of both transparency windows seems to increase in similar proportions. In opposition, for the heart muscle, the transparency window located at 230 nm presents higher magnitude increase than the transparency window located at 300 nm, especially for solutions containing more than 40% glycerol.

Considering treatments with 99% glycerol, some calculations were performed to obtain the protein dissociation rates in the two tissues under study. These results allowed to identify a higher protein content in the heart muscle.

REFERENCES

- [1] V. Tuchin, D. Zhu, E. Genina, Handbook of Tissue Optical Clearing (CRC Press), (2022).
- [2] Carneiro et al, J. Biophotonics 12, e201800333, 2018.
- [3] M. Saraiva, J. Photochemistry & Photobiology B: Biology 212, 112022, 2020.
- [4] Carneiro et al, J. Biophotonics 12, e201900181, 2019.
- [5] Carneiro et al, IEEE J. Selected Topics in Quantum Electronics 27, 7200108, 2021.

Phase transition monitoring in adipose tissue by multimodal approach

Irina YANINA^{1,2}, Viktor NIKOLAEV², Denis VRAZHNOV², Vyacheslav KOCHUBEY¹, Yuri KISTENEV² and Valery TUCHIN^{1,2,4}

¹*Institute of Physics, Saratov State University, Russia*

²*Laboratory of laser molecular imaging and machine learning, Tomsk State University, Russia*

³*Institute of Precision Mechanics and Control of RAS, Russia*

irina-yanina@list.ru

ABSTRACT

The present work demonstrates the temperature-mediated phase transitions of the components of adipose tissue. Pieces of abdominal fat were used as samples of adipose tissue. These samples were heated using a temperature-controlled table and observed using spectrophotometer SHIMADZU, the MPTflex two-photon microscope (JenLab GmbH) with fluorescence lifetime imaging microscopy (FLIM) mode and machine learning methods. The analysis of FLIM data was done with a software package “Becker&Hickl”. The developed approach has a great potential for obtaining accurate information on the phase-transition processes occurring during metabolism alterations.

Studies in recent decades have allowed us to look from a new angle at the causes and mechanisms of development of many diseases, especially of socially significant, such as atherosclerosis and coronary heart disease, hypertension, type 2 diabetes, liver disease, orthopedic diseases, some cancers (lipoma, liposarcoma, and etc.). Convincing evidence of the relationship of these diseases with excessive accumulation of body fat, i.e. with obesity was obtained [1-3]. In this regard, interest in studying the function of adipose tissue and its role in health and disease has increased [5]. Currently, it is generally accepted that the adipose tissue plays an important role in the metabolic regulation of both energy balance in the body and vascular homeostasis. However, it is not a passive conduit serving to save energy consumption and is responsible for changes in energy balance. Despite the seemingly unwanted fat, fat performs a lot of very important physiological functions [6]. Knowledge of these functions must be not only for understanding of the pathogenesis of obesity and related diseases, but also for its effective prevention and treatment.

Observation of temperature-mediated phase transitions between components of the adipose tissue has been proved. The spectra of total transmission and diffuse reflection coefficients of the samples were measured in the wavelength range of 350–2500 nm using a spectrophotometer UV-3600 with an integrating sphere LISR-3100 (Shimadzu, Japan). Various machine learning methods have been used. Images of abdominal adipose tissue at different temperatures were obtained with two-photon tomography with FLIM mode using MPTflex equipment (JenLab GmbH). The analysis of FLIM data was done with software package “Becker&Hickl”. Since the wavelength of fluorescence excitation did not change, similar (NADH) fluorophore groups were excited. But in the experiment we observed different lifetimes. This may be due to a change in the conformation or environment of the molecule. The method allows one to explore in space not only the molecules themselves but also the distribution of their states and environments. It has been found that structural changes in the fat cell observed as the temperature increases above 28 °C are statistically significant. The result obtained can be associated with both a decrease of the thickness of the sample under heating and a real change in the fluorescent abilities of adipose tissue.

Further work in this direction may be associated with a detailed study of the above dependences on a large sample of data and the construction of numerical distribution model for the dependences of the lifetime of the autofluorescence on temperature.

The developed approach has a great potential as an alternative method for obtaining accurate information on the processes occurring during metabolism change.

The study was supported by a grant Russian Science Foundation No. 24-44-00082, <https://rscf.ru/project/24-44-00082/>.

REFERENCES

- [1] H. Bahrami, D.A. Bluemke, R. Kronmal, et al., *J Am Coll Cardiol*. 51(18), 1775-1783 (2008)
- [2] J.B. Schwimmer, R. Deutsch, J. B. Rauch, C. Behling, R. Newbury, J.E. Lavine, *The Journal of Pediatrics* 143(4), 500–505 (2003)
- [3] N. J. Manek, D. Hart, T. D. Spector and A. J. MacGregor, *Arthritis & Rheumatism* 48(4), 1024–1029 (2003)
- [4] T. D. Brisbois, A. P. Farmer and L. J. McCargar, *Obesity reviews* 13(4), 347–367 (2012)
- [5] M.C. Michalski, C. Genot, C. Gayet, C. Lopez, F. Fine, F. Joffre, J.L. Vendevre, J. Bouvier, J.M. Chardigny, and K. Raynal-Ljutovac, *Prog. Lipid Res.* 52 (4), 354-73 (2013)

Computational augmentation of optical coherence tomography contrasts for label-free tissue dynamics and property imaging

Yoshiaki YASUNO¹

¹Computational Optics Group, University of Tsukuba, Japan

yoshiaki.yasuno@cog-labs.org

ABSTRACT

Computational contrast extensions of optical coherence tomography (OCT) and OCT microscopy (OCM) are presented. The intracellular motility and cellular metabolism are visualized through the combination of sequential OCT acquisition and subsequent time-statistical analysis. We also introduce a deep learning method to accelerate the acquisition speed of this label-free metabolism imaging. Finally, we will demonstrate tissue scatterer density estimation using a deep learning approach.

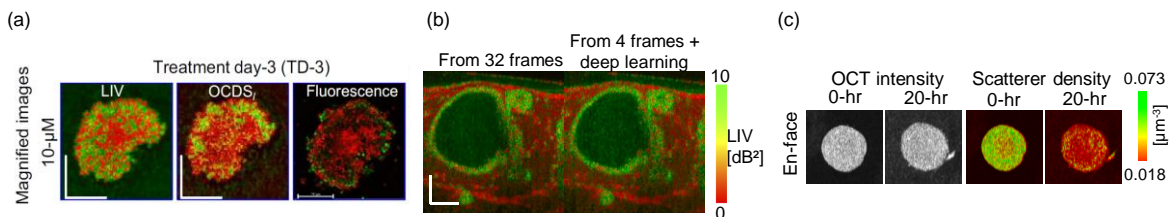
The recent development of drug development and basic clinical science heavily relies on *in vitro*, *ex vivo*, and small animal imaging. For these imaging modalities, a system with high imaging depth, high resolution, and label-free tissue activity visualization capability is required. Although OCT and OCM can potentially be used for such imaging, they only visualize tissue morphology.

Here in this talk, we introduce a group of contrast extensions of OCT and OCM, and it includes dynamic OCT (DOCT), its extension using deep-learning-based image generator, and deep-learning based scatterer density imaging.

One of the extended contrasts is dynamic OCT/OCM. This method is achieved by combining repetitive frame acquisition (typically a few tens to a few hundred frames) and subsequent time-sequential statistical signal processing. In our specific example, we utilized sequential acquisition of 32 frames and successfully visualized the metabolic activity of *in vitro* and *ex vivo* samples, such as tumor spheroids and organoids, as shown in Figure (a) [1]. We employed two types of DOCT algorithms: ‘logarithmic intensity variance’ (LIV) and ‘late OCT correlation decay speed’ (OCDS_L) [2]. LIV can be considered sensitive to the magnitude of the tissue dynamics, while OCDS_L is sensitive to the dynamics speed.

Although DOCT successfully visualizes cellular activity without labels, it requires a relatively long acquisition time. In our DOCT acquisition protocol, one volumetric scan takes around 1 min. Here, we employed a deep-learning method to generate DOCT images from only four sequential frames. It enables 8-fold improvement in acquisition speed. Figure (b) demonstrates that this deep-learning based method generate LIV image of *in vitro* alveolar (lung) organoids from only 4 frames/position, and it well resembles the original LIV image made from 32 frames/position [3]. See Ref. [4] for the details of the organoid study.

The scatterer density is associated with tissue density, and hence it might sensitive to tissue abnormality. We utilized a deep-learning method to estimate the density of scatterers in the tissue. For training the deep-learning network, we generated a massive amount of OCT speckle patterns numerically using a wave-optics simulator. Subsequently, we trained the network to estimate the scatterer density from local speckle patterns (i.e., small patches of OCT) [5]. An application example of this method applied to tumor spheroids is illustrated in Fig. (c).



Figures: (a) Dynamic OCT (DOCT) and fluorescence images of a breast cancer (MCF-7 cell line) spheroid. (b) LIV images of an alveolar organoid obtained from 32 frames (left) and 4 frames with the deep-learning methods (right). (c) OCT images of MCF-7 tumor spheroid (left) and scatterer density images (right). The measurements were performed at 0- and 20-hr time points after extracting the cultivation chamber.

REFERENCES

- [1] I. Abd El-Sadek et al., Sci. Rep. 14, 3366 (2024).
- [2] I. A. El-Sadek, et al., Biomed. Opt. Express 11, 6231–6248 (2020).
- [3] Y. Liu, et al., Biomed. Opt. Express 15, 3216–3239 (2024).
- [4] R. Morishita, et al., Biomed. Opt. Express 14, 2333–2351 (2023).
- [5] T. Seesan, et al., Biomed. Opt. Express 15, 2832–2848 (2024).

Raman spectroscopy and machine learning in the prognosis of patients with coronary heart disease complicated by chronic heart failure

Luydmila Bratchenko¹, Yulia Khristoforova¹, Maria Skuratova², Peter Lebedev³ and Ivan Bratchenko¹

1 Samara National Research University, Samara, Russia

2 Samara regional hospital named after V.I. Pirogov, Samara, Russia

3 Samara State Medical University, Samara, Russia

iabratchenko@gmail.com

ABSTRACT

Promising diagnostic methods, such as "optical biopsy" [1] and "liquid biopsy" [2], are in high demand for specific diseases biomarkers detection in biological tissues and fluids. Optical methods have the potential to overcome the limitations of traditional methods of clinical analysis. One of the most promising methods of optical analysis (and optical biopsy) is a Raman spectroscopy, which can contribute to understanding of molecular basis of diseases and creation of new bioanalytical tools for the diagnosis of diseases. Since each type of biological tissue and biofluid has an individual molecular composition and, thus, a unique spectral profile resulting from the transition of a molecule from one vibrational-rotational state to another, a set of such individual states of functional groups of nucleic acids, proteins, lipids and carbohydrates makes it possible to characterize component composition of tissues, which ultimately makes it possible to isolate disease markers [3]. Along with the use of optical biopsy methods, it is possible to apply a supersensitive technique for analyzing biofluids based on surface-enhanced Raman spectroscopy, which will be most effective for detecting low concentrations of disease markers in biological fluids. In the last decade, the development of nanotechnology has led to the creation of promising tools for solving new problems in the study of various human diseases, which is especially important for effective and targeted treatment and a deeper fundamental understanding of the biochemistry of diseases [2].

In this study we demonstrate application of conventional Raman spectroscopy for the analysis of skin tissues and application of SERS for serum analysis to determine the prognosis of patients with coronary heart disease (CHD) complicated by chronic heart failure (HF). We included 184 patients (mean age 70.78 ± 8.91 years) of both sexes with CHD complicated by severe (stage C: 42%) and severe (stage D: 58%) HF, examined clinically and instrumentally at baseline, in a prospective study. During the follow-up period (mean 1 year), 31 patients died. In overall we created a number of prognosis models based on standard clinical markers and optical and liquid biopsy.

Predictors of overall mortality in multivariate analysis using routine parameters were NTproBNP and glomerular filtration rate (model 1). Parameters of SERS were also used to create discrimination models for this outcome by the latent structure projection method. Sensitivity (model 2): 68%; specificity 84%; accuracy 81.4% have no significant differences from model 1. The most informative frequencies for discrimination were found to be: 628, 655, 820, 1357, 1660 cm^{-1} . The combined use of parameters of both models improves the quality of prediction. For the first time we have shown that SERS reflecting metabolic "portrait" of HF provides an opportunity for prediction of total mortality.

3 out of 5 Raman spectroscopy parameters significant for predicting mortality in patients with CHD coincide with the parameters characterizing Raman spectroscopy in patients with CHD, which allows us to confirm the significant prognostic impact of reduced glomerular filtration rate on survival in HF. However, the spectral differences cannot be explained entirely by the influence of creatinine and urea, the classic markers of CKD (chronic kidney disease).

By means of multivariate analysis, the informative spectral bands associated with the CHD during disease progression were identified. In addition, the analysis of the correlation between the serum spectral characteristics and urea, creatinine has made it possible to determine the spectral bands correlated with levels of creatinine and urea into the complex spectral characteristics of serum. In general, the reported approach may form the basis for monitoring the health status of CHD patients and find application in studying other pathological conditions of the human body [4]. Raman-based optical and liquid biopsy may be promising in non-communicable diseases identification, as it provides fast and rapid diagnosis.

REFERENCES

- [1] Yu.A. Khristoforova, et al. Raman spectroscopy in chronic heart failure diagnosis based on human skin analysis, *Journal of Biophotonics*, 16 (7), e202300016, 2023.
- [2] S.Z. Al-Sammaraie, et al. Human blood plasma SERS analysis using silver nanoparticles for cardiovascular diseases detection, 10 (1), 010301, 2024.
- [3] Yu.A. Khristoforova, et al. Raman-Based Techniques in Medical Applications for Diagnostic Tasks: A Review, *International journal of molecular sciences*, 24 (21), 15605, 2023.
- [4] L.A. Bratchenko, et al. Analyzing the serum of hemodialysis patients with end-stage chronic kidney disease by means of the combination of SERS and machine learning, *Biomedical Optics Express*, 13, 4926-4938, 2022.

Non-contact biomechanical imaging of cell and tissue using optical Brillouin microscopy

Jitao ZHANG

Department of Biomedical Engineering, Wayne State University, USA

zhang4@wayne.edu

ABSTRACT

Biomechanical interactions play crucial roles in regulating many cellular functions and system-level behaviors. To understand the mechanical interplay within cells and tissue, we need tools to identify mechanically related pathways, measure deformations and forces, and quantify the mechanical properties (e.g., elasticity) of materials. Many important techniques have been developed to assess material mechanical properties and can be loosely classified into three categories [1]. The first is contact-based techniques, including atomic force microscopy (AFM) and other cantilever-based indentation methods, micropipette aspiration, parallel-plate rheometer, and stretching substrate. Contact-based techniques can provide direct quantification of elasticity and are considered the gold standard. However, they need to physically touch and apply force to the sample during experiment, making the measurement invasive and mostly limited to the superficial layer of material. The second is bead-based techniques, including optical tweezer, magnetic tweezer, magnetic twisting cytometry, passive microrheology, and microdroplet-based sensors. These techniques have been extensively used to extract the localized mechanical properties of the sample, mostly at the cellular and subcellular scales. However, the injection of beads or droplets is required for experiments. The third is elastography techniques, where the application of an external force is coupled with imaging technologies to measure force-induced deformation and back calculate the strain. These include optical stretching, optical coherence elastography (OCE), and microfluidics-based deformers. OCE is powerful to characterize and map the mechanical properties of biological tissue in large scale, and the microfluidics-based techniques can assess cell biomechanics in medium with high throughput. In short, each of these techniques has strengths and limitations, leading to a specialization of their use for particular applications.

Here, we would like to introduce a new technology named optical Brillouin microscopy [2-4], which utilizes an entirely different approach to probing material mechanical properties. Brillouin microscopy is based on the physical principle of spontaneous Brillouin light scattering, where the incident light undergoes a frequency shift (i.e., Brillouin shift) after interaction with the sample being tested. The Brillouin shift Ω is proportional to the local longitudinal elastic modulus M' of the sample by $M' = K \cdot \Omega^2$, where the coefficient $K = \lambda\rho/(4n^2)$ for backward scattered light. λ is the known laser wavelength in air, ρ and n is the mass density and refractive index of the sample, respectively. With a known value of ρ/n^2 , the longitudinal modulus M' can be computed from the Brillouin shift Ω measured by a Brillouin spectrometer. A confocal Brillouin microscope is built by integrating a Brillouin spectrometer and a standard optical confocal microscope [4], allowing the mechanical mapping of material with diffraction-limited resolution in 3D. Brillouin microscopy only uses a laser beam to probe the mechanical modulus, making it a non-contact, non-invasive, and label-free mechanical testing tool.

The unique features of the Brillouin microscopy provide new opportunities for probing cell and tissue biomechanics in physiologically relevant conditions that are not easily accessible to conventional technologies, such as the nuclear mechanics in an intact cell, subcellular mechanics during confined migrations and in 3D *in vitro* microenvironments (e.g., 3D culture, spheroid, and organoid), and tissue mechanics of early-stage embryo. In this work, we will first talk about the innovation and instrumentation of several Brillouin technologies, including confocal Brillouin microscopy [4], line-scanning Brillouin microscopy [5], and Brillouin flow cytometry [6]. We will then show several biomedical research that is enabled by Brillouin technology, with a focus on cancer related research and embryo development [8-10].

REFERENCES

- [1] Bao, G et al., *Nature Materials*, 2: 715-725, 2003.
- [2] Scarcelli, G et al., *Nature Photonics*, 2: 39-43, 2008.
- [3] Scarcelli, G et al., *Nature Methods*, 12: 1132-1134, 2015.
- [4] Zhang, J et al., *Nature Protocols*, 16: 1251-1275, 2021.
- [5] Zhang, J et al., *Nature Methods*, 20: 677-681, 2023.
- [6] Zhang, J et al., *Lab Chip*, 17: 663-670, 2017.
- [7] Zhang, J et al., *Small*, 1907688, 2020.
- [8] Wisniewski, E et al., *Science Advances*, 6: eabas6506, 2020.
- [9] Roberts, A et al., *J Biomechanics*, 121: 110400, 2021.
- [10] Prevedel, R et al., *Nature Methods*, 16: 969-977, 2019.

Biophotonics methods for study the functional state of microcirculatory-tissue systems during long-term isolation in the ground model of a space station and in space flight conditions

Andrey DUNAEV

Research & Development Center of Biomedical Photonics, Orel State University, Russia

dunaev@bmecenter.ru

From the very beginning of human exploration of Space, considerable importance has been given to the study of the weightlessness effect on the cardiovascular system. Currently, there has been a steady increase in interest in the problems of non-invasive research not only of the microcirculatory bed as the final segment of the cardiovascular system, but also of the microcirculatory-tissue systems (MTS) of the human body. MTS are the smallest functional unit of the vascular system, where microvessels are in close interaction with the surrounding tissue and regulatory elements. The study of MTS functional state, both under the simulation of spaceflight (SF) conditions, like in an isolation experiment, and in a real SF, opens up new opportunities for a more detailed analysis of microvasculature and oxidative metabolism of biological tissue adaptation [1]. The purpose of this work is to demonstrate the capabilities of biophotonics methods for analyzing the functional state of MTS of the human body during long-term isolation in the ground model of a space station and in space flight conditions.

To study the MTS in the Space conditions wearable multimodal devices with laser Doppler flowmetry (LDF) and fluorescence spectroscopy (FS) channels “LAZMA PF” (SPE LAZMA Ltd., Russia; in EU/UK this device is made by Aston Medical Technology Ltd., UK as “FED-1b”) were used [2]. The following parameters were recorded and analysed: index of microcirculation (I_m), amplitudes of endothelial (A_e), neurogenic (A_n), myogenic (A_m), respiratory (A_r) and cardiac (A_c) oscillations, and the skin autofluorescence value (A_{NADH}) when probing with 365 nm light, normalised to the backscattered radiation.

MTS research is currently being conducted on volunteers under isolation conditions. The 360-day isolation experiment (SIRIUS-23 project) simulates the conditions of a long-term manned Space mission in order to study the biomedical and psychological problems in humans associated with isolation and restriction of space. The research protocol includes simultaneous registration of MTS parameters on the back of the wrist and the pads of the first toe. MTS parameters were recorded in a supine position for 10 min (basal conditions), then hyperventilation breathing (6 times per min) was performed for 5 min. The next part of the protocol was executed without the device on the toe since volunteer performed an orthostatic test (standing in upright position). Then volunteer took a horizontal position, and 3 min occlusion test was performed. Measurements of MTS during the simulation of individual SF factors were also performed and showed an active response of MTS parameters to functional tests. It was shown, that, when exposed to the overload during rotation of cosmonauts on a centrifuge, there is a decrease of I_m in the legs and forehead skin, showing the blood circulation is centralized. Changes in MTS parameters of participants of the SIRIUS-23 experiment reflect changes in their functional state due to physical inactivity and changes in psycho-emotional background.

During LAZMA experiment (from December 2021 to the present time) on the International Space Station (ISS) two devices were symmetrically placed on the pads of the middle fingers and big toes, on the back of the wrists and attached to the temples [3]. Measurements of each area lasted 8 min, during which the cosmonauts were in a state of complete physical and psychological rest. Subsequently, the experimental protocol was adapted and shortened to 30 min and included measurements in 3 areas of interest (forehead, fingers and toes). The obtained data demonstrates that the toes are the most stressed areas during the microgravity, which also reflects a decrease in the I_m and oxidative metabolism index in the first days of SF. A preliminary analysis of data on 1 cosmonaut and 1 space tourist showed that the most significant changes in MTS parameters occur in the temporal region of the head and in the region of the lower extremities on the 2nd and 3rd days of SF and are characterized by a significant decrease in I_m and an increase in vascular tone with gradual restoration of pre-flight values by the 6th day of SF. It can also be concluded that the human body strives to maintain the hemodynamics of the brain at a constant level and this area adapts most quickly to new conditions. Thus, for the first time, a technique has been developed for measuring MTS in the limbs of cosmonauts during the period of acute adaptation to microgravity conditions and readaptation after the completion of a SF. Obtaining the most important physiological information in real time under conditions of zero gravity will provide completely new data on the physiology of the MTS in humans under conditions of orbital flight.

Thus, the use of biophotonics methods in portable analyzers during space research (on Earth and in Space) makes it possible to assess the functional state of the MTS of the human body and individualize both the processes of preparing cosmonauts for space flight and their adaptation directly to weightlessness conditions.

[1] A. Dunaev, *J of Biomedical Photonics & Eng* 9(2), 020201, 2023.

[2] E. Zharkikh et al, *J. Biophotonics* 16 (9), e202300139, 2023.

[3] A. Dunaev et al, *Proc. of Int. Conf. Laser Optics (ICLO)*, 2022.

Master Slave OCT for ultra Fast Swept Sources

Adrian Podoleanu¹, Ramona Cernat¹, Adrian Bradu¹, Sylvain Rivet³, Patrick Bowen²
Alejandro Martinez Jimenez¹, Rene Riha¹ and Sacha Grelet^{1,2}

¹*School of Physical Sciences, University of Kent, UK*

²*NKT, Denmark*

³*Université de Bretagne Occidentale, IBSAM, Laboratoire OPTIMAG, France*

ABSTRACT

In order to reduce the distortion effects due to organ movement, fast tunable lasers (swept sources) have been designed and fast volume investigation optical coherence tomography (OCT) systems have been proven.

I will review the progress in the fast tunable lasers for OCT in Kent, presenting different principles leading to MHz and tens of MHz sweeping rate, such as dispersive cavity mode locked lasers and time stretch. Dispersive cavity mode locked laser swept sources represents a low cost alternative to time stretch technology. In addition, such a concept is compatible with swept source full field OCT systems, where the sweeping is slow, in fractions of a second.

I will also present the bottleneck in digital signal processing raised by the combination of an interferometer with a multi MHz tuning rate laser. Traditionally, in order to produce a volumetric image, a Fourier Transform (FT) is applied to the electrical signal delivered by reading the channeled spectrum at the interferometer output. The acquisition time is improved due to increase in the data acquisition speed, with data less affected by sample movement, but data collected in one sweep exceed the data transfer rate of Camera Link or Coax express, hence denying possibility of real time display.

The method of Master Slave (MS) will be presented. In Kent, we developed several facets of the MSOCT method. Master Slave [1], Complex Master Slave [2], Downconversion Master Slave [3]. In its version of down conversion, the MS method can serve delivery of *en-face* OCT images in principle at any high sweeping rates, of MHz or tens of MHz.

The Master Slave (MS) OCT method [1] employs a processor for each depth in the sample. In doing so, the MSOCT does not need to process the data in the way a conventional FT based OCT method does. To eliminate the nonlinearity in tuning, FT based OCT systems require spectral data to be organised along linear slots in time. In opposition, the MSOCT uses the data as they are but employs a different basis of sinusoidal or exponential terms, that are chirped due to nonlinear sweeping and due to dispersion in the interferometer. The spectral modulation of components of such basis is exactly that generated by the same interferometer driven by the same swept source at a given optical path difference (OPD). The basis of functions, termed as masks can be obtained experimentally, by collecting spectra at different OPD values, or theoretically inferred from a few experimental spectra for at least two different OPDs [2]. The MS method will be presented in comparison with the conventional method of using a FT block to process the photodetected signal. Experimentally, the masks can be generated by using the same interferometer employed to scan the sample examined, or by using separate Master interferometers [3]. In both cases, the interferometer equipped with the scanning head and sample plays the role of a Slave interferometer, where only the signal corresponding to the OPD of the mask is selected, i.e. from a depth in the sample dictated by the mask. Largely, we progressed the MSOCT along the utilization of a single interferometer, that in a first instance is used at a Master stage to inform a protocol for calculation of masks, using a mirror as sample. In the second stage, Slave, the same interferometer is used at the Slave stage, where the object subject to investigation is scanned. This method leads to complex masks [2] with advantages in terms of signal to noise ratio and phase processing, but requires a fast digitizer, similar to that used for the FT block in conventional OCT systems. However, if the sweeping speed curve varies in time, masks require to be recalculated. In this case, better is to produce the masks in real time by using a second interferometer, Master [3]. The same digitizer is employed as before, to perform the MSOCT protocol, where instead of a stored mask, a real time mask is generated in synchronism with spectral acquisition of data from the object. This requires a digitizer with two inputs, hence referred here as method D. The D method is different from that of FT based OCT signal processing, where the digitizer is clocked by a fixed optical path interferometer in the swept source and should produce similar results. Comparisons of the three methods, CMS, D and downconversion will be presented in terms of axial resolution and axial range achievable [3]. Even more, by downconversion the digitizer can be eliminated, where an analogue mixer is employed to perform analogue multiplication of the photodetected signals from the two interferometers, Master and Slave.

I will show how these three methods can contribute towards incorporation of fast tuning lasers within the armamentarium of fast swept source driven OCT instruments.

REFERENCES

- [1] A. Podoleanu et al, Opt Express 21(16):19324-19338 2013.
- [2] S. Rivet et al, Opt. Express 24, 2885-2904 2016.
- [3] A. Podoleanu et al, Biomed Opt Express.;10(2):772-788 2019.

Qualitative and quantitative analysis of gas samples THz and IR absorption spectra for medical and ecological applications

Yury KISTENEV, Vladimir PRISHEPA, Vladimir SKIBA, Viktor NIKOLAEV, Georgy Raspopin, Didar MAKASHEV
and Alexey BORISOV
LMIML Laboratory, Russia
Tomsk State University, Tomsk
yuk@iao.ru

ABSTRACT

Spectral analysis of gas samples has numerous applications in medicine and ecology including medical diagnostics through analysis of volatile molecular biomarkers in the patient exhaled air or industrial molecular pollutions and greenhouse gases in the atmosphere. Laser absorption spectroscopy allows analyzing operatively and in the field or near a patient's bed properties of gas probes. But meaningful analysis of absorption spectra of a multi-components gas mixture of natural origin is very hard because of a priori unknown molecular composition. Applications of chemometrics and machine learning methods in gas samples and groups of samples absorption spectra decomposition, funding latent dependencies, and classification will be discussed.

Qualitative and quantitative analysis of gas probes is associated with operative control of industrial molecular pollutions and greenhouse gases in the atmosphere. It is also the base of perspective and intensively developing now methods of noninvasive medical diagnostics [1-3]. Here, qualitative analysis is associated with establishing the presence of a definite molecular component in the gas probe. Quantitative analysis is aimed on a specific component concentration evaluation. IR and terahertz (THz) absorption spectroscopy has the following advantages in relation to other methods of spectral analysis: possibility to work in the field or in a hospital, high sensitivity, a simple and low-cost operation procedure. Usually, absorption spectra decomposition can be conducted by iterative algorithms like multivariate curve resolution, which need a priori knowledge what components are present in a studied probe. We plan to discuss machine learning methods and specific chemometrics methods suitable for this task. This procedure, in fact, is the step of informative features extraction, which then can be used for funding latent dependencies in groups of samples and creation of prediction data model for their classification. The examples of appropriate machine learning pipeline implementation will be presented.

The work was conducted with the financial support of the Ministry of Science and Higher Education of Russia (Agreement No. 075-15-2024-557 dated 04/25/2024).

REFERENCES

- [1] Y.V. Kistenev et al. Journal of Biophotonics. Vol. 16, № 9. Art. num. e202300198, 2023. DOI: 10.1002/jbio.202300198
- [2] A.A. Boiko et al, Journal of Biomedical Photonics & Engineering. Vol. 8, № 4, 1–9, 2022. URL: <http://jbpe.ssau.ru/index.php/JBPE.L>.
- [3] A.V. Borisov et al, Journal of Breath Research. Vol. 15, No 2. 027104, 2021. DOI: 10.1088/1752-7163/abebd4

Revolutionizing Vascular Diagnostics: the Role of Wideband Ultrasound Detectors in Laser Optoacoustic Angiography

Pavel SUBOCHEV¹

¹Laboratory of Ultrasound and Optoacoustic Diagnostics, Department of Radiophysical Methods in Medicine, Institute of Applied Physics named after A.V. Gaponov-Grekhov of the Russian Academy of Sciences, Russia

pavel@ipfran.ru

ABSTRACT

Laser optoacoustic (OA) angiography combines molecular optical specificity with ultrasound's diagnostic depth and resolution. The sensitivity and bandwidth of ultrasonic detectors are important cornerstones of vascular diagnostics in both clinical and preclinical research. My presentation will cover the basics of optoacoustic imaging through the prism of piezopolymer ultrasound technology that can leverage the true multi-scale potential of optoacoustics. Recent advancements in detector design, such as the highly sensitive miniature needle PVDF-TrFE ultrasound sensor for optoacoustic microscopy [1], will be highlighted, showcasing their contribution to superior image fidelity and diagnostic accuracy. Applications in diagnosing and treating vascular abnormalities will be discussed, emphasizing high-resolution, real-time imaging capabilities. Noninvasive optoacoustic microangiography's role in revealing radiation-induced deep tumor vasculature remodeling [2] and scanning optoacoustic angiography's use in assessing post-thrombotic syndrome [3] will be highlighted. Challenges, limitations, and future research directions will also be addressed, illustrating the potential of wideband ultrasound detectors to redefine optoacoustic imaging standards.

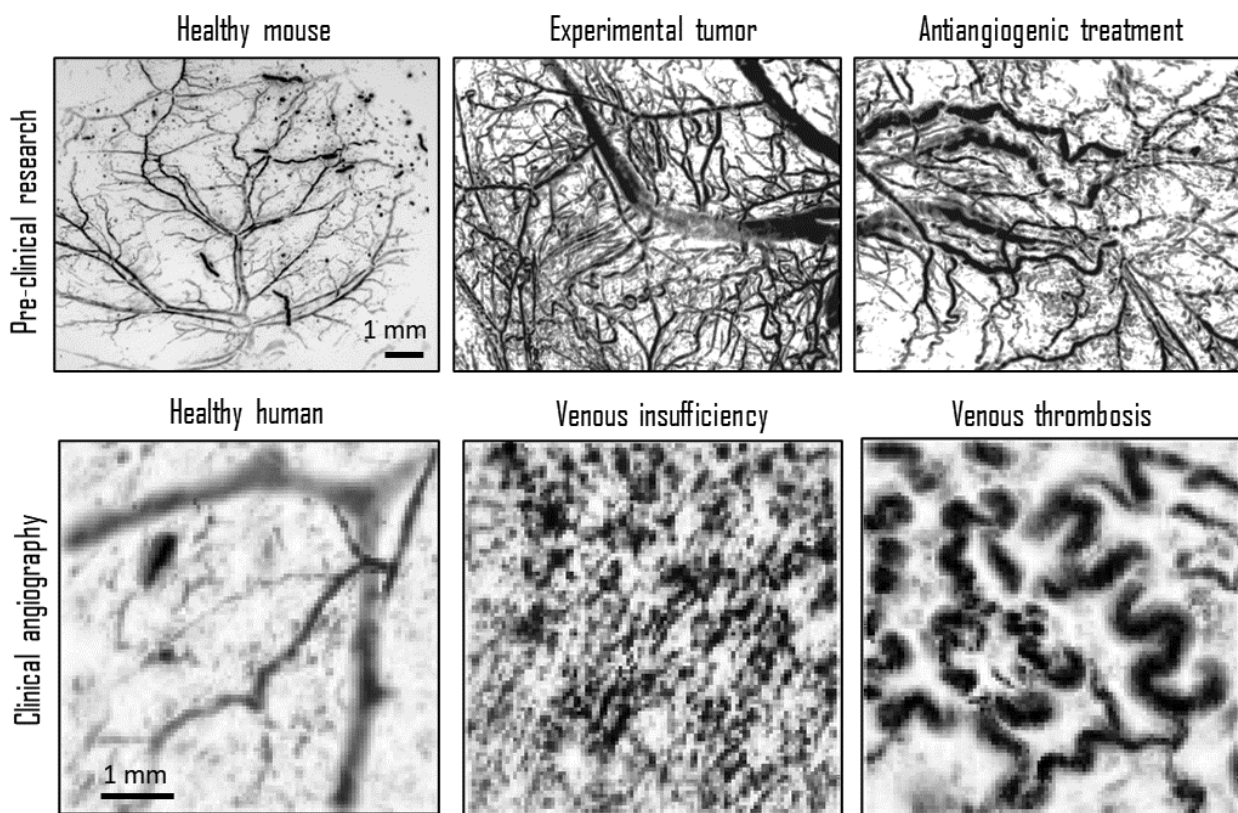


Figure 1: Wideband optoacoustic angiography in clinical and preclinical research.

ACKNOWLEDGMENT

Pavel Subochev acknowledges support by the Center of Excellence "Center of Photonics" funded by the Ministry of Science and Higher Education of the Russian Federation, Contract No. 075-15-2022-316.

REFERENCES

- [1] Liu, Y. H., Kurnikov, A., Li, W., Subochev, P., Razansky, D. (2023). Highly sensitive miniature needle PVDF-TrFE ultrasound sensor for optoacoustic microscopy. *Advanced Photonics Nexus*, 2(5), 056006-056006.
- [2] Orlova, A., Pavlova, K., Kurnikov, A., Maslennikova, A., Myagcheva, M., Zakharov, E., ... Subochev, P. (2022). Noninvasive optoacoustic microangiography reveals dose and size dependency of radiation-induced deep tumor vasculature remodeling. *Neoplasia*, 26, 100778.
- [3] Nemirova, S., Orlova, A., Kurnikov, A., Litvinova, Y., Kazakov, V., Ayvazyan, I., Subochev, P. (2024). Scanning optoacoustic angiography for assessing structural and functional alterations in superficial vasculature of patients with post-thrombotic syndrome: A pilot study. *Photoacoustics*, 100616.

Development of FF-SS-OCT systems for structural and bleach-induced functional retinal imaging.

Robert ZAWADZKI^{1,2}, Ratheesh MELEPPAT¹, Denise VALENTE^{2,3}, Soohyun LEE⁴, Ewelina PIJEWSKA^{1,2}, Nathan DOBLE^{4,5} and Ravi JONNAL²

¹ UC Davis Eye-Pod Small Animal Ocular Imaging Laboratory, Department of Cell Biology and Human Anatomy, University of California Davis, USA

² Center for Human Ocular Imaging Research (CHOIR), Dept. of Ophthalmology & Vision Science, UC Davis, USA

³ Department of Physics, University of Pernambuco, Recife, Brazil.

⁴ College of Optometry, The Ohio State University, 338 West 10th Avenue, Columbus, Ohio 43210, USA

⁵ Department of Ophthalmology and Visual Sciences, Havener Eye Institute, The Ohio State University, 915 Olentangy River Road Suite 5000, Ohio 43212, USA

rjzawadzki@ucdavis.edu

ABSTRACT

The development of optical methods to assess retinal structure and function simultaneously is of great interest to clinical and experimental ophthalmology. If successful, it would revolutionize clinical practice that relies on an independent evaluation of disease-related changes in retinal morphology and its function. Full-field swept-source optical coherence tomography (FF-SS-OCT) has emerged as a powerful tool for *in vivo* retinal imaging in humans and experimental animals. The flexibility afforded by a tunable laser source with adjustable sweep rate and sweep range, in conjunction with a fast 2D CMOS camera, allowed exploration of variable sweep (volume) rates imaging. Additionally, excellent phase stability between consecutive volumes made it an ideal tool for acquiring bleach-induced changes in retinal morphology using phase-based approaches. This presentation will review our recent progress in developing and applying FF-SS-OCT systems built at UC Davis for human and small experimental animal evaluation. It will discuss the criteria used to choose a specific implementation for each system, evaluate the quality of the acquired retinal data, and discuss current limitations and directions for future development.

Optical coherence tomography (OCT) is the gold standard for clinical retinal imaging [1,2]. One of the major factors affecting the ability to use OCT for functional retinal imaging is the reduction of motion artifacts, which is often achieved by increased data acquisition speed. This can be achieved by increasing the point scan rate or implementing parallelization of illumination and data acquisition. However, increasing the lateral scanning rate decreases sensitivity because fewer photons are collected per A-scan. Increasing the illumination irradiance can compensate for this, but this is ultimately limited by the maximum permissible exposure (MPE) safety limits. As methods to parallelize the acquisition of A-scans and circumvent limits imposed by mechanical scanning, line-scan (LS) and full-field (FF) OCT configurations have been demonstrated for human retinal imaging [3,4]. The highest level of parallelization is accomplished with FF-OCT, which utilizes a 2D camera to acquire the backscattered light from an illuminated area of the retina. In recent years, the capability of full-field SS-OCT (FF-SS-OCT) systems employing high-speed CMOS detectors has been explored to attain effective A-scan rates substantially higher than traditional flying-spot OCT in human retinal imaging [5-7]. However, the FF-OCT scheme suffers an inherent issue of coherent crosstalk between neighboring image points, limiting the quality of retinal images. Strategies for reducing this crosstalk by reducing spatial coherence have been explored, such as the use of a lengthy multimode fiber, a rapidly moving diffuser, or other conventional incoherent sources [6]. This presentation will describe two FF-SS-OCT systems built at UC Davis. An adaptive optics AO-FF-SS-OCT system working in an off-axis configuration was built and used to study bleach-induced changes (optoretinography, ORG) in individual photoreceptors over small FOV (2° x 2°) in human subjects [8]. An FF-SS-OCT system working in an on-axis configuration has been built and used to study the morphology and bleach-induced changes (ORG) over large FOV (28.5° x 14.25°) in the retinas of mice. A real-time fundus view and low-resolution B-scans allowed for the effective alignment of subjects during the imaging session.

REFERENCES

- [1] D. Huang et al, Science 254, 1178, 1991.
- [2] W. Drexler et al, Progress in retinal and eye research 27, 45, 2008.
- [3] D. J. Fechtig, et al., Biomed. Opt. Express 6, 716, 2015.
- [4] T. Bonin, et al., Opt. Lett. 35, 3432, 2010.
- [5] D. Valente, et al., Biomed. Opt. Express 11, 5995, 2020.
- [6] E. Auksoorius, et al., iScience 25, 2022.
- [7] D. Hillmann, et al., Opt. Express 25, 27770, 2017.
- [8] R.S. Jonnal, Ann Transl Med 9, 1270, 2021.

Photon Time-of-Flight Sensing for Color-Bias-Free Pulse Oxymetry

Stefan ANDERSSON-ENGELS^{1,2,3}, Claudia NUNZIA GUADAGNO³, Suraj KUMAR KOTHURI¹, Hui MA¹, Pranav LANKA¹, Rekha GAUTAM¹ and Sanathana KONUGOLU VENKATA SEKAR^{1,3}

¹Biophotonics@Tyndall, Tyndall National Institute, Ireland

²School of Physics, University College Cork, Ireland

³BioPixS Ltd., Ireland

stefan.andersson-engels@tyndall.ie

The future of biomarker sensing technology is led by non-invasive optical biomarker sensing (OBS) devices for blood saturation, heart rate, respiration rate, hydration, body temperature, glucose and more. Such sensing will be conducted by pulse oximeters, smartwatches, glucose monitors and hydration monitors, etc. The most widely used OBS device is the pulse oximeter. Despite 40+ years since its clinical introduction and recommended use in various critical clinical settings, pulse oximeters are unreliable and suffer from skin color bias and inaccuracies [1]. The color bias phenomenon was identified as early as the 90s [2], and despite efforts, the bias remains present even today. Recently during the COVID-19 pandemic, racial bias in OBS devices was suspected to have contributed to the loss of many lives in darkly pigmented patients [3]. Current state-of-the-art OBS devices use continuous wave (CW) light technology which is inherently limited in accuracy and results are sensitive to signal contamination from superficial melanin skin color pigmentation [4].

In this work we explore transformational multilayer photon time-of-flight spectroscopy (pTOFS) to address the shortcomings of CW technology and with the aim to significantly reduce or eliminate racial bias while significantly improving the accuracy of OBS devices.

Monte Carlo simulations were conducted to show that the shape of a pTOFS curve depends on the absorption and scattering properties of multilayered tissue studied. The absorption of the superficial layer (melanin pigmentation) turns out to only affect the overall attenuation of the pTOF curves, while the shape remains more or less constant (to be presented). The deep tissue absorption will, on the other hand, affect the shape, and also the scattering affects the peak position and broadening of the pTOF. The simulation results are further backed by experimental results on realistic two layers (skin, muscle) tissue-mimicking phantoms (Fig. 1a). The top layer absorption was changed across 3 skin color types (light, medium, dark with equivalence $\mu_{a1} = 1, 3, 7 \text{ cm}^{-1}$, respectively) and the muscle layer was kept constant at $\mu_{a2} = 0.1 \text{ cm}^{-1}$. The pTOF curves of the three skin color configuration are shown in Fig. 1b. The preliminary recovered optical properties results using a novel multilayer model is shown in Fig. 1c. From the results, it is evident that changing the absorption of the skin layer affects only the CW technology equivalent signal whereas the recovered muscle layer absorption is independent of variation in the skin layer. This novel feasibility results show bias-free recovered absorption (μ_{a2}) of the muscle layer independent of realistic skin pigmentation (skin absorption- μ_{a1} (light, medium, dark)). It further suggests possible pathways for OBS devices to become a gold standard for bias-free and reliable tools in clinical and personal biomarkers sensing applications.

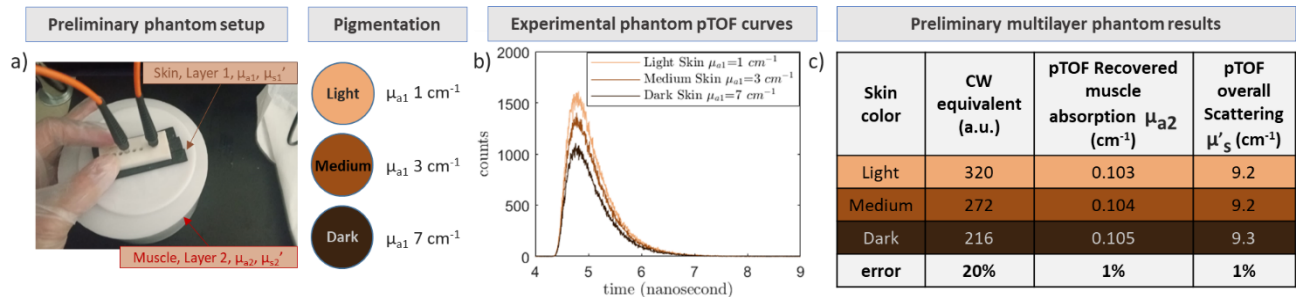


Figure 1: Results on phantoms a) experimental setup of two-layer phantom and TDDOS probe b) pTOF curves of the two-layer phantom with changing skin color (light, medium, dark) layer c) preliminary bias-free extraction of deep layer absorption with varying skin pigmentation, changing the pigment of skin layer does not affect the estimated deep layer (muscle) absorption (μ_{a2})

REFERENCES

- [1] C. Shi, M. Goodall, J. Dumville, J. Hill, G. Norman, O. Hamer, A. Clegg, C. L. Watkins, G. Georgiou, A. Hodkinson, C. E. Lightbody, P. Dark, and N. Cullum, medRxiv 2022.02.16.22271062 (2022).
- [2] A. Jubran and M. J. Tobin, Chest 97(6), 1420–1425 (1990).
- [3] M. J. Tobin, F. Laghi, and A. Jubran, Am. J. Respir. Crit. Care Med. 202(3), 356–360 (2020).
- [4] M. J. Tobin and A. Jubran, Ann. Intensive Care 12(1), 2021–2022 (2022).

Photodynamics of Molecular Probes in Solutions, Cells, and on Organic Surfaces

Oleg VASYUTINSKI¹

¹*Ioffe Institute Russian Academy of Sciences, Russia*

osv@pms.ioffe.ru

ABSTRACT

The lecture presents the review of recent studied that have been carried out in the Ioffe Institute, Russian Academy of Sciences in the field of photodynamics of photosensitizers (PS) and biomolecules in solutions, living cells, and on organic surfaces by means of time-resolved fluorescence polarization spectroscopy and fluorescence lifetime imaging microscopy (FLIM).

Detailed investigations of the fluorescence of coenzymes NADH and FAD in water-alcohol mixtures (methanol, ethanol, propylene glycol) and of a photosensitizer Chlorin e6 that is now widely used for photodynamics therapy of oncology diseases and for photodynamic purification of organic surfaces have been carried out [1]. A significant increase of fluorescence quantum yield in NADH and FAD with increase of alcohol concentration was observed. A new model has been developed for elucidation of the effect observed. The model takes into consideration several possible energy transfer channels in the coenzyme excited states after excitation with ultrashort laser pulses. The model results to a new expression for time-dependent intensity of fluorescence from the lowest excited state of the coenzyme and allows for separation of the fast sub-nanosecond nonradiative relaxation processes from more slow nanosecond radiative and nonradiative relaxation processes. The mechanisms of these relaxation processes were analyzed for each type of coenzymes under study.

Fluorescence anisotropy of PS Chlorin e6 in various solutions and the dependence of the fluorescence decay time on microenvironmental conditions in solutions and living cells have been investigated. A significant difference between the fluorescence anisotropy under one- and two-photon laser excitation has been observed within wide excitation spectrum and possible reasons for the difference of the fluorescence anisotropies observed have been analyzed [2]. We also observed a significant gain of the Chlorin e6 fluorescence quantum yield and a non-monotonous increase of the fluorescence decay time in solution with pH in the range of 5-7 [3]. The effects observed were then applied for investigation of PS Chlorin e6 distribution with FLIM in living cells and for the mapping of pH distribution inside cells. A new effective method of singlet oxygen generation on organic surfaces has been developed [4]. The method is based on the excitation of a PS dissolved in an appropriate solution and pulverized on the surface by a gas spray. Singlet oxygen generation quantum yield and PS Chlorin e6 photobleaching on various organic and non-organic surfaces were under study. An intriguing decrease by several decades of the photobleaching rate of PS on organic surfaces with respect to non-organic surfaces has been observed. The investigation of the photobleaching rate allowed for understanding of the photobleaching mechanism. As was shown, the PS photobleaching on organic surfaces occurred mainly due to interaction with oxygen molecules.

REFERENCES

- [1] I. Gorbunova et al, *J. Photochem. Photobiol. A: Chemistry*, 436, 114388, 2023.
- [2] I. Gorbunova et al, *Photonics*, 10, 9, 2023.
- [3] A. Belashov et al, *J. Photochem. Photobiol. B: Biology*, 243, 112699, 2023.
- [4] A. Zhikhoreva et al, *J. Photochem. Photobiol. B: Biology*, 228, 112395, 2022.

Nanostructures for Multi-response Selective Volatile Organic Compound Sensing

Anna ORLOVA

ITMO University, Russia

a.o.orlova@itmo.ru

ABSTRACT

The early detection of oncological diseases represents a significant challenge for contemporary society [1]. The development of effective strategies to reduce cancer mortality and shorten cancer therapy periods is contingent upon the convergence of modern theranostics and sensorics. In recent years, there has been a notable advancement in the development of techniques for detecting volatile organic compounds, which serve as markers of oncological diseases [2]. The detection of elevated concentrations of these compounds in exhaled breath samples may indicate the presence of a specific malignant neoplasm. Certain compounds act as "markers," including acetone, acetonitrile, methanol, ethanol, and others.

At present, the most promising avenue of research in the field of sensor technology is the development of sensing elements based on nanomaterials. The high surface-to-volume ratio, the capability to modify the shape and chemical composition of nanomaterials enables precise tuning of the physical and chemical properties of the sensing elements, thereby enhancing their performance, sensitivity, and selectivity. Luminescent colloidal quantum nanocrystals (NCs), which include quantum dots, rods, tetrapods, and nanoplatelets, as well as graphene-family materials, such as graphene, reduced oxide graphene, graphene nanobelts, and carbon nanotubes, are the two most extensively researched classes of nanomaterials for modern sensorics [3]. Despite the significant success in research and development of luminescent and electrical sensors based on these nanomaterials, the problem of selectivity represents a major concern in the detection of VOC, which have a similar chemical composition. In an early study, we combined quantum dots (QDs) and graphene or graphene nanobelts to demonstrate the enhancement of the electrical response to ammonia vapour due to efficient energy and charge transfer from QDs to graphene [4,5]. This approach allows for an improvement in the sensitivity of the sensor response in comparison with pure graphene, but does not allow for an increase in the selectivity of the recognition of VOC.

Now we present an approach to selective detection of several VOC with similar chemical composition analyzing luminescent and electrical responses simultaneously from several sensing elements utilizing layers of rGO nanosheets, CdSe/ZnS QDs, CdSe nanoplatelets (NPs) and multilayered hybrid structured based on combination of QDs (QDs/rGO) and NPs (NPs/rGO). We demonstrate that both types of nanostructures facilitate effective photoexcitation energy transfer and photoinduced electron transfer from QDs and NPs to rGO layers. These processes are accompanied by a luminescence quenching of QDs and NPs. We have demonstrated that the rates of quenching and rising of luminescence of CdSe/ZnS QDs and CdSe NPs layered onto dielectric slides and in hybrid structures with rGO depend on several factors: (i) the concentration of the analyte, (ii) the rate of analyte sorption to the surface of samples, and (iii) the rate of photoinduced desorption of analyte molecules from the surface of samples. Our results demonstrate that the combination of luminescent and electrical signals from our samples allows us to obtain a unique response for several VOCs with similar chemical compositions. Our findings demonstrate that the luminescent response of CdSe NPs to acetonitrile molecules is negative for NPs layers on dielectric slides and positive for NPs/rGO hybrid structures.

We show that the photoelectric response from rGO layers and NPs/rGO hybrid structures is also oppositely directed. This indicates that the photoinduced electron transfer from NPs to the rGO layer, rather than FRET, is the primary contributor to the observed change in conductivity. Additionally, we have shown that the interaction of acetonitrile molecules with the NPs/rGO structure results in a significant alteration in the dark and photoconductivity of the structures. We have developed a model to explain the electronic relaxation pathways in the NPs/rGO structure under acetonitrile action. Our results indicate the potential for the development of multi-parametric selective sensors based on the combination of hybrid structures with different quantum nanocrystals and graphene-like materials.

ACKNOWLEDGEMENTS

The research was supported by the Ministry of Education and Science of the Russian Federation, State assignment, Passport 2019-1080 (Goszadanie 2019-1080).

REFERENCES

- [1] Crosby D et al, *Science*, 375, 6586, 2022.
- [2] Magnano M. et al, *TrAC Trends in Analytical Chemistry*, 176, 117739, 2024.
- [3] Malik S. et al, *Heliyon*, 9, 9, 2023.
- [4] Gromova Yu. Et al, *J. Appl. Phys.*, 118, 10, 2015
- [5] Reznik I. et al., *Nanomaterials*, 10, 4, 714, 2020

Hyperspectral Imaging of Intestinal Ischemia Supported by Machine Learning

Valery SHUPLETSOV¹, Ilya GORYUNOV, Nikita ADAMENKOV^{1,2} and Viktor DREMIN^{1,3}

¹Research & Development Center of Biomedical Photonics, Orel State University, Russia

²Orel Regional Clinical Hospital, Russia

³College of Engineering and Physical Sciences, Aston University, UK

viktor.dremin@bmecenter.ru

ABSTRACT

The study focuses on developing a hyperspectral imaging (HSI) system to assess intestinal wall ischemia, which is traditionally determined visually through mesenteric vessel pulsation, peristaltic contractions, and colour assessment. These traditional methods are subjective and limited. HSI offers an objective and noninvasive alternative, combining digital imaging and spectral analysis to provide detailed information on tissue viability [1,2].

A portable imaging system was constructed on the basis of the SpecimIQ hyperspectral pushbroom camera (Specim, Spectral Imaging Ltd., Finland) providing spectral data within the total range of 400-1000 nm. A broadband illumination unit is based on the fibre-optic ring illuminator and the halogen irradiation source, providing uniform distribution of light intensity in the camera focal plane.

Animal studies were conducted on six Wistar rats, simulating ischemia by ligating the main vessels supplying the intestine. The animals were monitored at intervals of 1-, 6- and 12-hours post-ligation to assess tissue changes. Histological analyses were performed to correlate spectral data with the extent of ischemia. Tissue saturation was calculated using a two-wave approach based on the different absorption properties of oxygenated and deoxygenated haemoglobin [3], producing two-dimensional colour maps of tissue saturation.

A machine learning (ML) algorithm, specifically XGBoost, was applied to classify intestinal tissue into three categories: intact, possibly reversible ischemia, and irreversible ischemia. The model was trained on preprocessed hyperspectral data, using principal component analysis (PCA) for feature reduction. Data were labelled based on the Park/Chui histologic grading. The ML model effectively classified tissue viability with high accuracy (99%). The classification maps visually correspond to the saturation maps (Fig. 1), which indicates a high ML potential for processing raw HSI data.

The HSI system was also tested on patients with intestinal obstruction. The system successfully identified areas of reduced saturation correlating with ischemic tissue. HSI, combined with ML, offers a promising method for intraoperative assessment of intestinal viability. It provides objective, noninvasive diagnostics without contrast agents.

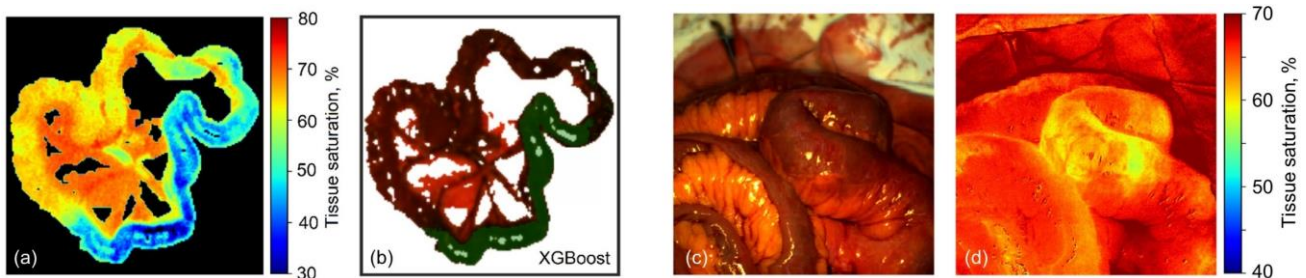


Figure 1: (a) Example of a two-dimensional tissue saturation map for possibly reversible ischemia of the rat intestine, and (b) corresponding classification map based on the XGBoost algorithm, (c) clinical example of intestinal obstruction, and (d) corresponding tissue saturation map.

REFERENCES

- [1] E. Zherebtsov et al, Biomed. Opt. Express 10(7), 3545-3559, 2019.
- [2] V. Dremin et al, IEEE Trans. Med. Imaging 40(4), 1207-1216, 2021.
- [3] E. Potapova et al, Human Physiol. 43(2), 222-228, 2017.

Optical monitoring of intrafollicular drug delivery by means of vaterite carriers

Yulia SVENSKAYA¹, Valery TUCHIN¹

¹Science Medical Center, Saratov State University, Russia

svenskaya@info.sgu.ru

ABSTRACT

Administration of pharmacologically active molecules via skin appendages is gaining tremendous scientific interest, especially with regard to delivery to specific targeted regions and the reduction of systemic toxicity. However, the design of an appropriate effective method for clinical use remains challenging. We report on a novel non-invasive approach for topical delivery based on accommodation of drug-loaded submicron particles in hair follicles followed by sustained release of active molecules into the skin [1, 2]. The proposed delivery system is represented by submicron porous biodegradable vaterite carriers, which provide the degradation-driven *in situ* release of the loaded substance. By means of scanning electron microscopy, optical coherent tomography and confocal laser scanning microscopy, we demonstrated a deep and plentiful filling of hair follicles with the topically applied carriers *in vivo* under the sonophoresis. This group of optical methods was also utilized to monitor degradation of the delivered carriers in rats and mice *in vivo* [1-5]. The described method provides intra- and transdermal drug administration for the purposes of localized and systemic adsorption and was adopted for delivery of photosensitizers [6-8], antifungal drugs [4, 9-11], vaccines [12] and glucocorticoids [5]. The use of vaterite particles allowed us to enhance dermal bioavailability of the applied drugs while targeting to specific areas in skin. In such a manner, by means of various optical methods we demonstrated that our protocol in non-invasive and easily practicable protocol for transdermal and topical drug administration.

The study is supported by Russian Science Foundation (project № 22-73-10194).

REFERENCES

- [1] Yu. Svenskaya et al, ACS Appl Mater Int 11 (19), 17270-17282, 2019.
- [2] Yu. Svenskaya et al, Patent RU2698871C1, 2018.
- [3] Yu. Svenskaya et al, Izv. Sarat. Univ. Physics 21(1), 80–85, 2021.
- [4] O. Gusliakova et al, Mater. Sci. Eng. C. 119, 111428, 2021.
- [5] M. Saveleva et al, J Mat. Chem. B. 12, 4867– 4881, 2024.
- [6] Y. Svenskaya et al, Brit J Dermatol, 182(6), 1479-1481, 2020.
- [7] Y. Svenskaya et al, Patent RU2698871C1, 2018.
- [8] S. Utz et al, Vestn Dermatol Venerol., 95(1), 21-29, 2019.
- [9] E. Lengert et al. Mater. Lett. 248, 211-213, 2019.
- [10] M. Saveleva et al, Biomat. Sci. 10, 3323, 2022.
- [11] R. Verkhovskii et al, ACS Infect. Dis. 9(5), 1137-1149, 2023.
- [12] Yu. Svenskaya et al, J Mat. Chem. B. 11(17), 3860-3870, 2023.

Pulsed Laser Trigger Released of Gene and Drug from Lipid Nanoparticles

Michel MEUNIER¹, Leonidas AGIOTIS¹, Amélie BARON¹, Isabelle LARGILLIÈRE¹ and Pieter CULLIS²

¹ Polytechnique Montreal, Department of Engineering Physics, Canada

² University of British Columbia, Department of Biochemistry and Molecular Biology, Canada

michel.meunier@polymtl.ca

Lipid-based nanoparticles (LNPs) are rationally designed 100nm spherules of concentric biodegradable phospholipids able to entrap many water or lipid-soluble therapeutic cargos. As such, LNPs hold great potential in the development of gene and drug-delivery-based applications as they further exhibit numerous attractive properties, such as long-term stability in biological environments [1]. They can be further designed to exhibit the ability to release their cargo in the presence of a trigger, either locally (pH changes or enzymes), or remotely (ultrasound, light, magnetic field) [1-2].

Here we propose a pulsed laser-triggered release approach based on the interaction of a single laser pulse with (5nm) gold nanoparticles (AuNPs) contained within engineered LNPs [3], resulting in rapid release of encapsulated therapeutic cargos. (see Fig. 1) We have examined two different approaches of triggered release, by performing both simulations and experiments.

In the first approach [4], a nanosecond laser pulse is employed for the release of the anti-cancer drug Doxorubicin (DOX) from LNPs. The latter are engineered oligolamellar vesicles containing clustered AuNPs within junctions of lipid bilayers and DOX at their aqueous core [3]. The laser is tuned near the plasmon resonance of the AuNPs, therefore, their interaction leads to the opening of the LNP by a heating process. Specifically, we demonstrate through simulations and experimentally that laser irradiation gives rise to sufficiently high temperatures for thermal decomposition of the surrounding lipids near the AuNPs, yet, without affecting the integrity of the drug [4]. Overall, the demonstrated increased efficacy of the proposed approach in the treatment of human breast adenocarcinoma cells *in vitro* holds promise for further improvements in cancer chemotherapy strategies [4].

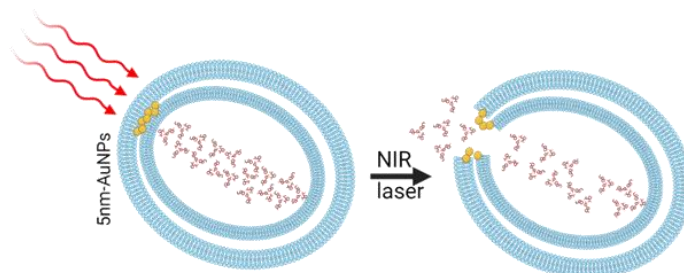


Figure 1: Schematics of laser trigger Gene/Drug release from Lipid Nanoparticles containing small gold nanoparticles

The second approach consists of laser-triggered liberation of genetic material instead of DOX. In this case, a femtosecond laser pulse is employed to interact with the clustered AuNPs out of the plasmon resonance. The LNP opening mechanism is proposed based on plasmon-induced hot spots of broadband laser-field amplification leading to highly localized photochemical decomposition of the surrounding lipid chains and release of the encapsulated substances. We, therefore, propose applying the triggered gene release by ultrashort laser pulses in ophthalmology, specifically for retina degenerative diseases.

References:

- [1] T. M. Allen and P. R. Cullis, *Adv. Drug Delivery Rev.* (2013): 65, 36;
- [2] S. Bibi et al., *J. Microencapsul* (2012): 29, 262;
- [3] I. V. Zhigaltsev, et al., *Langmuir* (2022): 38, 7858;
- [4] A. Uzel, et al., *Small* 19.52 (2023): 2305591.

NIR-II fluorescence functional imaging of immune cells in cancer immunotherapy

Xiaolong Liu¹

¹ Mengchao Hepatobiliary Hospital of Fujian Medical University, P.R. China.

xiaoloong.liu@gmail.com

ABSTRACT

[Body Text style] The biodistribution, viability, and functionality of immune cells play key roles in the cancer immunotherapy process. Thus, developing a method for characterizing immune cells *in vivo* is critical to understanding the effectiveness and the mechanisms of cancer immunotherapy, however, it remains challenging. The NIR-II fluorescence imaging, one of relatively safe and simple optical imaging modes, holds high-sensitivity and specific imaging ability in biological system due to minimal autofluorescence, low tissues light scattering, and enhanced penetration depth, and also can be used for multispectral and multiplexing imaging, which suitable for bioimaging the intrinsically complicated immune system. In recent years, we focused on the *in vivo* functional imaging of immune cells in cancer immunotherapy by NIR-II fluorescence imaging. We have developed a series of NIR-II fluorescence probes with different optical performances, which were used (1) to quantitatively track the natural killer (NK) cells viability in adoptive immunotherapy via ratiometric NIR-II fluorescence imaging mode, (2) to image the T cell migration and biodistribution in tumor microenvironment via aptamer modified NIR-II probe for imaging CD8 and PD1 expression of T cells, and (3) to evaluate the T cells activation via a novel granzyme B (immunoactivation-related biomarker) responsive NIR-II ratiometric fluorescence imaging probes. Our NIR-II fluorescence imaging probes provided a novel and safe noninvasive evaluation approach for cancer immunotherapeutic research in living animals.

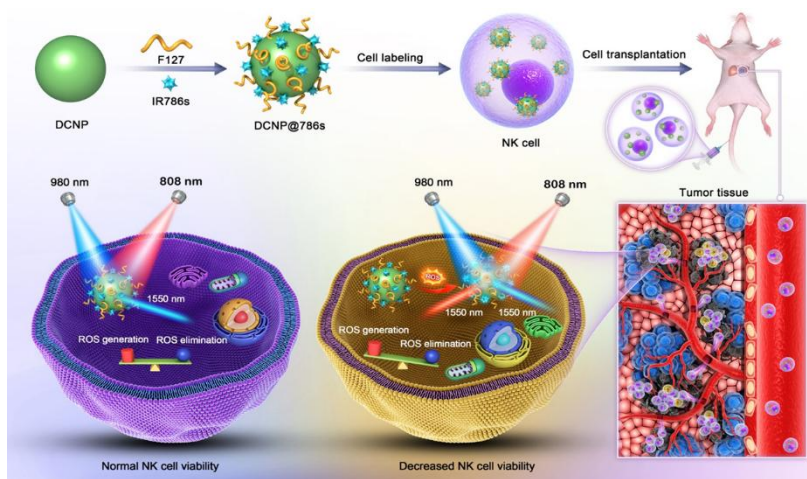


Figure 1. Schematic illustration of DCNP@786s with ratiometric NIR-II fluorescent signal for tracking NK cell viability *in vivo*.

REFERENCES

- [1] Liao N, Su L, Zheng Y, et al. In Vivo Tracking of Cell Viability for Adoptive Natural Killer Cell-Based Immunotherapy by Ratiometric NIR-II Fluorescence Imaging[J]. *Angewandte Chemie International Edition*, 2021, 60(38): 20888-20896.

Tissue optical clearing imaging: from in vitro to in vivo

[Main Title Style]: Times new Roman, Font size 14, Bold, centred

Dan ZHU

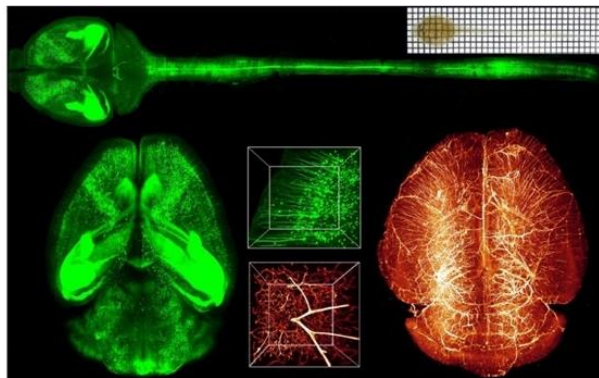
Britton Chance Center for Biomedical Photonics - MoE Key Laboratory for Biomedical Photonics, Advanced Biomedical Imaging Facility, Wuhan National Laboratory for Optoelectronics, Huazhong University of Science and Technology, China

dawnzh@mail.hust.edu.cn

ABSTRACT [HEADING 1 STYLE]

Biomedical optical Imaging techniques provide powerful tools for observing biomedical tissue structural and functional information. However, the high scattering of biological tissues limits the penetration of light, and decreases imaging resolution and contrast as light propagates deeper into the tissue. Fortunately, novel tissue optical clearing technique provide a way for solving the above problem. Tissue optical clearing technique combined with a variety of fluorescent labelling and microscopic optical imaging, is to reveal the working mechanism of organism, from the perspective of space for the life sciences, especially neuroscience discoveries open a door.

This presentation will introduce some progress in tissue optical clearing imaging. Based on the established *in vitro* tissue optical clearing methods, such as FDICSO and MACS we developed, the neurovascular distribution of various tissues and organs was obtained, which help us to identify cerebral ischemia-reperfusion vessels in mice, neural development of different skeletal muscles, changes in neurovascular structures of normal and pathological tissues and organs. *In vivo* cranial window allows us to observe cortex nerve, blood vessel and microglia. Combined with photodynamic effects, we realized the cortex blood vessels targeted to open the blood-brain barrier, targeted vascular embolization, evaluate the effect of different intervention. This has very important theoretical significance and broad application prospects for life science research.



(a)

(b)

Figures: tissue optical clearing imaging (a)neuro& vascular image of mice brain. (b)skull optical clearing window for cortical imaging

REFERENCES

- [1]. H. Xie et al, Nat. Biomed. Engin 10.1038/s41551-023-01155-6, 2023
- [2]. S. Liu et al, Commun. Biol. 6, 1239, 2023
- [3]. Y. Li et al, Theranostics 13(1), 403-416, 2023
- [4]. J. Xu et al, Commun. Biol 5, 1200, 2022
- [5]. D. Li, eLight 2, 15, 2022
- [6]. J. Zhu et al, Adv. Sci., 201903185, 2020
- [7]. Y. Qi et al, Sci. Adv 5(1), eaau8355, 2019
- [8]. Y. Zhao et al, Light Sci Appl 7, 17153, 2018
- [9]. Chao Zhang et al, Theranostics 8(10), 2696-2708, 2018

Terahertz Spectroscopy of Body Fluids for Cancer Diagnosis

Olga CHERKASOVA^{1,2}, Nazar NIKOLAEV^{1,3}

¹*Institute of Automation and Electrometry, Siberian Branch of the Russian Academy of Sciences, Russia*

²*National Research Centre "Kurchatov Institute", Moscow, Russia*

³*Institute of Laser Physics, Siberian Branch of the Russian Academy of Sciences, Russia*

o.p.cherkasova@gmail.com

ABSTRACT

Cancer is one of the major diseases that seriously affect human health and threaten human life. The World Health Organization and the health departments of governments in all countries have listed tackling cancer as a top priority. For most cancer patients, early detection can enable them to receive timely treatment and have a greater chance of a cure. Therefore, the early screening and diagnosis of tumors are of great significance. However, currently used various imaging techniques cannot recognize the disease in its early stages. At the same time, with the appearance and development of tumors, the molecular composition of body fluids (blood plasma or serum, saliva, urine, cerebrospinal fluid) changes significantly, which can be a good diagnostic criterion for early cancer diagnosis. Early cancer diagnosis can be achieved by analyzing body fluids using optical spectroscopy methods [1, 2]. Terahertz time-domain spectroscopy (THz-TDS) provides the possibility of measuring directly the medium refractive index and absorption coefficient, and hence the complex dielectric permittivity of the biological sample, in a single scan and in a broad frequency range of 0.1–3 THz [3]. THz radiation has great potential in biomedical detection, which could lead to the development of new methods of cancer diagnostics [4-6].

In this work, we propose approaches to increase the sensitivity of THz-TDS to cancer diagnosis: a) an integral assessment of the difference in the THz response of body fluids from the response of water. The full amplitude of the THz waveform was analyzed after normalization to the reference signal passing through the water [7]. It allows to reveal subtle differences between samples; b) analysis of lyophilized blood plasma for better separation of samples from patients and healthy individuals. Lyophilization was used to boost THz spectroscopy's informativity [8] because the water contribution to the THz blood plasma spectrum predominates over the other components; c) the use of machine learning techniques for the analysis of THz spectral data [8-11]. THz spectroscopy is sensitive to the presence of biomolecules in a sample. However, molecules' absorption bands overlapping in the THz spectral range make it difficult to discover specific metabolites in blood samples by conventional analysis. Machine learning techniques enable the resolution of these issues, the creation of predictive data models, and the discovery of useful frequencies; d) the use of THz metamaterials for the identification of cancer biomarkers [11, 12]. All these approaches pave the way for the application of THz-TDS for early cancer diagnosis.

The work was carried out within the framework of the State assignment project of the IA&E SB RAS # FWNG-2024-0025. The work of O.C. was partially supported within the state assignment of NRC "Kurchatov Institute".

REFERENCES

- [1] J.M. Cameron, et al, *Neurooncol. Adv.*, 4, vdac024, 2022.
- [2] D. Vrazhnov et al, *Pharmaceutics*, 15, 203, 2023.
- [3] O.A. Smolyanskaya et al, *Progress in Quantum Electronics*, 62, 1, 2018.
- [4] O. Cherkasova, et al., *Photonics*, 8(1), 22, 2021.
- [5] O. Cherkasova, et al, *J-BPE*, 9 (3), 030308, 2023.
- [6] K.I. Zaytsev et al, *Journal of Optics*, 22 (1), 013001, 2020.
- [7] M.M. Nazarov, et al., *Opt. Spectrosc.*, 126, 721-729, 2019.
- [8] M.R. Konnikova, et al., *Biomed. Opt. Express*, 12, 1020-1035, 2021.
- [9] O. Cherkasova, et al., *Appl. Sci.*, 13, 5434, 2023.
- [10] D. Vrazhnov, et al., *Appl.Sci.*, 12, 10533, 2022.
- [11] D. Vrazhnov et al, *Appl. Sci.*, 14, 2872, 2024.
- [12] S. Kuznetsov, et al., *Journal of Physics: Conference Series*, 2316 (12), 012016, 2022.
- [13] M.R. Konnikova et al., *Quantum Electron.*, 52 (1), 2, 2022.

Photonic 3D printing of human tissue models for disease research and treatment

Edik U. Rafailov & Sergei G. Sokolovski*

AiPT, The College of Engineering and Physical Sciences, Aston University, Birmingham, UK

In the realm of modern cell molecular biology and neuroscience, the quest for replicating the intricate architecture and functionality of human organs and neural networks has taken a pivotal turn with the advent of 3D bioprinting technologies. Traditionally, two-dimensional (2D) cell cultures have been the cornerstone of cellular and molecular research, offering critical insights into cellular responses under various conditions. However, the limitations of 2D cultures in mimicking the three-dimensional (3D) complexity of human tissues and organs have led to the development and adoption of 3D tissue models and bioprinting techniques. These advanced methodologies are revolutionizing the field by providing more realistic platforms for drug and cosmetics development, disease modelling, and the study of complex human attributes such as consciousness and the underlying mechanisms of neurological disorders^{3,4}.

3D bioprinting technology stands at the forefront of this innovation, allowing for the creation of artificial tissues using a mix of cell types, growth factors, and extracellular matrix components. This method involves the fabrication of microporous 3D scaffolds that replicate the extracellular matrix, thereby facilitating cell migration, proliferation, and tissue growth. This technique leverages various methods, including extrusion, laser-induced forward transfer, and two-photon polymerization, to create microporous scaffolds that mimic the extracellular matrix, thus providing an enhanced environment for cell migration, proliferation, and tissue growth. Specifically, in the context of neuroscience, the human-induced pluripotent stem cell (iPSC)-derived neuronal cultures and innervated tissue models is addressing the critical need for more relevant human cell models. By identifying suitable materials for the generation of scaffolds and employing two-photon polymerised materials, we aim to create functional multilayer tissue models. Human full-thickness skin equivalents (FSE), closely mirroring actual skin, play a significant role in fundamental research, drug testing, and clinical studies. FSEs are engineered using skin cells or TRET-immortalized keratinocytes and fibroblasts, aiming to replicate and graft 3D human organs. For detailed analysis, optical imaging and spectroscopy are indispensable, offering insights into the morphology and biochemical characteristics of 2D cell cultures and 3D tissues. Key to assessing metabolic activity, the fluorescence of nicotinamide adenine dinucleotide (NADH) and flavin adenine dinucleotide (FAD) serves as biomarkers. These markers, significant in cellular aging and maturation, are present in FSE keratinocytes and fibroblasts, with the redox ratio (RR) offering additional metabolic information. Our research introduces a biocompatible 3D scaffold paired with a novel dual-channel system combining optical coherence tomography (OCT) and fluorescence spectroscopy (FS) for comprehensive morphological and metabolic evaluation of engineered FSE, highlighting a groundbreaking approach in tissue engineering and cellular analysis.

Moreover, optical imaging techniques can provide essential insights into the morphological and biochemical aspects of these 3D human tissue models, highlighting the significant role of endogenous fluorophores as biomarkers for cellular metabolism and aging. Our research aims to combine 3D bioprinting and cell molecular biology advancements with developing a dual-channel system that marries morphological and metabolic assessments of 3D-engineered human tissues, ie. full-thickness skin equivalents, setting a new standard for biocompatible scaffold creation and evaluation.

Through this synthesis, we highlight the transformative impact of 3D bioprinting and scaffold-based tissue engineering in advancing our understanding of human tissue/organ biology in health and disease. These technologies offer unprecedented opportunities for creating more accurate models of human tissues and neural networks, thereby facilitating groundbreaking research in cellular biology, neuroscience, and medicine.

Reference

1. Duval K, Grover H, Han LH, et al. Modeling Physiological Events in 2D vs. 3D Cell Culture. *Physiology*. 2017;32(4):266-277. doi:10.1152/physiol.00036.2016
2. Kim J, Koo BK, Knoblich JA. Human organoids: model systems for human biology and medicine. *Nat Rev Mol Cell Biol*. 2020;21(10):571-584. doi:10.1038/s41580-020-0259-3

Advanced Fiber Spectroscopy for Life Science Applications

Viacheslav ARTYUSHENKO¹

¹art photonics GmbH, Germany

sa@slavart.de

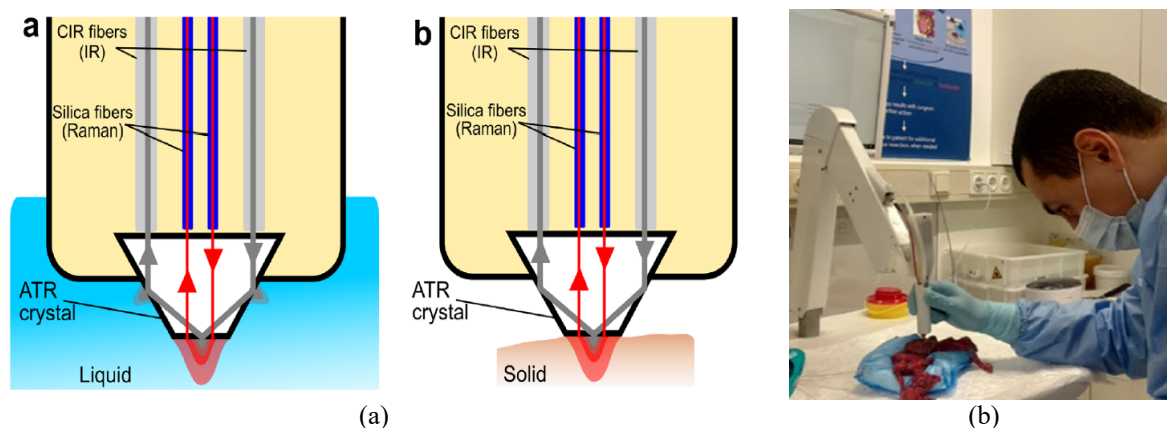
ABSTRACT

The latest innovative fiber solutions to be reviewed for biomedical applications in 0.3-18 μ m range, including multispectral diagnostics to define tumor margins, QCL-fiber coupled probes to detect osteoarthritis in 5-15 μ m range, design of IR-endoscopes for inter-corporal IR-imaging and unique fiber catheters for laser angioplasty – used to recanalize arteries blocked by plaques.

Composition of tissue and bioliquids can be analyzed by several spectroscopic methods: reflection and transmission, fluorescence, and Raman scattering. Spectroscopy enables real-time label-free chemical and structural evaluation of tissues and bioliquids for medical diagnostics *ex-vivo* in real time or *in-situ* and *in-vivo*. Fiber-optic probes provide flexible, sterilizable, and compact solutions for simultaneously analyzing tissue samples with several spectroscopic modalities. Review of various fiber probes for all these methods is secured by the set of various fiber types: drawn from Silica and IR-glasses, PIR-fibers extruded from AgCl:AgBr crystals and by hollow glass waveguides. The 1st results to be presented on new development of multispectral combi-fiber probes for biomedical applications [1]. Strong advantages of spectral data fusion from 2 complimentary spectroscopy methods will be demonstrated for differentiation of malignant and normal tissue using fiber probes.

The most advanced clinical applications will be presented about the development and validation of a high-wavenumber Raman spectroscopic technology used to oral cancer diagnostics *ex-vivo*, for a quick and objective intraoperative measurement of resection margins on fresh specimens. It employs a thin fiberoptic needle probe of 150 μ m diameter, which is inserted into the tissue, to measure the distance between a resection surface and the tumor [2].

Broad spectra applications for various fiber coupled spectrometers and sensors open many promising applications in spectral diagnostics of tissues, bioliquids, exhalation and in the future theranostics.



Figures: (a) Multimodal fiber optic probe for Mid-IR-absorption & Raman spectroscopy of liquid and solid samples.
b) Intraoperative assessment of resection margins for oral cancer by Raman spectroscopy from RiverD to guide oral cancer surgery

REFERENCES

- [1] Novikov, A., et al. Sci Rep **14**, 7430 (2024) <https://www.nature.com/articles/s41598-024-57539-4>
- [2] Yassine Aaboubout et al, Analyst, The Royal Society of Chemistry 2023, DOI: 10.1039/d3an00650f

Clinically translatable molecular photoacoustic imaging

Ananthakrishnan Jeevarathinam¹, Claire Jones¹, Mohammed Kawelah², Cayla Wood¹, Yunfei Wen³, Anil Sood³, Alexander Marras², Thomas Truskett², Keith Johnston², Richard Bouchard¹ and Konstantin Sokolov¹.

¹*Department of Imaging Physics, The UT M.D. Anderson Cancer Center, U.S.A.*

²*McKetta Department of Chemical Engineering, The University of Texas at Austin, U.S.A.*

³*Department of Gynecologic Oncology and Reproductive Medicine, The UT M.D. Anderson Cancer Center, U.S.A.*

ksokolov@mdanderson.org

ABSTRACT

Here we will present development of molecular photoacoustic imaging (PAI) with clinically translatable contrast agents that are based on FDA approved indocyanine green (ICG) dye. Specifically, the agents are based on ICG J-aggregates that are stabilized by encapsulation in either liposomes [1] or polymersomes [2] resulting in *ca.* 100 nm particles. The molecular specificity is rendered by directional conjugation of monoclonal antibodies. We showed that molecular PAI with encapsulated ICG J- aggregates (en-ICGJ) significantly improves the feasibility of combined quantitative functional and molecular PAI. Further, we demonstrated the detection limit of *ca.* 100 total ovarian and breast cancer cells labeled with en-ICGJ in tissue mimicking phantoms. Our cell culture and in vivo studies in orthotopic murine models of ovarian cancer showed a good correlation between an expression profile of folate receptor alpha (FR α) – a biomarker of ovarian cancer – and molecular PAI with FR α -targeted an-ICGJ. These studies provide foundation for further development of molecular PAI with en-ICGJ for applications in image-guided personalized therapy of ovarian and breast cancer patients.

REFERENCES

- [1] C. Wood et al, Nature Comm 12, 5410, 2021.
- [2] M. Kawelah et al, ACS Appl Mat Interfaces, 2024.

Non-invasive *in vivo* imaging of the multi-colored tattoo inks in the skin using two-photon excited fluorescence lifetime imaging

Maxim DARVIN¹, David LOPEZ², Victor NIKOLAEV², Yury KISTENEV² and Marius KRÖGER¹

¹Independent Researcher, Germany

²Laser Molecular Imaging and Machine Learning, Tomsk State University, Russia

maxim.darvin@protonmail.com

ABSTRACT

The trend of multicolored tattoos has increased in the young population in recent decades, however, the location and kinetics of tattoo ink, its impact on the skin after application and during recovery are not well understood, partly due to a lack of *in vivo* imaging methods [1]. For the first time, we visualize the deposition of tattoo ink of different colors (black, blue, green, yellow and red) in human skin with old tattoos (applied more than one year ago) *in vivo* and non-invasively to a depth of ≈ 150 μm using two-photon excited fluorescence (TPE-AF) and fluorescence lifetime imaging (TPE-FLIM) technique. We excited the skin fluorophores with the tunable titanium sapphire laser at 760 nm, generating 100 fs pulses at 80 MHz with a power lower than 50 mW, which is superior to single-photon excitation microscopy in terms of spatial resolution and imaging depth [2]. The dermal matrix was additionally visualized by a second harmonic generation (SHG) signal originating from collagen-I in the dermis. The distinct TPE-AF and TPE-FLIM parameters and morphological features were sufficient to classify dermal mast cells [2], dermal macrophages [3] and different compartments in native skin [4].

In tattooed skin, tattoo ink agglomerates have been observed in different skin layers from the stratum corneum to the reticular dermis [4]. In the fully recovered old tattoos, cellular intake of ink nanoparticle agglomerates has been clearly visible in the dermis: papillary dermis (Fig. 1a, yellow-orange-marked areas), suspected resting and activated mast cells (Fig. 1b, blue-yellow-marked areas), suspected macrophage (Fig. 1c) and suspected fibroblast (Fig. 1d) absorb/phagocytose ink aggregates and serve as a long-term reservoir that retains tattoo ink for the lifespan of the cell. The extracellular matrix has been shown to be free of tattoo inks after the initial skin regeneration of 3 weeks. Tattoo ink residues have been observed in the keratinocytes, dendritic cells, and basal cells of the constantly renewed epidermis even in old tattoos, indicating the continuous release of a very small amount of tattoo ink throughout the basal layer of old tattoo. Tattoo inks have also been observed in the stratum corneum, but we could not determine whether they are stored in the corneocytes or in the intercellular lipid matrix.

Thus, loading with tattoo particles, with the distinct TPE-AF and TPE-FLIM parameters (mainly characterized by the short TPE-FLIM and the high TPE-AF intensity), enables the *in vivo* visualization of dendritic cells in the epidermis and fibroblasts in the dermis, which are not fluoresce and cannot be visualized under native conditions without staining [4,5]. The TPE-FLIM technique could be useful in clinical dermatological and cosmetic practice to manage patients with tattoo-related complications and to provide important information about the cellular penetration pathways and accumulation time of exogenous substances in the different skin layers and to understand their effects on the skin compartments.

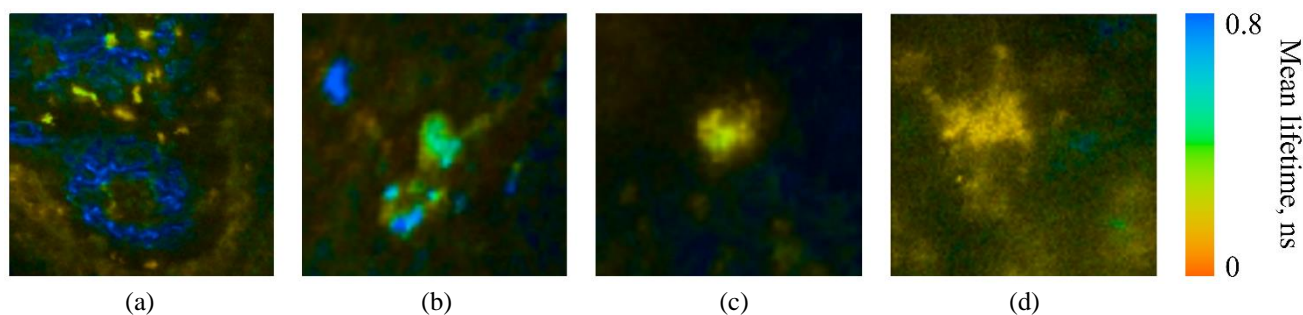


Figure 1: *In vivo* TPE-FLIM images (colour gradient of mean lifetime from red – 0 ns to blue – 0.8 ns) of the dermis of tattooed human skin at a depth of 70–80 μm . (a) Papillary dermis, green ink, image size 70 μm (b) Suspected resting and activated mast cells, green ink, image size 34 μm (c) Suspected macrophage, red ink, image size 28 μm (d) Suspected fibroblast, green ink, image size 42 μm .

REFERENCES

- [1] W. Bäuml, *Curr. Probl. Dermatol.* 48, 176–184, 2015.
- [2] M. Kröger et al, *Sci. Reports* 10, 14930, 2020.
- [3] M. Kröger et al, *eLife* 11, e72819, 2022.
- [4] M. Kröger et al, *Dermatology* 239, 478–493, 2023.
- [5] V. Nikolaev, *J. Biophotonics* 17, e202300223, 2024.

Imaging, spectroscopy and therapy enhanced by tissue optical clearing

Valery TUCHIN

*Institute of Physics and Science Medical Center, Saratov State University, Russia
Institute of Precision Mechanics and Control, FRS "Saratov Scientific Centre of the RAS", Russia
Laboratory of Laser Molecular Imaging and Machine Learning, Tomsk State University, Russia*

tuchinvv@mail.ru

ABSTRACT

The method of immersion optical tissue clearing (TOC) is an effective means for improving the quality of optical images of tissues and organs, and holds great promise for depth spectroscopy and effective photodynamic and photothermal therapies [1-6]. Biocompatible TOC technologies continue to be successfully developed and applied in increasingly new and relevant areas of biomedical science and practice. The presented work summarizes the latest achievements in the development of the TOC method for solving problems of optical imaging, spectroscopy and therapy. The method is based on the creation of new virtual and expansion of known transparency windows of various tissues in a wide range of wavelengths from deep UV to THz waves. In addition to increasing optical transparency, the study of the kinetic properties of the response of tissue transparency to the action of probe molecules of optical clearing agents (OCAs) allows reliable differentiation of healthy and pathological tissues in addition to data on absorption or refractive contrast. The principles and achievements of TOC based on the temporary and reversible suppression of light scattering in tissues using biocompatible OCAs, their delivery to living tissue to ensure its temporary transparency in a wide spectral range with the possibility of obtaining spectroscopic information and images from greater depth and better contrast in optics will be discussed, as well as the compatibility of the technology with traditional spectroscopy and imaging methods such as ultrasound, CT and MRI.

New areas of biomedical applications of this technology will be demonstrated for optical imaging, drug delivery monitoring, effective antitumor and antimicrobial phototherapy, optical communications and charging of smart implants in the human body.

This work was supported by grant of the Russian Science Foundation # 23-14-00287.

REFERENCES

- [1] L. Oliveira, V.V. Tuchin, *The Optical Clearing Method: A New Tool for Clinical Practice and Biomedical Engineering*, Springer Nature Switzerland AG, Basel, 2019.
- [2] V.V. Tuchin, D. Zhu, and E. A. Genina (Eds.), *Handbook of Tissue Optical Clearing: New Prospects in Optical Imaging*, Taylor & Francis Group LLC, CRC Press, Boca Raton, FL, 2022.
- [3] A.B. Bucharskaya et al., *Biophysical Reviews* 14, 1005–1022 (2022).
- [4] V.V. Tuchin et al., *Advanced Drug Delivery Reviews* 180, 114037 (2022).
- [5] I.S. Martins et al., *Biomedical Optics Express* 14, 249–298 (2023).
- [6] A.S. Shanshool et al., *Progress in Quantum Electronics* 94, 100506 (2024).

Advanced Image-Based Techniques in Miniaturized Devices for Biosensing Applications

H. Cumhuri TEKIN^{1,2}

¹*Department of Bioengineering, Izmir Institute of Technology, Turkey*

²*METU MEMS Center, Turkey*

cumhurtekin@iyte.edu.tr

ABSTRACT

Sensitive detection of biomarkers is crucial for accurate diagnosis and prognosis. Image-based detection methods offer robust, low-cost, and simplified biomarker analysis, making them suitable for integration into miniaturized intelligent devices for automated and accessible diagnostics. Here, we discuss various image-based approaches for detecting a range of biomarkers. First, we present a novel electromechanical platform for detecting serum creatinine levels to evaluate kidney function. Utilizing a simple smartphone camera, measurements in the hue, saturation, and value (HSV) color space on this platform demonstrated sensitive and cost-effective point-of-care analysis [1]. Additionally, we developed a portable Jaffe-based serum creatinine detection platform with an onboard heating and illumination system, providing sensitive and robust analysis. HSV analysis enhanced the performance of creatinine detection, surpassing that of bulky and expensive spectrometric methods. Furthermore, we applied HSV analysis in a point-of-care electromechanical device for detecting SARS-CoV-2 viral RNA using reverse-transcription loop-mediated isothermal amplification [2]. This compact, portable, and low-cost device did not require perfectly focused sample images for analysis and could automatically halt operations upon obtaining positive test results. Magnetic levitation (MagLev) technology was employed to measure the density and magnetic properties of micro and nanoparticles, as well as cells, in a microcapillary channel by monitoring their levitation heights [3]. We demonstrated a magnetic susceptibility-based protein detection method by observing the levitation heights of diamagnetic microparticles that acted as mobile microsensors to capture and detect proteins labeled with magnetic nanoparticles [4]. This platform was integrated with a lensless holographic microscopy setup for standalone and automated analysis of the levitation heights of microparticles and cells [5]. Moreover, we developed a deep learning-based detection scheme for automated analysis of microparticles and cells for MagLev-based cytometry applications and applied this method for label-free identification of cancer cells [6]. These image-based approaches have significant potential for further application in the sensitive, easy-to-use, and point-of-care detection of various biomarkers.

ACKNOWLEDGEMENT

This study was supported by the Scientific and Technological Research Council of Turkey (TUBITAK) under Grant Number 22AG032 and 217S518. The authors thank TUBITAK for their support.

REFERENCES

- [1] B. Karakuzu et al, ACS Omega 7, 25837–25843, 2022.
- [2] E.A. Tarim et al, Talanta 254, 124190, 2023.
- [3] N.D. Durmus et al, PNAS 112, E3667-E3668, 2015.
- [4] S. Yaman et al, Anal. Chem. 93, 12556-12563, 2020.
- [5] K. Delikoyun et al, ACS Sensors 6, 2191-2201, 2021.
- [6] K. Delikoyun et al, Proc SPIE 11655, 1165509, 2021.

Where does photonics meet acoustics and nanostructured materials for biomedical applications?

Dmitry GORIN

Skolkovo Institute of Science and Technology, Moscow, Russia

d.gorin@skoltech.ru

ABSTRACT

This talk will review the combination of photonic and acoustic tools and nano- and microstructured materials that can be used for visualization of pathological tissue and organs, navigation of drug delivery carriers and remote-controlled release of encapsulated bioactive substances, and last but not least, the application of optical sensors for early diagnosis and evaluation treatment efficiency. There are many biological objects that can be used as markers of various pathological states including cancer. These comprise, but are not limited to, proteins, exosomes, and circulation tumor cells. Exosomes are a very promising marker for early cancer diagnosis and even for evaluating treatment efficiency. An exosome is a small vesicle at 100 nm size produced by a cell. The exosomes can be sent by both normal and pathological cells. It can be used for early diagnosis of neuro, cardio, and onco-diseases. The combination of a photonic integrated circuits (PIC), a microfluidic devices (MF) and a surface modification improves not only the sensitivity but also the specificity of exosome's detection [1].

The application of photonic and acoustic tools can be used for visualization, navigation of multifunctional carriers and remote-controlled release of bioactive substances. These particles will combine the ability to deploy drugs in a controllable manner with physical triggering, multimodal detection, and visualization as well as sensing of important biological markers. It is required to apply a new bottom-up method as layer by layer assembly [2] and freezing induced loading [3] and their combination [4]. It can be allowed us to vary the volume fraction of components and their chemical composition led to the control of the optical and thermal properties of multifunctional carriers [5]. Raman spectroscopy is perspective method for in situ monitoring of freezing induced loading method [6]. Physical targeting of carriers was realized by the magnetic field gradient [4], optical tweezers approach [7]. Acoustics has a good perspective for the same purpose. The carrier sensitivity to external influences such as laser irradiation, ultrasound (US) treatment can be changed by variation of volume fraction and chemical composition of inorganic nanoparticles and/or organic dyes in the carrier shells. The same approach is applied for drug delivery carriers imaging by MRI, fluorescence imaging (FI), USI and optoacoustics (OA) [4,8]. Additionally, there are some trends of modern biophotonics: 1) combination of OA, US and FI[9]; 2) transfer to mid-IR [10]; 3) preparation of multimodal contrast agents, that can be provided the contrast by some clinical methods including OA, FI, MRI, USI etc. [8]; 4) using minimally invasive OA [11,12] by developing PIC based US transducers [13] using biomimetic approach for preparation a sensitive part (membrane) of such type of sensors [14,15]; 5) using optical clearing approach [16]; 6) realization of theranostic approach by the submicron polymer shells containing dyes and nanozymes [17]. In talk will be presented also the results of *in vivo* optoacoustic applications and besides both optoacoustic mesoscopy and tomography. Particular attention will be devoted to the implementation of near and mid-IR for OA microscopy and endoscopy and the prospects for its application for *in vitro* and *in vivo* studies.

Thus, the combination of photonic and acoustic tools with nanostructured materials has a good perspective for biomedical applications.

This work was supported by Russian Science Foundation (RSF) grant № 22-14-00209.

REFERENCES

- [1] A. Kuzin et al, Applied Physics Letters, 2023, 123, 193702.
- [2] M.V. Novoselova et al, J. Biophotonics, 12 (4), 2019, e201800265
- [3] S.V. German et al, Scientific Reports, 8, 2018, 17763
- [4] M.V. Novoselova et al, Colloids and Surfaces B, 2021, 111576
- [5] R. E. Noskov et al, Adv. Mater. 2021, 2008484
- [6] S.V. German et al, Langmuir, 2021, 37,4, 1365
- [7] E.S. Vavaev et al, ACS Applied Nano Materials, 2022 5 (2), 2994
- [8] E.A. Maksimova et al, Laser & Photonics Reviews, 2023, 2300137
- [9] M.D. Mokrousov et al, Biomedical Optics Express, 12(6), 2021, 3181
- [10] M.A. Pleitez et al, Nat. Biotechnol., 38(3), 2020, 293
- [11] H. Guo et al, J. Biophotonics, 13(12), 2020, 1–20
- [12] N. Kaydanov et al, ACS Photonics, 8, 11, 2021, 3346
- [13] W. J. Westerveld et al, Nature Photonics, 15, 202, 341
- [14] J. Cvjetinovic et al. Scientific Reports, 13, 2023, 5518
- [15] J. Cvjetinovic et al, Applied Physics Letters, 2023, 123 (18), 184101
- [16] M.V. Novoselova et al, Photoacoustics, 2020, 100186
- [17] I.S. Sergeev I. S. et al, Particle & Particle Systems Characterization, 2024, 2300149.

Novel Photo-Activated Treatments in Ophthalmology

Susana MARCOS^{1,2}, Rocío GUTIERREZ¹, Mar FERNANDEZ¹, Carmen MARTINEZ³, Patricia GALLEGO³, Lupe VILLEGAS¹, Andres DE LA HOZ¹, Fernando ZVIETCOVICH¹, James GERMANN^{1,2}, Rushnan ISLAM², Wayne KNOX² and Irene KOCHEVAR⁴

¹*Instituto de Optica, CSIC, Spain*

²*The Institute of Optics & Center for Visual Science, University of Rochester, USA*

³*Cellular Biology, Genetics, Histology and Pharmacology Department, Universidad de Valladolid, Spain*

⁴*Wellman Center of Photomedicine, Harvard Medical School, USA*

smarcos2@ur.rochester.edu

ABSTRACT

Since the advent of laser refractive surgery and photodynamic therapy, light-ocular tissue interaction underlies multiple successful treatments in the eye. Optical techniques to assess the outcomes of these treatments have become mainstream diagnostic tools in ophthalmology and/or in the laboratory. We present emerging photo-activated treatments that modulate the mechanical and structural properties of cornea and sclera (photo-crosslinking, CXL, and laser-induced refractive index change, LIRIC) and facilitate wound healing or functional implants (photo-bonding, PB). We evaluated the success of these treatments in rabbits *ex vivo* & *in vivo*, using custom-developed imaging technologies (3D quantitative OCT, air-puff OCT corneal deformation imaging, ultrasound excitation optical coherence elastography OCE, second harmonic generation microscopy SHG, histology and immunohistochemistry).

Photo-crosslinking is aimed at creating covalent bonds intra and inter collagen fibers to stiffen corneal tissue in keratoconus and the sclera in myopia. We explored two different modalities of photo-crosslinking (Rose Bengal (RB)/green light, RGX, and Riboflavin/ultraviolet light, UVX, with different dosages and photo-activator formulations). We found consistent increase of tissue stiffness (reconstructed from extensimetry, air puff OCT and OCE), with significant differences across CXL techniques. In the sclera, the efficacy depended on the treatment location. The lower RGX penetration minimized cell-death, while producing similarly effective stiffness. Changes were also observed in the organization of the collagen fibers as imaged by SHG.

Photo-bonding, first proposed to replace sutures, has also proved effective in securing polymer-based implants. PB is key in the operation of our shape-changing accommodating IOL, to engage the IOL haptics to the capsular bag periphery and capture the equatorial ciliary muscle forces. We demonstrated intraocular bonding of the IOL with the capsular bag using RB and green light (RGB).

We have recently developed a family of ocular implants exploiting the properties of silk fibroin (SF). SF is transparent, fully biocompatible, tunable, and a well-suited platform for smart, flexible photonics. SF-based corneal bandages mimic the properties of the standard-of-care (donor-dependent) amnion membranes for corneal wound healing and (RGB) to corneas *ex vivo* and *in vivo*. Using other SF-based biomaterial formulations, we have developed corneal inlays which have shown long-residency time and high biocompatibility when implanted in rabbit corneas (>2 months after implantation). Furthermore, LIRIC treatments on this material has shown high linearity and reproducibility of index change, opening the possibility of non-tissue subtraction post-surgery refraction tuning.

REFERENCES

- [1] N. Bekesi et al *Invest Ophthalmol Vis Sci.* 58, 1612-1620, 2017.
- [2] E. Lorenzo-Martín et al. *Invest Ophthalmol Vis Sci.* 59, 4821-4830, 2018.
- [3] J.A. Germann et al. *Invest Ophthalmol Vis Sci.* 61, 28, 2020.
- [4] A. Curatolo et al *Biomed Opt Express* 11, 6337-6355, 2020.
- [5] D. Bronte-Ciriza et al. *Biomed Opt Express* 12, 6341-6359, 2021.
- [6] N. Alejandre-Alba et al. *Transl Vis Sci Technol* 7, 27, 2018.
- [7] S. Marcos et al. *Invest. Ophthalmol. Vis. Sci* 64, 1693, 2023.
- [8] R. Gutierrez-Contreras et al. *Invest. Ophthalmol. Vis. Sci.* 64, 3126, 2023.

Surgery guidance with optical spectroscopy: from bench to bedside

Evgeny SHIRSHIN^{1,2}

¹*Physical Department, M.V. Lomonosov Moscow State University, Russia*

²*Endocrinology research center, Russia*

eshirshin@gmail.com

ABSTRACT

Despite low light penetration depth, photonic technologies have found certain applications in the field of biomedical diagnostics. One of the most successful examples is the optical spectroscopy-based surgery guidance, when using the optical response through the endoscope or directly from the tissue surface allows discriminating between different areas. In this research area, the holy grail is to detect the tumor margin, making it possible for a surgeon to cut all the cancer cells and reduce the possibility of cancer recurrence. However, other problems also exist such as laser energy automation during lithotripsy, parathyroid detection during thyroidectomy, assessment of cartilage or ligament mechanical properties and so on. A battery of optical methods can be potentially applied to perform molecular and/or morphological analysis, including diffuse reflectance spectroscopy, fluorescence spectroscopy (and also FLIM, fluorescence lifetime imaging), NIR region and Raman spectroscopy. Those methods are widely applied for surgery guidance-related tasks, mostly ex vivo, however, the progress clinical translation is also evident during the past decade. In this talk, we will discuss the results of our group in the development, clinical probation and translation of a few optical methods for surgery guidance with a focus on the development of medical devices for clinicians.

Breaking the Speed Barrier: High-Speed Light-Field Microscopy for KiloHertz to Terahertz 3D Imaging

Liang Gao¹

¹*Department of Bioengineering, UCLA, USA*

gaol@ucla.edu

ABSTRACT

Light-field microscopy offers unprecedented capabilities for 3D visualization of biological samples down to the sub-cellular level. Despite its strengths, the technique has historically faced limitations in imaging speed due to the acquisition of large-format light field data. This bottleneck has restricted its use in high-speed bioimaging applications like voltage imaging or fluorescence lifetime imaging microscopy (FLIM). In this presentation, I will discuss our innovative approaches [1, 2] to overcoming this challenge by leveraging advancements in computational optics and detector technology, enabling a volumetric frame rate from kilohertz to terahertz.

REFERENCES

- [1] Wang Z, Zhao R, Wagenaar DA, Kang W, Lee C, Schmidt W, Pammar A, Zhu E, Wong GCL, Liang R, Hsiai T, Gao L. KiloHertz volumetric imaging of in-vivo dynamics using squeezed light field microscopy. bioRxiv [Preprint]. 2024 Mar 27:2024.03.23.586416. doi: 10.1101/2024.03.23.586416. PMID: 38585760; PMCID: PMC10996549.
- [2] Ma Y, Huang L, Sen C, Burri S, Bruschini C, Yang X, Cameron RB, Fishbein GA, Gomperts BN, Ozcan A, Charbon E, Gao L. Light-field tomographic fluorescence lifetime imaging microscopy. Res Sq [Preprint]. 2023 May 10:rs.3.rs-2883279. doi: 10.21203/rs.3.rs-2883279/v1. PMID: 37214842; PMCID: PMC10197779.

Engineering Biomedical Sensing Technologies to Advance Human Health

Hatice CEYLAN KOYDEMIR¹

¹Department of Biomedical Engineering, Texas A&M University, United States of America

²Center for Remote Health Technologies and Systems, Texas A&M Engineering Experiment Station, United States of America

hckoydemir@tamu.edu

ABSTRACT

Advancements in semiconductor fabrication technology have enabled new communication tools with better cameras, connectivity, and data processing tools. These technologies advance lifestyle and result in the development of novel diagnostic technologies that provide high sensitivity and specificity to facilitate diagnostics at the point of care. In this talk, I will present how we converted a regular smartphone to a flow meter without using an external lens and a specific brand of smartphone [1, 2]. The design utilizes a 3D printed box (Fig. 1), of which the inside is illuminated using two LEDs to provide uniform illumination and prevent external light disturbances. The box has a smartphone holder tilted with 30 degrees. It costs less than 10\$. The microfluidic cartridges are made by laminating a PET layer, an adhesive tape, and a microscope slide. The channel structure was patterned using a laser cutting machine on the adhesive tape.

After loading the microfluidic cartridge on the sample holder, the video of the sample flow is captured using the regular smartphone application. The sample is introduced to the sample loading zone on the microfluidic cartridge. The video is processed digitally using custom-developed image processing algorithms to track the flow in the channel with time. We tested the device's performance using solutions with different glycerol concentrations in water and demonstrated that it can detect the flow changes in nanolitres per second. We demonstrated its use for point-of-care diagnostics use by screening blood coagulation. We mixed the human blood with a coagulation reagent and introduced it into the channel. As the blood mixes with the reagent in the channel, it changes its form from liquid to gel and stops the flow. This stopping time was correlated with the coagulation levels. The device demonstrated about 90% accuracy compared to the standard clinical laboratory test results when 47 different human clinical samples were used. The approach used in determining flow in the microfluidic cartridges can be used for many other biomedical and analytical measurements. The engineered device can be a helpful and cost-effective analytical tool for non-invasive contactless flow measurement in microfluidic designs.

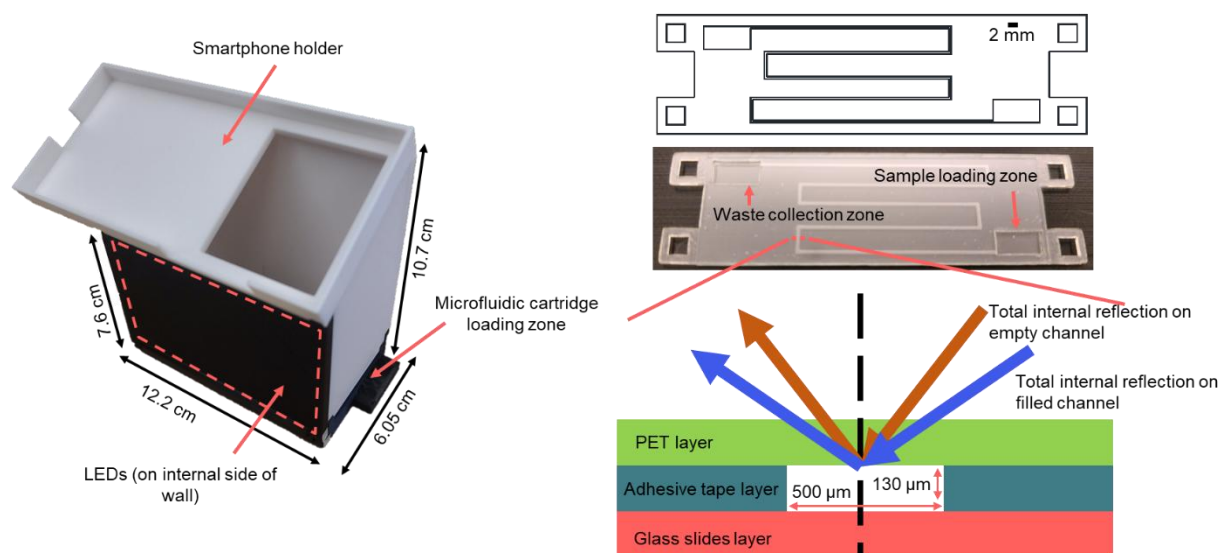


Figure 1: (Left) 3D printed holder for microfluidic flow analysis (Top Right) Photo of the laminated microfluidic channel (Bottom Right) Schematic illustrating the principle behind the flow meter in nanolitre precision.

REFERENCES

- [1] W. Xu, M. Althumayri, A. Mohammad, H. Ceylan Koydemir, Foldable low-cost point-of-care device for testing blood coagulation using smartphones, *Biosensors & Bioelectronics*, 2023, <https://doi.org/10.1016/j.bios.2023.115755>.
- [2] W. Xu, A. Y. Atik, L. Beker, H. Ceylan Koydemir, Digital monitoring of the microchannel filling flow dynamics using a non-contactless smartphone-based nano-liter precision flow velocity meter, *Biosensors & Bioelectronics*, 2024, <https://doi.org/10.1016/j.bios.2024.116130>.

Multi-modal, label-free, optical imaging of metabolic function: From mitochondria to humans

Irene GEORGAKOUDI^{1,2}, Yuhang FU^{1,2}, Einstein GNANATHEEPAM¹, Matthew LINDLEY², Nima NAJAFI GHALEHLOU^{1,2}, Christopher POLLEYS¹, Maria SAVVIDOU¹, Yang ZHANG¹, Mihaela BALU³, Afshin BEHESHTI⁴, Anand GANESAN³, Jessica SHIU³, Hong-Thao THIEU⁵, Elizabeth GENEGA⁵, David KAPLAN¹, Pramesh SINGH⁶ and Abani PATRA⁶

¹Thayer School of Engineering, Dartmouth College, U.S.A

²Biomedical Engineering Department, Tufts University, U.S.A

³Biomedical Engineering Department, University of California at Irvine, U.S.A

⁴Blue Marble Space Institute of Science, U.S.A

⁵School of Medicine, Tufts Medical Center, U.S.A

⁶Data Intensive Studies Center, Tufts University, U.S.A

Irene.georgakoudi@dartmouth.edu

ABSTRACT

Label-free, two-photon imaging provides a unique platform for assessing metabolic and mitochondrial function and/or dysfunction in living tissues. The high spatiotemporal resolution and non-destructive nature of these measurements are key enabling features for such functional assessments within specimens varying in scale from isolated mitochondria to living humans. The main source of contrast for such imaging is autofluorescence intensity and lifetime of NAD(P)H and flavoproteins (FP), two co-enzymes that play a critical role in several key metabolic pathways utilized to maintain health, growth, and reproduction of cells, tissues, and organisms. The high resolution of two-photon images enables assessments of the spatiotemporal heterogeneity of metabolic and mitochondrial dysfunction, which is recognized increasingly as a significant driver of events that determine the development and/or treatment response of numerous diseases. For example, we have shown that the NAD(P)H image intensity variations can be analyzed using automated, fast, Fourier-based approaches to extract quantitative information regarding the mitochondrial organization as a function of epithelial tissue depth. Associated metrics can be used to identify distinct mitochondrial and metabolic function states in cervical precancerous lesions and in vitiligo lesions. The optical redox ratio, extracted from the ratio of FP/(NAD(P)H+FP) images provides additional information regarding tissue redox status. Finally, lifetime measurements can yield important insights regarding the local environment of NAD(P)H. In combination, these metrics yield exquisite sensitivity and potential specificity to changes in a wide range of metabolic pathway changes, including oxidative phosphorylation, glycolysis, glutaminolysis, fatty acid synthesis and oxidation (1). Recent findings to highlight such measurements in the context of cancer, vitiligo, and neurodegeneration will be presented utilizing engineered brain tissues, freshly excised human tissues, and living patients, building on our extensive studies in this area (2-7). We will also demonstrate the complementary nature of optical and transcriptomic readouts of metabolic function, highlighting the potential of optical metabolic imaging to provide important functional insights. In addition, we will identify challenges in autofluorescence-based assessments of metabolism and some potential approaches to overcome them. Specifically, we will discuss how information from spectral images can be leveraged to identify potential contributions from other fluorophores, such as lipofuscin, along with methods to quantify their content and to perform robust metabolic measurements in their presence. In summary, we expect our presentation to provide an overview of the range of studies that can be performed using two-photon, label-free imaging and the unique capabilities and challenges of such measurements to assess metabolic and mitochondrial function in living specimens.

REFERENCES

1. Liu Z, Pouli D, Alonzo CA, Varone A, Karaliota S, Quinn KP, et al. Mapping metabolic changes by noninvasive, multiparametric, high-resolution imaging using endogenous contrast. *Sci Adv.* 2018;4(3):eaap9302.
2. Polleys CM, Singh P, Thieu H-T, Genega EM, Jahanseir N, Zuckerman AL, et al. Rapid, high-resolution, non-destructive assessments of metabolic and morphological homogeneity uniquely identify high-grade cervical precancerous lesions. *BiorXiv.* 2024.
3. Liaudanskaya V, Fiore NJ, Zhang Y, Milton Y, Kelly MF, Coe M, et al. Mitochondria dysregulation contributes to secondary neurodegeneration progression post-contusion injury in human 3D in vitro triculture brain tissue model. *Cell Death Dis.* 2023;14(8):496.
4. Georgakoudi I, Quinn KP. Label-Free Optical Metabolic Imaging in Cells and Tissues. *Annu Rev Biomed Eng.* 2023.
5. Yerevanian A, Murphy LM, Emans S, Zhou Y, Ahsan FM, Baker D, et al. Riboflavin depletion promotes longevity and metabolic hormesis in *Caenorhabditis elegans*. *Aging Cell.* 2022;21(11):e13718.
6. Pouli D, Thieu HT, Genega EM, Baecher-Lind L, House M, Bond B, et al. Label-free, High-Resolution Optical Metabolic Imaging of Human Cervical Precancers Reveals Potential for Intraepithelial Neoplasia Diagnosis. *Cell Rep Med.* 2020;1(2).
7. Shiu J, Lentsch G, Polleys CM, Mobasher P, Ericson M, Georgakoudi I, et al. Noninvasive Imaging Techniques for Monitoring Cellular Response to Treatment in Stable Vitiligo. *J Invest Dermatol.* 2024;144(4):912-5 e2.

Portable fNIRS for measuring brain activity anytime, anywhere

Audrey BOWDEN^{1,2}, Seth CRAWFORD¹, Daniel LIU¹ and Tiffany-Chau LE¹

¹Biomedical Engineering, Vanderbilt University, USA

²Electrical and Computer Engineering, Vanderbilt University, USA

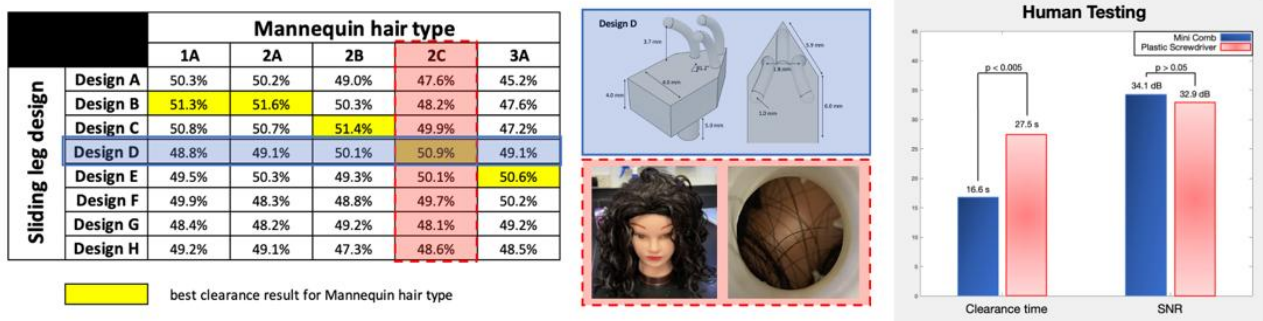
a.bowden@vanderbilt.edu

ABSTRACT

Every year, 51.4 million patients risk developing postoperative delirium (POD) following surgery, imposing an annual \$33-152 billion dollar cost to the U.S. healthcare system [1]. POD is a poorly understood condition defined by an acute change in cognitive ability and increased risk of developing neurological disorders. The risk of POD increases with age, with 72% of patients aged 70-79 and 92% of patients aged 80-89 being identified with POD following a surgical procedure [2]. Past studies have strongly correlated hyperoxic cerebral reperfusion and reduced functional connectivity of cortical regions during surgery to onset of delirium [3]. Thus, perioperative monitoring of blood oxygen levels across the whole cortex could shed light on the risk-factors of POD, reducing the overall burden and improving patient outcomes. However, many conventional neuroimaging techniques including MRI/fMRI and PET scans are bulky, expensive, and require the immobilization of the patient for long periods of time. This leads to many logistical challenges in the operating room (OR) and causes patient discomfort and significant noise artifacts in measurements. To combat this issue, we are developing a portable, wireless, whole-cortex functional near-infrared spectroscopy (fNIRS) system capable of performing real-time neuromonitoring in perioperative settings.

The system electronics comprise multiple LEDs at wavelengths of 740nm and 850 nm that emit light in a continuous-wave fashion. The signal is detected using silicon photodiode detectors. To validate the electronics of the device, measurements and tests were performed to confirm that the wavelength spectra and pulse times meet the expected specifications. The photodiodes were ensured to operate within their linear working range under realistic light levels, guaranteeing accurate signal detection. Using a pressure-standardized tissue-mimicking phantom apparatus, a platform was developed to analyze the system's reliability by enabling cross-validation and consistent performance of the electronics. In addition, preliminary breath-holding data was collected on a 33-channel prototype of the system to show that a well-characterized cerebral hemodynamic plot could be reproduced. These results collectively confirmed the successful validation of the device concept. Further work will be done to improve the system's data rate which is currently at ~7Hz and enable BLE connections to multiple controller boards simultaneously in order to achieve whole-cortex coverage.

To ensure the device is compatible with patients of all demographics, we specifically undertook steps to facilitate clearance of different hair types. To this end, we developed a versatile attachment for fNIRS systems that we call the "Mini Comb," which is able to reduce the hair-clearance time and whose design can be optimized to work on different hair types. Initial tests of the Mini Comb used on commercial fNIRS systems show that it can reduce hair clearance time by nearly 50% while achieving similar SNR to existing hair clearance tools such as plastic screwdrivers. Further, to better understand how changes in body posture may affect the collected fNIRS signal during the perioperative workflow, we are testing the influence of different body postures on the auditory cortex fNIRS signal. We expect to find changes that should be considered when evaluating fNIRS data.



Figures: (left) Results from testing of Mini Comb on mannequins with different wig types. (middle) Image of sliding legs associated with Design D of the Mini Comb and corresponding clearance achieved on a wigged mannequin with long, curly hair (c) Preliminary results of clearance time and SNR differences achieved during human testing of the Mini Comb.

REFERENCES

[1] Hshieh, T. T. et al, J. of Alzheimer's Assoc, 19, 1901, 2023.

[2] Robinson TN et al, Ann Surg, 249, 173-178, 2009.

[3] Lopez MG et al, Free Radic Biol Med., 103, 192-198, 2017.

Non-obvious features imaging in OCT

G.V. Gelikonov¹

¹*Department of Nonlinear Dynamics and Optics, Institute of Applied Physics Russian Academy of Sciences, Russia*

grgel@ipfran.ru

ABSTRACT

Low-coherence interferometry has occupied a special niche not only in measurements of physical quantities, but also in sensor and diagnostic systems and devices. The most striking example of such an application is Optical Coherence Tomography. Despite its apparent simplicity, the measurement of low-coherence interference is associated with a number of features that significantly affect the result. Often these features are not obvious. We will discuss the issues of the observed optical noise and achieving its minimum values, calculating the dispersion characteristics of an object when direct measurement is impossible, and the influence of the spectrometer resolution on the attenuation of the spectral OCT signal with depth.

The optical noise contains fundamental and technical parts. Technical noise has multiple sources and can be eliminated. Fundamental noises consist of shot and beat noises of the spectral components, due to the incoherent nature of the radiation sources for low-coherence interferometry. In the case of weak reflection or scattering from the observed object, the intensity of the reference radiation in the Michelson interferometer has an optimum, which is achieved by attenuating this radiation in the reference arm while maintaining the division ratio of 50/50. [1, 2]

When using a tandem scheme with a measuring interferometer and an additional interferometer that compensates for the difference in the path of the measuring one, both waves of the compensating interferometer must have the same intensity. In this case, the excess noise cannot be completely subtracted, and its value will differ by $\sqrt{1.5}$ times from the original one. [3]

In the case of impossibility of directly measurement the dispersion characteristics of the object of study (for example, when examining the retina), they can be calculated from the registered interference signal. [4]

The axial motion that distorts OCT images could be corrected during or after scanning using the phase information in the OCT signal [5]. This method requires overlapping A-scans in in B-scan and could be realized using Fourier transform.

In spectral optical coherence tomography, the signal decay with depth, in addition to the general scattering and absorption factors, is also determined by the resolution of the measuring spectrometer. An improved model of the spectrometer is presented, which more accurately describes the signal decay with depth. [6]

Acknowledgements: The work was supported under IAP RAS State financing, project #FFUF-2024-0029

REFERENCES

- [1] Feldchtein F., Bush J., Gelikonov G., Gelikonov V., Piyevsky S. Cost effective, all-fiber autocorrelator based 1300 nm OCT system // *Progress in Biomedical Optics and Imaging - Proceedings of SPIE*. V. 5690. P. 349-355 (2005)
- [2] Bush J., Feldchtein F., Gelikonov G., Gelikonov V., Piyevsky S. Cost effective, all-fiber autocorrelator for Optical Coherence Tomography imaging // *Proceedings of SPIE - The International Society for Optical Engineering*. V. 5855 PART I. P. 254-257 (2005)
- [3] Gelikonov V.M., Romashov V.N., Gelikonov G.V. Excess broadband noise at equal intensities in the interferometer arms. // *Quantum Electronics*. V.51, №.5, P. 377-382.(2021)
- [4] Gelikonov G.V., Gelikonov V.M. Measurement and Compensation for the Amplitude and Phase Spectral Distortions of an Interference Signal in Optical Coherence Tomography for the Relative Optical-Spectrum Width Exceeding 10%. // *Radiophysics and Quantum Electronics*. V.61, №.2, P. 135-145.(2018)
- [5] Ksenofontov, S. Y., Shilyagin, P. A., Terpelov, D. A., Gelikonov, V. M. & Gelikonov, G. V. Numerical method for axial motion artifact correction in retinal spectral-domain optical coherence tomography. *Frontiers of Optoelectronics* 13, 393-401, doi:10.1007/s12200-019-0951-0 (2020).
- [6] Sherstnev E.P., Shilyagin P.A., Terpelov D.A., Gelikonov V.M., Gelikonov G.V. An Improved Analytical Model of a Spectrometer for Optical Coherence Tomography. // *Photonics*. V.8, №.12, P. 1-10. (2021)

Pre-clinical and clinical investigations on Hyperspectral Imaging

Adrian RÜHM^{1,2}, Matthäus LINEK¹, Ester PACHYN¹, Christian FREYMÜLLER^{1,2}, Maximilian AUMILLER^{1,2}, Marco SEEGER¹, Daniel HAPPACH¹, Prishita MIRCHANDANI¹, Ina STADLER¹, Veronika VOLGGER³, Axelle FELICIO-BRIEGEL³ and Ronald SROKA^{1,2}

¹Laser-Forschungslabor, LIFE-Zentrum, LMU University Hospital, LMU Munich, Germany

²Department of Urology, LMU University Hospital, LMU Munich, Germany

³Department of Otorhinolaryngology, LMU University Hospital, LMU Munich, Germany

Adrian.Ruehm@med.uni-muenchen.de

ABSTRACT

The interest in hyperspectral imaging as a tool for medical applications is growing continuously. By detailed spectral analysis of the light collected in each pixel, after interaction with biological tissue, a wealth of information can be derived about that tissue. In principle, regions of different tissue types can be located within the tissue and characterized regarding their optical properties. In practice, however, the obtainable information is limited, due to the limited resolution of the involved diffuse optics and the related need for simplifying assumptions, based on previous knowledge about the tissue.

The suitability of different hyperspectral imaging systems has been explored for different diagnostic applications. This includes the assessment of the perfusion of the radial forearm, as a source for free flaps to be used for reconstructive head and neck surgery. Subsequently, after transplantation of suitable free flaps into the oral cavity, their blood and oxygen supply was monitored postoperatively. In a different study, blood contaminations on different substrates were examined over long periods of time, in order to assess the potential of hyperspectral imaging for forensic applications.

Arm-mounted, handheld and endoscopic hyperspectral imaging systems were used and compared. In the first place, geometric and temporal boundary conditions determine the suitable device options. Additional challenges may be brought about by the type of tissue to be examined and environmental conditions. Image artefacts and calibration issues may complicate the automated data interpretation. Reflections from the tissue surface and the influence of skin tone have to be taken into consideration, and the use of suitable reference samples is highly recommendable. This becomes crucial with the trend towards a detailed analysis of the spectra, rather than restricting the interpretation to the indices commonly derived to estimate oxygenation, water content and perfusion in the tissue. Model-based data analysis is just one of the steps required in addition to obtain depth-resolved information about the tissue.

REFERENCES

- [1] M. Linek, I. Schrader, V. Volgger, A. Rühm, R. Sroka, Proc. SPIE 11919, 119190C, 2021, doi: 10.1117/12.2614462.
- [2] V. Volgger, A. Felicio-Briegel, C. Freymüller, A. Rühm, M. Linek, R. Sroka, Proc. SPIE 11919, 119190G, 2021, doi: 10.1117/12.2614471.
- [3] M. Linek, A. Felicio-Briegel, C. Freymüller, A. Rühm, A. S. Englhard, R. Sroka, V. Volgger, Lasers Surg. Med. 54(2), 245-255, 2022, doi: 10.1002/lsm.23479. Erratum in: Lasers Surg. Med. 54(10), 1321, 2022, doi: 10.1002/lsm.23587.
- [4] V. Volgger, M. Linek, R. Sroka, A. Felicio-Briegel, Laryngorhinootologie, 101(S 02), S23, 2022, doi: 10.1055/s-0042-1747149. English version: S243-S244, doi: 10.1055/s-0042-1746505.
- [5] A. Felicio-Briegel, M. Linek, R. Sroka, A. Rühm, C. Freymüller, M. Stocker, P. Baumeister, C. Reichel, V. Volgger, Lasers. Surg. Med. 56(2), 165-174, 2024, doi: 10.1002/lsm.23756.
- [6] E. Pachyn, M. Aumiller, A. Buchner, C. Freymüller, M. Linek, V. Volgger, R. Sroka, Proc. SPIE 12627, 126271U, 2023, doi: 10.1117/12.2670934.

Ultracompact multimodal femtosecond fiber multiphoton tomograph

Karsten König^{1,2}

¹Department of Biophotonics and Laser Technology, Saarland University,
66123 Saarbrücken, Germany

²JenLab GmbH, Johann-Hittorf-Strasse 8, 12489 Berlin, Germany

ABSTRACT

Multiphoton tomography is a clinical imaging method to obtain high-resolution optical biopsies of human skin and to perform optical metabolic imaging (OMI) by two-photon fluorescence lifetime imaging (FLIM) of autofluorescent coenzymes (1-3).

We report on the PRISM AWARD 2024 winning multimodal multiphoton tomograph MPT_{compact} run by batteries that can be powered by flexible solar panels. The air-cooled fiber laser head is located inside the 360° imaging head that is attached to a flexible mechanical arm. Imaging modalities include two-photon imaging, SHG imaging, FLIM, and confocal reflectance microscopy with 80 MHz, 100 fs laser pulses at 780 nm wavelength (4).

We report on a long-term MPT-OMI study during oxygen inhalation (5-7). Metabolic changes of epidermal cells have been recorded twice daily for one week. Specific intratissue cells could be imaged with subcellular resolution over two hours during oxygen inhalation. It was found that the ratio free to bound NADH changed more significantly in the basal cell layer close to the capillaries compared with the stratum granulosum.



REFERENCES

1. K. König (editor). Multiphoton microscopy and fluorescence lifetime imaging. De Gruyter (2018) ISBN 978-3-11-042998-5. Free download.
2. K. König. Review: Clinical in vivo multiphoton FLIM tomography. *Methods Appl Fluoresc* 8 (2020) 034002.
3. K. König. Medical Femtosecond Laser. *J Eur Opt Society-Rapid Publ* 19(2023)36
4. K. König. Multimodal multiphoton tomography with a compact femtosecond fiber laser. *Journal of Optics and Photonics Research* 1(2024)51-58.
5. M. von Ardenne. Oxygen multistep therapy: physiological and technical foundations. Thieme 1990, ISBN 978-3137435013
6. M. Stücker et al. The cutaneous uptake of atmospheric oxygen contributes significantly to the oxygen supply of human dermis and epidermis. *J Physiol* 1(2002)985-994.
7. M. Balu et al. In Vivo Multiphoton NADH Fluorescence Reveals Depth-Dependent Keratinocyte Metabolism in Human Skin *Biophys J* 104(2013)258-267.

Multispectral Light Scattering Imaging for Precancer Detection and Cell Analysis

Mark F. COUGHLAN, Xuejun ZHANG, Paul UPPUTURI, Umar KHAN, Yuri ZAKHAROV, Lei ZHANG, Le QIU
and Lev T. PERELMAN

*Center for Advanced Biomedical Imaging and Photonics,
Beth Israel Deaconess Medical Center
Harvard University
USA*

ltpere@bidmc.harvard.edu

ABSTRACT

Optical spectroscopy emerged as a valuable tool to study live biological tissue at various scales and detect early disease in the human body. While fluorescence and Raman spectra are sensitive to molecular properties of tissue, light scattering spectra, originating from the extracellular matrix, subcellular structures, and other tissue inhomogeneities, carry information about microscopic and macroscopic organization of tissue [1]. In this talk we will discuss how scattered light can be used for noninvasive detection of invisible pre-cancer in such diverse organs as the esophagus [2], pancreas [3], or bile duct [4] that seem to have little in common. Since pre-cancer in many organs is characterized by certain microscopic changes in epithelial cells, such as increase in nuclear size and nuclear density, light scattering signatures of those pre-cancers are quite similar, allowing early cancer imaging and detection without the need for external markers. At the same time, multiple scattering randomizes the signal from the underlying connective tissue which obscures the desired light scattering signals from epithelial cells. In order to extract diagnostic information from the reflected signal, the multiple scattering component related to connective tissue scattering and absorption must be removed. This is accomplished using various gating methods implemented with endoscopically compatible fiber optic probes. For organs with large epithelial surfaces, such as the esophagus, polarization gating provides rapid non-contact interrogation of the entire epithelial area [2]. For organs located deep in the abdomen which are difficult to access, such as pancreatobiliary system, spatial gating, which can be implemented in a much more compact package, is the preferred approach [3,4].

Light scattering signatures could also be used for sensing the subnuclear and subcellular structure of live cells, e.g. organelle organization or chromatin packing. Nanoscale changes in the nuclear structure have been shown to play a critical role in genetic and transcriptional alterations and are a hallmark of neoplasia. However, due to the lack of technologies for label-free nanoscale-sensitive measurements in live cells, many aspects of these phenomena have remained unknown. The approach based on the combination of confocal microscopy and spectroscopy of scattered light helps to solve this problem [5], providing several critical advantages over the existing methods. For example, coherent confocal light absorption and scattering spectroscopic (C-CLASS) microscopy is capable of label-free detecting changes in chromatin packing density in live cells [6], which is indicative of gene expression states. Using C-CLASS microscopy we monitored chromatin changes in cultured untreated human pancreatic ductal epithelial cells (HPDEC) and the same cells treated for 24 hours with nicotine-derived nitrosamine ketone (NNK), a well known mutagen causing carcinogenesis in cells. The C-CLASS microscopy measured a chromatin packing parameter [6] for the benign and NNK-exposed cells exhibit a statistically significant increase in heterochromatin in treated cells. This result agrees well with the literature, where NNK-exposed cells have shown increased levels of gene silencing [7].

REFERENCES

- [1] L.T. Perelman et al, *Phys. Rev. Lett.* 80, 627-630, 1998.
- [2] L. Qiu et al, *Nat. Med.* 16, 603-606, 2010.
- [3] L. Zhang et al, *Nat. Biomed. Eng.* 1, 0040, 2017.
- [4] D.K. Pleskow et al, *Nat. Commun.* 14, 1-2, 2023.
- [5] D.K. Pleskow et al, *ACS Photonics*, 8, 2050-2059, 2021.
- [6] G. Pettinato G et al, *Science Adv.* 7, eabj2800, 2021.
- [7] P. Srinivasan et al, *Am. J. Physiol. Gastrointest. Liver Physiol.* 310, 874–883, 2016.

Dynamic imaging and optogenetic control of mammalian embryonic cardiogenesis

Michaela A. McCown, Guzel R. Musina, and Irina V. Larina*

Baylor College of Medicine, Department of Integrative Physiology,
One Baylor Plaza, Houston, Texas 77030, USA

* larina@bcm.edu

Blood flow, heart contraction, and tissue stiffness are important regulators of cardiac morphogenesis and function during embryonic development. Defining how these factors are integrated is critically important to advance prevention, diagnostics and treatment of congenital heart defects. Mammalian embryonic development is taking place deep within the female body, which makes cardiodynamic imaging and analysis during early developmental stages in humans inaccessible. With thousands of mutant lines available and well-established genetic manipulation tools, the mouse is a great model to understand how biomechanical factors are integrated with molecular pathways to regulate cardiac function and development. Toward this goal, we have developed a set of novel methods for live dynamic volumetric imaging of the developing heart in cultured mouse embryos. Our methodology combines live mouse embryo culture protocols, state-of-the-art structural and functional Optical Coherence Tomography (OCT), and computational analysis. By taking advantage of the periodicity of the heartbeat, we developed a functional OCT method for the segmentation of the blood inside the beating heart. Building off advancements in Doppler OCT and quantitative OCT angiography, we present dynamic, volumetric (4D) speed analysis of blood flow in the embryonic cardiovascular system. Our new flow-tracking method is based on time-at-pixel measurements, blood cell size statistics, and the periodicity of the cardiac cycle. We also integrated optogenetic control for spatial mapping of cardiac pacemaker cells and track these cell population dynamics through development. Together, these methods are bringing us closer to understanding how specific mutations impact heart wall dynamics, and how this influences flow patterns and cardiogenesis.

Photoacoustic tracking of stem cells

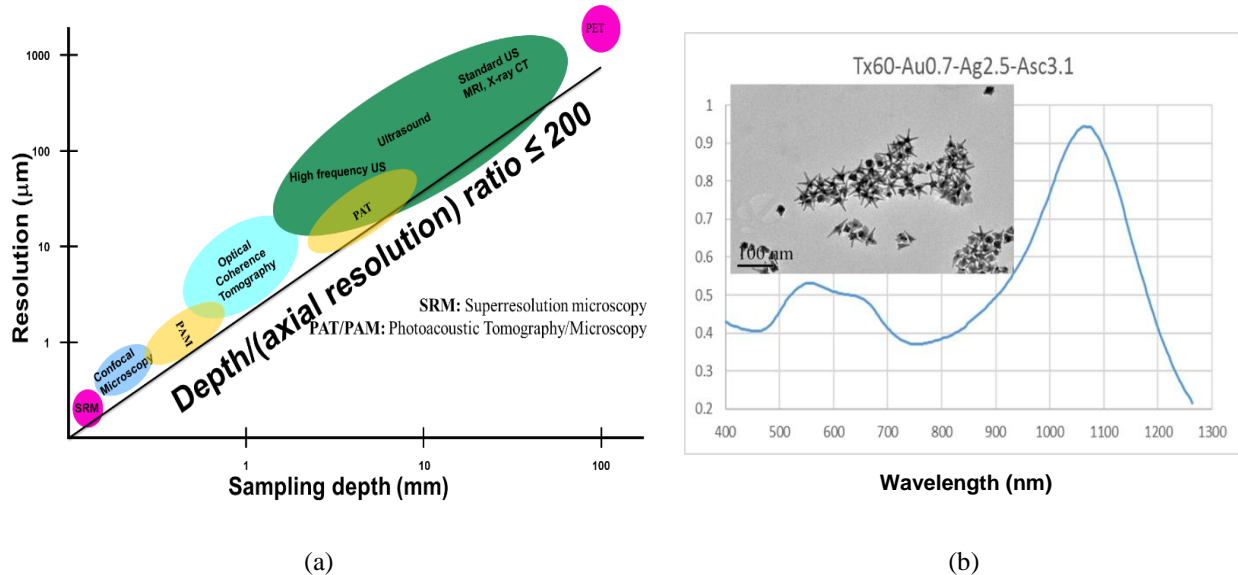
Martin LEAHY¹, Cerine LAL¹, Soorya JAMES¹, Anand ARANGATH¹, Rajib DEY¹, Niamh DUFFY¹ and Sergey ALEXANDROV¹

¹ Chair of Applied Physics, School of Natural Sciences, University of Galway
IRELAND

martin.leahy@universityofgalway.ie

Stem cell therapies promise to allow the blind to see, the lame to walk and those enslaved to thrice weekly dialysis to be free. However, they have not yet fulfilled their potential, partly because we don't know where stem cells go and what they do deep inside organs of real living humans. We recently identified a general limit of medical imaging which encapsulates the challenge; current technologies do not allow visualization of objects more than 200 times smaller than the depth; see figure 1. For example, typical cells, of 10 micron diameter, more than c. 2 mm into typical human tissues like the skin cannot be imaged by any technology [1]. The TOMI lab won a €6M EU H2020 grant to develop technologies to see deeper and smaller and with greater sensitivity than ever before. We go beyond the depth/resolution limit by demonstrating nanosensitive OCT to follow structural changes in cells and tissues at the nanoscale.

Using a unique star-shaped gold nanoparticle developed in Galway, which resonates in the low scattering and absorption window, allows us to see deeper and with greater sensitivity than ever before. To make it largely immune to skin colour variation, the particle is optimized for energy deposition at 1064 nm. The combination of long wavelength, tip field enhancement and energy transfer make this particle the brightest ever made. We combine this with photoacoustic imaging, so that we can use diffuse light to illuminate the tissue and ultrasound which is not scattered, to see where it was absorbed. A key patent allows photoacoustic images to be calibrated for the first time, allowing quantitative measurements of stem cell concentration, blood oxygen etc. The particle is also visible in MRI. We demonstrated this enhanced imaging in Cambridge during stem cell therapy for osteoarthritis of sheep knee.



Figures: (a) Imaging depth v axial resolution (b) Tuning the shape for energy deposition at 1064 nm

REFERENCES

- [1] C. Lal, Leahy M. *Microcirculation* **23**: 345–363, 2016.
- [2] M. Leahy, “A photoacoustic tomography method and system” EP3096678A1. granted in 2019

tSNIP Transient Selective Neural Inhibition via Photobiomodulation

Michael Moffitt¹, Andrew Buzza¹, Aaron, Skubal¹, and Michael Jenkins^{1,2}

¹Department of Biomedical Engineering, Case Western Reserve University, USA

²Department of Pediatrics, Case Western Reserve University, USA

mwj5@case.edu

ABSTRACT

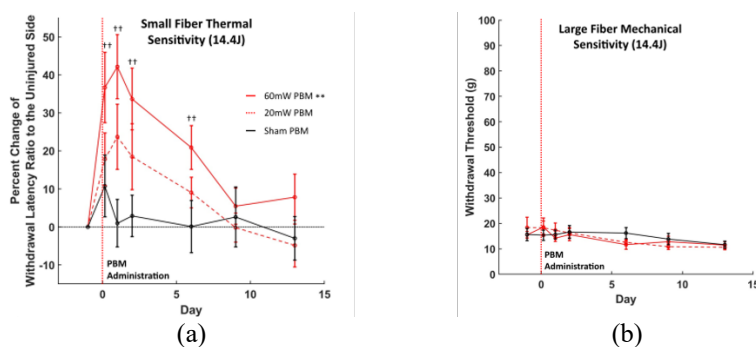
We will review our recent progress using Transient Selective Neural Inhibition via Photobiomodulation (tSNIP) to alleviate pain^{1,2}. tSNIP involves the application of red or near-infrared light to selectively block action potential transmission in small-diameter nerve fibers without the use of exogenous agents or inducing a thermally mediated response. Pain remains a significant reason people seek medical assistance, yet current pain management strategies often have limited efficacy and can result in severe side effects, including opioid addiction. The concept of selectively blocking nociceptors to "switch off" pain while preserving the function of large sensory fibers (maintaining non-painful touch) and motor fibers (ensuring unaffected motor function) offers a promising and innovative approach. This method has the potential to revolutionize pain management by providing a targeted solution that alleviates pain without compromising sensory or motor abilities.

Red and infrared light has been explored for alleviating pain in the past, but its wide adoption has been hindered by marginal results. These results can be attributed to the difficulty of delivering the correct light dose to the pertinent tissue. Non-optimal dosing arises from several factors. First, light's interaction with tissue is complex, involving multiple mechanisms that could potentially lead to pain relief. We believe that blocking the small-diameter fibers carrying pain signals is the most effective route to pain relief, as it provides a specific target and aligns with other pain-relieving strategies. However, clinical trials and most basic research have not focused on targeting these small fibers.

Second, most approaches deliver light from outside the body and report the light output at the emitter. Since target tissues can be located at various depths within the body, researchers often have little understanding of the actual light dose reaching the target tissue. This results in the use of various doses with highly variable outcomes. To achieve effective pain relief, it is essential to deliver the optimal dose to the correct tissue.

We demonstrate our efforts to determine the optimal dosing for Transient Selective Neural Inhibition via Photobiomodulation (tSNIP). Using pain models such as spared nerve injury (neuropathic pain model) and capsaicin injections (nociceptive pain model), along with behavioral tests like the Hargreaves test, von Frey, and pin prick tests, we have sought to identify effective dosing parameters. Additionally, we employed Monte Carlo photon propagation modeling of previous studies to refine our approach.

In Figure 1a, rats subjected to spared nerve injury and subsequently treated with 2.23 W/cm² of 808 nm light at the nerve for four minutes exhibited a significant reduction in hypersensitivity, lasting approximately one week. Figure 1b demonstrates that this light treatment had no impact on the mechanical sensitivity of large sensory fibers responsible for touch. Our data, combined with modeling based on previous publications, indicate a clear therapeutic window for tSNIP.



Figures: Laser irradiation at 14.4 J reduces hypersensitivities associated with small-diameter nerve fibers (a) Reduction of withdrawal latency ratio for individual rats during Hargreaves test is increased by over 20% for both the high and low power groups. (b) Mechanical hypersensitivity assessed by a von Frey test is unchanged by tSNIP. Statistical tests: treatment differences evaluated via 2-way ANOVA ($p < 0.05$ as indicated by ** (60 mW)); day-to-day differences via t-test with Dunn-Sidak correction (†† (60 mW)).

REFERENCES

- [1] A. Buzza et al, Lasers in Surgery and Medicine 56, 305-314, 2024.
- [2] A. Buzza et al, J. Photochemistry Photobiology B: Biology 256 112929, 2024.

AI Assisted Rapid Quantitative Optical Cytopathology of Cancer

Anna N Yaroslavsky

Advanced Biophotonics Laboratory, University of Massachusetts Lowell, Lowell, MA, USA

Anna_Yaroslavsky@uml.edu

ABSTRACT

We have developed an accurate approach for rapid quantitative detection of thyroid cancer in single cells that utilizes fluorescence polarization (Fpol) imaging and a 2D U-Net convolutional neural network for cell analysis. Its clinical implementation holds the potential to shift the paradigm of cellular level cancer diagnosis from subjective visual assessment to objective measurement, reduce incidence of cytologically indeterminate samples, and provide an accurate diagnosis within an hour from fine needle aspirate acquisition.

Fine needle aspirates (FNAs) from freshly excised thyroid tissues were stained in aqueous methylene blue (MB) solution and smeared onto a glass slide. Fluorescence images were acquired as described in [1]. Images were analyzed manually and by the deep learning model. Fpol values were calculated using: $Fpol = \frac{I_{co} - G \times I_{cross}}{I_{co} + G \times I_{cross}}$, where I_{co} is the co-polarized fluorescence emission, I_{cross} is the cross-polarized fluorescence emission, and G is the system calibration factor, equal to 0.75. Cell areas segmented as well as MB Fpol values and their standard deviations were determined for all the cells and specimens analyzed. Clinical diagnoses were obtained from BayState Medical Center and correlated with the optical imaging assessments.

In total, 12 fine needle aspirates (652 cells) were imaged and analyzed including 5 cancerous (272 cells) and 7 benign (380 cells). Malignant FNAs included 3 papillary thyroid (PTC) and 2 oncocytic carcinomas. Benign specimens included 3 follicular thyroid adenoma (FTA) and 4 multinodular goiter.

Fig. 1A shows malignant PTC cells annotated by manual segmentation (cyan regions). Fig. 1B presents the same cells outlined by automated processing (yellow regions). Figs. 1C and 1D display benign FTA cells segmented by manual and automated methods, respectively. Average MB Fpol was higher in cancerous cells as compared to noncancerous (Fig. 1E).

Overall, the differences in Fpol values obtained through manual vs. automatic cell segmentation agreed within $\pm 15\%$. Optical imaging results demonstrated higher MB Fpol values for cancerous as compared to benign cells and correlated well with histopathology. The rapid cell handling protocol reduced the time needed for cell preparation and imaging from ~ 30 hours to ~ 30 minutes. Utilization of the deep learning-based model reduced the time necessary for cell segmentation and processing to ~ 3 seconds from an hour required for manual segmentation. The results of the study indicate that rapid MB Fpol cytology may facilitate reliable and accurate thyroid cancer detection at the cellular level.

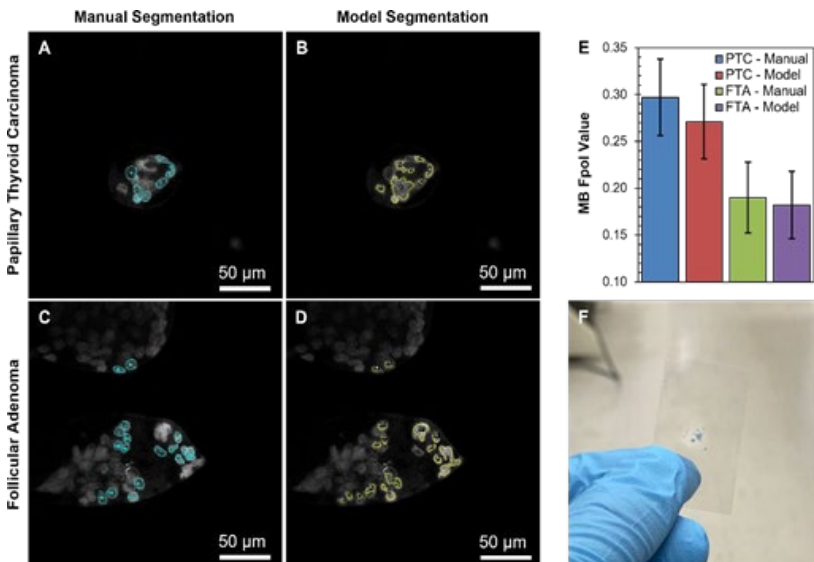


Figure 1: MB fluorescence emission images of PTC cells analyzed using (A) manual and (B) automated segmentation. Methylene blue fluorescence emission images of FTA cells analyzed using (C) manual and (D) automated segmentation. (E) Histogram of MB Fpol values (error bars are standard deviation). (F) Thyroid cytology slide prepared using rapid protocol.

REFERENCE

[1] Jermain PR, Fischer AH, Joseph L, Muzikansky A, Yaroslavsky AN. Fluorescence Polarization Imaging of Methylene Blue Facilitates Quantitative Detection of Thyroid Cancer in Single Cells. *Cancers*. 2022; 14(5):1339

Revealing the Micro-Scale Mechanics of Cancer Using Optical Coherence Elastography

Brendan Kennedy^{1,2,3}

¹*BRITELab, Harry Perkins Institute of Medical Research, QEII Medical Centre, Nedlands and Centre for Medical Research, The University of Western Australia*

²*Department of Electrical, Electronic and Computer Engineering, School of Engineering, The University of Western Australia*

³*Institute of Physics, Faculty of Physics, Astronomy and Informatics, Nicolaus Copernicus University in Toruń*

Brendan.kennedy@uwa.edu.au

ABSTRACT

It is well-established that cancer modifies the mechanical properties of tissue. For centuries, physicians have used stiffness as a biomarker for disease by palpating suspicious regions of tissue both prior to and during surgical procedures. In medical imaging, palpation inspired the development of clinical elastography, which is now an established clinical method in many procedures, for example, in detecting both breast cancer and liver cancer. In clinical elastography, a medical imaging modality, mainly ultrasound imaging or magnetic resonance imaging, is used to map tissue deformation in two or three dimensions. Then, a mechanical model of tissue deformation is used to estimate a mechanical property from measured deformation.

Whilst clinical elastography provides valuable clinical information, it is restricted to the macro-scale. However, cancer manifests at the micro-scale. As such, elastography techniques capable of mapping micro-scale mechanics have the potential to contribute to the treatment and understanding of cancer. For example, a tool capable of visualizing cancer on the micro-scale could help surgeons to detect tumour margins intraoperatively [1]. Additionally, mapping micro-scale mechanics could provide insight in cancer mechanobiology, where the goal is to understand the relationship between the mechanical micro-environment of cancer and cellular behaviour [2].

In this talk, I will describe our work demonstrating a variant of compression optical coherence elastography (OCE) called quantitative micro-elastography (QME) to image cancer. I will give an overview of the methodology we have developed and present a summary of our results in two main areas. Firstly, the development of OCE as a tool for intraoperative tumour margin assessment in breast-conserving surgery and, secondly, as a novel method to image cancers cells and spheroids on the sub-cellular scale. In Figure 1, an example of OCE imaging of freshly excised human breast tissue is presented. Lastly, I will present preliminary results extending OCE to the detection of prostate cancer.

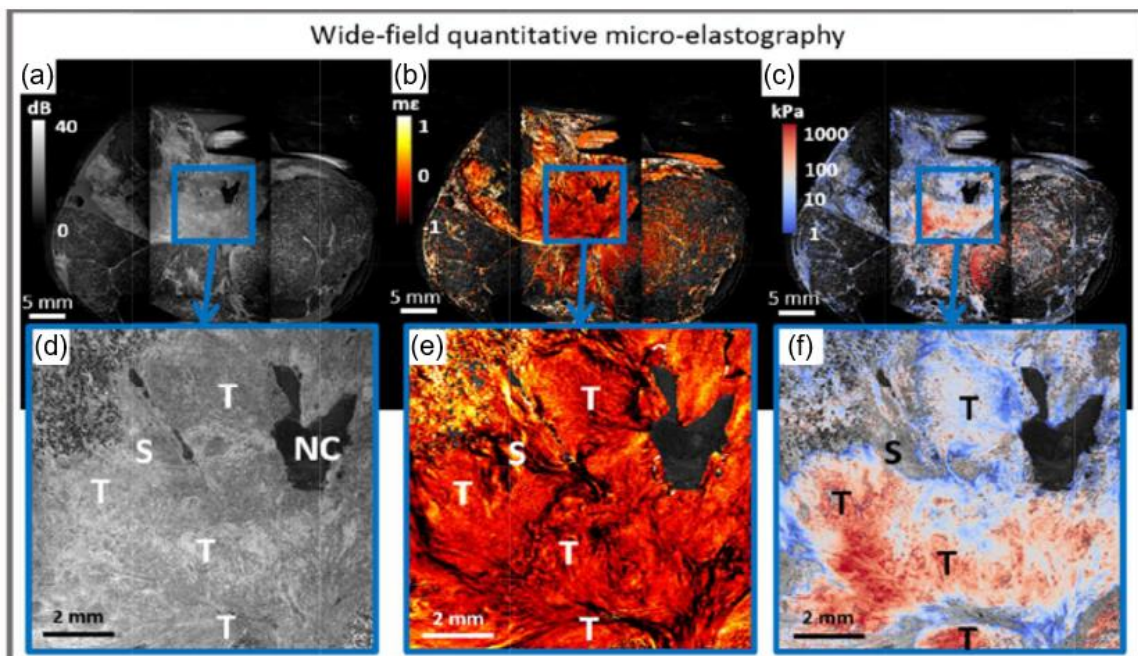


Figure 1: Example of QME on human breast tissue [3]. En face (a) OCT, (b) qualitative micro-elastogram (strain imaging), and (c) quantitative micro-elastogram from wide-field QME. Magnified en face (d) OCT, (e) qualitative micro-elastogram (strain imaging), and (f) quantitative micro-elastogram from wide-field QME. A, adipose; T, invasive tumor; NC, non-contact; S, uninvolved stroma.

REFERENCES

- [1] K. M. Kennedy et al, *Cancer Res.* 80, 1773–1783, 2020.
- [2] D. Vahala et al, *Adv. Healthcare Mater.* 12, 2301506, 2023.
- [3] W. M. Allen et al, *Biomed. Opt. Express* 9, 1082–1096, 2018.

Milling Microscopy: A Platform for Large-Scale Sub-Cellular 3D Histology

Jiaming Guo¹, Wilna Moree², Meher Niger¹, Maximillian Bluhm¹, and Jason Eriksen³, and David Mayerich¹

¹Electrical and Computer Engineering, University of Houston, USA

²Swift Front, LLC, USA

³Department of Pharmacological and Pharmaceutical Sciences, University of Houston, USA

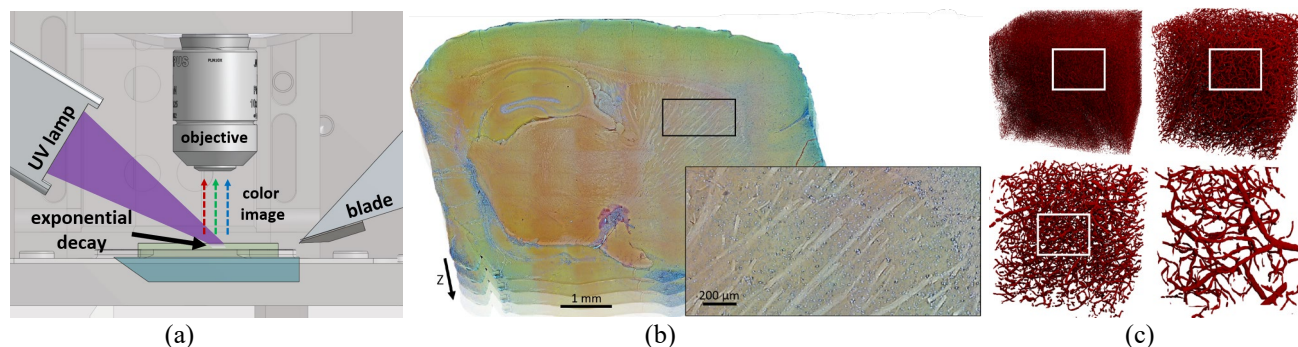
mayerich@uh.edu

ABSTRACT

Comprehensive models of whole-organ microstructures are needed to understand the large-scale impacts of disease across organs and organ systems. These models include microvascular and neuronal networks, as well as the distributions and classifications of individual cells and subcellular structures. The ability to compare models across phenotypes will provide insight into disease progression, as well as an array of biomarkers for both diagnosis and tracking treatment efficacy. Current approaches for whole-organ imaging are labor intensive and provide limited resolution.

We have developed an acquisition and segmentation framework for low-cost imaging and modeling of tissue microstructures using wide-field imaging at three-dimensional resolutions comparable to confocal microscopy [1]. Image acquisition relies on block-face fluorescence imaging using deep ultraviolet excitation. Tissue samples are labeled *en bloc* using traditional fluorescent dyes and embedded in a hard polymer or traditional paraffin wax. Three-dimensional images are acquired using MUSE microscopy [2], which leverages deep-ultraviolet light to limit acquisition to a thin layer at the sample surface. The imaged tissue is then ablated using a microtome or other automated milling system. By fully automating this procedure, the resulting three-dimensional image stack is aligned and processed to build an explicit model of the tissue.

Segmentation algorithms are developed to take advantage of similarity and connectivity seen across large tissue volumes. Convolutional neural network (CNN) architectures such as U-Net are adapted to efficiently segment cells and microvessels [3]. We have also developed highly parallel and GPU-based level sets extract microvascular structure and connectivity embedded in the images. The microvasculature network is stored such that the connectivity graph can be exploited to quantify the organ-scale angiome and facilitate data mining at the terabyte scale. Future work in this area focuses on identifying whole-organ labeling methods compatible with UV excitation, new embedding compounds that limit excitation penetration to improve resolution, and algorithms and data structures to store and characterize large volumes of microstructures.



Figures: (a) Milling and imaging using MUSE. Deep UV (~ 280 nm) illumination is used to excite visible fluorescence at the tissue surface. This illumination is blocked by both the tissue and embedding compound, limiting excitation to ~ 10 μm . (b) Mosaic images and image stack of a sagittal brain section labeled using eosin and Hoechst, with an inset showing cellular and vascular features. (c) GPU-based active contours using RSF level sets are used to segment the sample, building a large-scale model of the microvascular surface and connectivity.

REFERENCES

- [1] Guo, et al., Nature Scientific Reports, 2019
- [2] Fereidouni, et al., Nature Biomedical Engineering, 2017
- [3] Saadatfard, et al., MICCAI, 2020

Mueller matrix microscopy for digital pathology

Hui MA

Shenzhen International Graduate School, Tsinghua University, China

mahui@tsinghua.edu.cn

ABSTRACT

Mueller matrix microscopy is becoming an increasingly attractive digital pathology technique for characterizing complex biological tissues. A Mueller matrix image (MMI) contains rich optical and microstructural information in all the pixels, comprehensively encoded in the high-dimensional polarization feature space. Since the contrast mechanism does not rely on absorption and is sensitive to scattering features down to a fraction of wavelength, the technique is label-free and non-invasive, capable of cross-scale and quantitative measurements and ideal for probing biomedical samples including tissues and cells. Despite all the apparent advantages of Mueller matrix microscopy for quantitative characterization of the microstructural properties, how to extract polarization features of pathological significance remains challenging for clinical applications [1-3]. In this report, we propose polarization super-pixels approach to exploit pixel-level polarization features for pathological applications.

For MMIs, polarization features are encoded in the density distribution of pixels in polarization feature space. Using clustering techniques, we can group together pixels of similar polarization properties to obtain a collection of polarization super-pixels (PSP), which are characterized by their centroid position, standard deviation and pixel population [4]. The set of PSPs provide an approximate representation of the MMIs in polarization space,

For pathological slides of liver cancer tissues, we took MMIs for multipole region-of-interest (ROI) and calculated 1024 PSPs for each MMI. Then for all the PSPs of the ROIs, we applied UMAP for dimension reduction followed by hierarchical clustering. Different clusters correspond to different pathological components of the liver tissues, such as normal and malignant nuclei, cytoplasm and fibrous structures. The decomposition method helped doctors to identify more specific indicators for pathology auxiliary diagnosis.

If pathological features are spatially labelled, we can compute the relative-contributions of individual PSPs to the labelled area and assign weight coefficients. The set of PSPs with weights forms a polarization feature template, or PFT, which can be used for label spreading by highlighting pixels of similar polarization features to those within the labelled areas. Results demonstrate that we can construct the PFT from small patches of labelled lung adenocarcinoma, and spread the label to the entire field of view. PFT essentially functions as the linkage, connecting polarization features to the spatial pattern of the specimen. Leveraging PSP and PFT the approach provides the capability to identify specific pathological features for assisted diagnosis, effectively reducing labor and time costs for pathologists.

REFERENCES

1. Pengcheng Li, et al, "Polaromics: deriving polarization parameters from a Mueller matrix for quantitative characterization of biomedical specimen", *J. Phys. D: Appl. Phys.* 55, 034002, 2022
2. Yang Dong, et al, "Deriving Polarimetry Feature Parameters to Characterize Microstructural Features in Histological Sections of Breast Tissues", *IEEE Transactions on Biomedical Engineering*, 68(3), 881-892, 2021.
3. Yang Dong, et al, "A Polarization-Imaging-Based Machine Learning Framework for Quantitative Pathological Diagnosis of Cervical Precancerous Lesions", *IEEE Transactions on Medical Imaging*, 40(12), 3728-3738, 2021
4. Jiachen Wan, et al, "Unsupervised learning of pixel clustering in Mueller matrix images for mapping microstructural features in pathological tissues." *Communications Engineering*, 2 (1): 88, 2024.

Correlation of Endothelium Function with Optically Measured Blood Microcirculation Parameters in Healthy Volunteers and Patients Suffering from Cardiac Diseases

Alexander PRIEZZHEV¹, Petr ERMOLINSKIY¹, Yuri GURFINKEL² and Andrei LUGOVTSOV¹

¹Physics Department, Lomonosov Moscow State University, Russia

²Medical Research and Education Centre, Lomonosov Moscow State University, Russia

avp@biomedphotonics.ru

ABSTRACT

This study aimed to identify a relationship between blood microcirculation parameters (MP) and endothelial function (EF) in healthy volunteers and two groups of patients suffering from cardiovascular diseases, specifically coronary heart disease (CHD) and atrial fibrillation (AF). These diseases pose significant health risks and require accurate diagnostic tools to assess the severity and progression of the diseases. Traditional diagnostic methods have limitations in providing detailed information about blood flow characteristics, particularly in the microcirculation.

Digital optical capillaroscopy was employed to assess such MP as blood flow velocity, the size of red blood cell aggregates, and the number of aggregates per min and per running mm measured in the finger nail bed capillaries of the subjects included into the study groups. The digital capillaroscope Kapillaroskan-1 (AET, Russia) was utilized to visualize the capillaries. It was equipped with a high-speed CCD-camera (1/3" monochrome progressive scan IT CCD sensor, resolution 640 × 480 px, frame rate 200 fps full frame), specifically the TM-6740GE (JAI, Japan). The illumination of the nail bed was achieved using an LED-based illuminating system. Two sets of total magnification were employed: 125× and 400×. The 125× magnification was used to capture panoramic images of the capillaries, facilitating the selection of higher quality images among capillaries in the nail bed, while the 400× total magnification allowed for more detailed imaging of individual capillaries. This higher magnification also facilitated the measurement of static parameters such as capillary length and diameter in various parts of the capillary, as well as the assessment of capillary blood velocity in different capillary segments. To quantitatively estimate the EF we used the experimental device "Angiochek" (Russia), in which the method of pulse tonometry was implemented. Highly sensitive acoustic sensors located in the projection of the brachial artery and wrist arteries were used for measuring the amplitudes of pulse waves of the arteries.

The study of microcirculation involved 132 adults including 44 healthy volunteers, 44 patients with CHD and 44 patients with AF. The measurements were performed in three groups for comparison: control group (healthy volunteers), group of patients with CHD and group of patients with AF. An additional study of the correlation between MP and EF included 47 adults extracted from an initial sample of 132 adults for whom EF was measured. Patients with AF, as well as CHD patients presented in this study, take oral anticoagulants (mainly apixaban and rivaroxaban) according to the protocol adopted by the cardiology department.

The results indicate significant alterations in blood flow characteristics among patients with CHD and AF compared to healthy volunteers [1]. For example, capillary blood flow velocity is statistically significantly decreased in the case of CHD and AF compared to the healthy volunteers. Additionally, the correlation between the measured parameters is different for the studied groups of patients and healthy volunteers. The correlation between the MP and the EF is higher for the patients with CHD. Specifically, an increase in EF measured on the wrist leads to a significant decrease in the blood aggregate size. These findings highlight the potential of digital optical capillaroscopy as a non-invasive tool for evaluating blood flow abnormalities (red blood cell aggregates and decreased capillary blood flow velocity) in cardiovascular diseases, aiding in early diagnosis and disease management.

This research was funded by the Russian Science Foundation Grant No. 22-15-00120.

REFERENCE

[1] P. Ermolinskiy et al., Life 13, 2043, 2023.

Explainable AI (XAI) Applied to Laser Applications in Life Sciences

Olga M. CONDE*^{1,2,3}, José A. GUTIERREZ^{1,2}, Verónica MIEITES^{1,2}

¹Photonics Engineering Group, University of Cantabria, Spain

²IDIVAL - Valdecilla Biomedical Research Institute, Spain

³CIBER-BBN – Instituto de Salud Carlos III, Spain

olga.conde@unican.es

ABSTRACT

Advanced optical imaging technologies including HyperSpectral Imaging (HSI), Optical Coherence Tomography (OCT), Polarization Sensitive-OCT (PS-OCT), and Mueller polarimetry, provide valuable and rich chemical and morphological information about biological tissues. These techniques help clinicians to improve and facilitate better decision-making processes while performing surgery, pathological assessment, diagnosis, etc. Under this perspective, the adoption of optical imaging techniques within the biomedical field will enhance CADe (Computer-Aided Detection) and CADx (Computer-Aided Diagnosis) [1] disciplines. Nowadays, most CADe and CADx attempts rely on Artificial Intelligence (AI) that, unless attaining accurate diagnostic performances, provide results under the “black box” approach that has led to significant concerns about their decision-making processes. Explainable Artificial Intelligence (XAI) [2][3] comes to overcome this “black box” nature, incorporating reliable, trustful and understandable mechanisms that can help to correlate their performance to physical and comprehensible evidence.

On the other hand, the information from advanced optical imaging can sometimes be redundant, requiring careful data fusion or selection for the optimal features that best extract the distinguishing and discriminative properties of the tissue specimen. Understanding the physics of light-tissue interaction mechanisms helps to obtain accurate optical properties (absorption and scattering coefficients, birefringence, anisotropy, etc.) that can be used for diagnosis. In general, and due to the heterogeneity of tissues, this problem is affected by a multiparametric nature that cannot be addressed by deterministic or empirical approaches. Analysing this complex data is where AI strategies take advance, but where it is difficult to understand how they arrive to conclusions. This lack of transparency becomes a hurdle in critical fields like medical diagnosis.

XAI techniques cover different perspectives: including feature importance methods that select the most significant data to improves model outputs while removing the influence of redundant information; visualizations techniques to provide a more intuitive understanding of the model; attention mechanisms in ANN (Artificial Neural Networks) to find the influential data; etc. This work reviews the state of the art and specific implementations [4]-[7] to the advanced optical imaging technologies in the field of tumor margin delineation, cardiovascular diagnosis, brain imaging, etc.

REFERENCES

- [1] M. Firmino, et al., *BioMed Eng OnLine* 15, 2, 1-17, 2016.
- [2] A. Adadi and M. Berrada, *IEEE Access* 6, 52138-52160, 2018.
- [3] A. Barredo et al., *Information Fusion* 58, 82-115, 2020.
- [4] P.B. García-Allende et al., *Journal of Biomedical Optics* 14, 3, 034034, 2009.
- [5] P.B. García-Allende et al., *NDT & E International* 42, 1, 56-63, 2009.
- [6] A. Eguizábal et al., *Biomed Opt Express* 12, 4(7), 1104-1118, 2013.
- [7] V. Mieites et al., *Proc. SPIE* 13010, 130100G, 2024.

Fractional Laser Treatment of Cartilage: Review of Recent Ex Vivo and Clinical Data

Ilya Yaroslavsky

*IPG Medical, IPG Photonics, Marlborough, MA, USA
iyaroslavsky@ipgphotonics.com*

Fractional laser treatment of cartilage has been proposed as a potential remedy for degenerative disk disease (spinal disks) and osteoarthritis (articulated joints). For both conditions, laser-induced regeneration of cartilage is postulated as underlying pathway leading to clinical benefits.

This talk will review recent results of both ex vivo studies and clinical research addressing efficacy and safety of the technique. Mechanism of action will be discussed as well as current status of the technique in the armamentarium of cartilage-regenerating methods.

Progress on imaging neurovascular coupling in the retina

Kostadinka BIZHEVA^{1,2,3}

¹Department of Physics and Astronomy, University of Waterloo, Canada

²School of Optometry and Vision Sciences, University of Waterloo, Canada

³Systems Design Engineering Department, University of Waterloo, Canada

kbizheva@uwaterloo.ca

ABSTRACT

Neurodegenerative ocular diseases such as diabetic retinopathy, glaucoma and age-related macular degeneration, can change the cellular structure of the retina and cause abnormalities in the retinal blood flow and blood perfusion, as well as alter the normal response of retinal neurons to visual stimulation. A number of optical imaging modalities such as scanning laser ophthalmoscopy (SLO), optical coherence tomography (OCT), Doppler flowmetry, Doppler OCT, OCT-based optical microangiography (OCTA), fluorescence-based angiography and two-photon microscopy, have been used in the past to investigate structural, vascular and functional changes in the human and animal retina in health and disease. Here, we utilize a combined OCT+ERG system to investigate the relationship between neuronal and blood flow responses to visual stimulation (so called neurovascular coupling) in the healthy and glaucomatous retina.

For this study we used a fiber-optic based SD-OCT system that is powered by a superluminescent diode-based light source. The detection end of the system is comprised of a high-resolution spectrometer and a linear array camera with 250 kHz maximum readout rate. A telecentric pair of achromat lenses was used to generate a 2 mm wide optical beam incident on the cornea with optical power of 1.1 mW. A visual stimulator comprised of 4 LEDs (blue, red, green and white) and pair of achromat lenses was integrated into the OCT retinal imaging probe to deliver Maxwellian illumination of the retina. The visual stimulator was connected to a commercial electroretinography system (ERG), that allowed for precise control of the color, intensity, duration and pattern of the visual stimulus that was delivered to the human retina. Functional retinal OCT and ERG data were recorded synchronously from human subjects and rats (rodent model of glaucoma). The imaging studies have received full ethics clearance from the University of Waterloo Office of Research Ethics. OCT+ERG recordings were acquired over period of 10 seconds with 2s pre-stimulus period. The color, intensity, duration and pattern of the visual stimulus were varied to explore dependence of the recorded physiological and blood flow changes on these parameters. Custom Matlab-based algorithms were used to process and analyze the OCT data.

Figure 1 shows high resolution morphological images of the healthy human retina: (A) B-scan where all major retinal layers are resolved, enface images of the (B) retinal surface, (C) the outer plexiform layer showing capillary network, (D) inner – outer segment photoreceptors junction, (E and D) magnified views of the same layer showing reflections from individual cones. Note that all images are single-shots and no averaging or post-processing was applied. Figure 2 shows results from a functional blood flow test with the following stimulus parameters: color – blue (440 nm); pattern – flicker, duration – 1s, intensity – 0.8 Cd.s/m². An enface view of the retinal ONH, generated from a volumetric OCT image is shown in Fig. 2A. The red lines show the approximate location of the circular scans. A circular B-scan (Fig. 2B) shows cross-sections of major retinal blood vessels at the ONH. Fig. 2C shows stimulus-induced changes in the blood flow of a single retinal blood vessel over a period of 10s. The black and red lines correspond to the measured raw and filtered blood flow data respectively. The blue area in the graph marks the timing and duration of the visual stimulus. The blood flow shows ~ 500% peak increase relative to the baseline (dark recording). The latency of the peak response was ~2s relative to the onset of the visual stimulus.

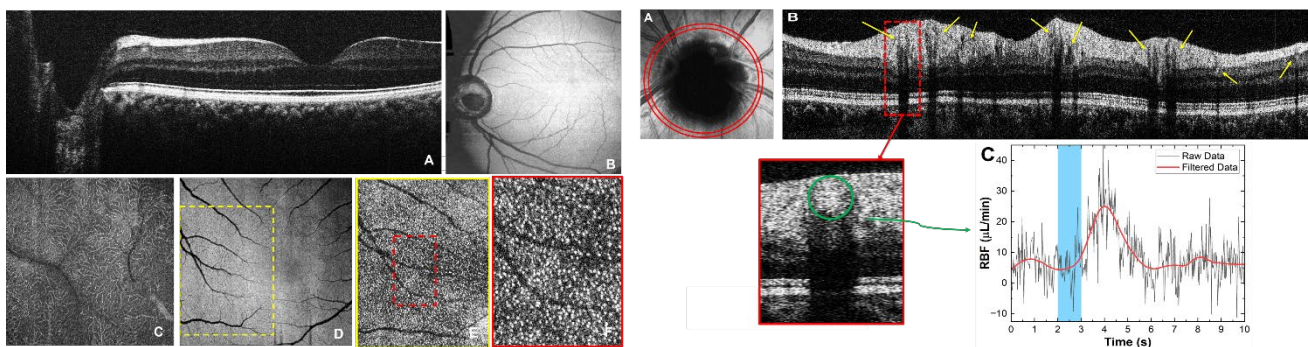


Figure 1: (A) B-scan and (B) En-face view of the healthy human retina. En-face views of (C) the outer plexiform layer showing capillary network, (D) inner-outer segment junction, (E) magnified view of the ROI marked with yellow dashed line, (F) magnified view of the ROI marked with red dashed line where white dots correspond to reflections from cone photoreceptors.

Figure 2: (A) Enface view of the ONH with red circles marking the OCT scanning pattern. (B) Circular B-scan showing retinal blood vessels around the ONH (yellow arrows); (C) Transient changes in the blood flow measured from a blood vessel in response to blue flicker stimulation.

Multimodal imaging platform to study cartilage degeneration using compression-based depth-resolved polarisation-sensitive optical coherence tomography and vibrational spectroscopy

Frédérique VANHOLSBECK^{1,2}, Darven Murali THARAN^{1,2}, Pierre DABOT, Marco BONESI^{1,2}, Daniel EVERETT^{2,4}, Matthew GOODWIN^{1,2}, Sue McGLASHAN³, Cushla McGOVERIN^{1,2}, and Ashvin THAMBYAH⁴

¹Department of Physics, ²The Dodd-Walls Centre for Photonic and Quantum Technologies, ³Department of Anatomy and Medical Imaging, ⁴Department of Chemical and Materials Engineering, The University of Auckland, New Zealand

f.vanholsbeeck@auckland.ac.nz

ABSTRACT

Osteoarthritis (OA) affects millions worldwide, incurring substantial healthcare and productivity costs, particularly in Aotearoa New Zealand. Early OA onset disrupts the collagen network of the articular cartilage (AC), compromising its mechanical integrity and altering tissue birefringence and biochemical composition. To meet the urgent need for early OA detection, we are developing a multimodal imaging platform to study cartilage deformation in real time during compression. Our aim is to mimic standard mechanical tests done on cartilage while allowing real time imaging. This platform utilizes polarization-sensitive optical coherence tomography (PS-OCT), vibrational spectroscopy and displacement sensors. Our research examines AC under compression to evaluate its response to mechanical stimuli.

PS-OCT allows to identify micro-scale collagen network disruptions indicative of early-stage damage. In healthy AC, collagen fibrils form a characteristic chevron pattern that effectively dissipates compressive forces [1]. The loss and/or deformation of this chevron boundary is a clear indicator of AC degeneration.

We introduce, for the first time to our knowledge, a dynamic depth-resolved PS-OCT approach that enables mechanical testing of biological tissues under creep loading using a custom-built PS-OCT system paired with a compression imaging head. By applying a fixed load on the cartilage with the compression head, we simultaneously acquire a time sequence of high-resolution PS-OCT data to observe cartilage deformation under creep loading.

Our experimental setup enables depth-resolved quantification of the optical axis (OpAx) and birefringence, correcting for erroneous effects commonly seen in cumulative PS-OCT imaging. Birefringence reflects the organization of fibrillar structures, while OpAx indicates the orientation of these fibrils. We have developed a novel tractography algorithm called density encoded line integral convolution (DELIC) to enhance the visualization of the OpAx. This method builds upon the traditional line integral convolution technique by incorporating sample birefringence into the tractography density. DELIC operates by using a sparse texture composed of points whose density is determined by the sample's birefringence. These points are then convolved based on the OpAx vector field. Conceptually, this process is akin to placing ink droplets on a plane at varying densities and smearing them to reveal the underlying OpAx vector field. To achieve a point density that accurately represents the birefringence, we employ weighted Centroidal Voronoi Tessellation (CVT)[2]. Our results demonstrate that compression-based PS-OCT enables non-destructive observation of the distinctive chevron pattern in cartilage and its changes during creep loading. The location and shape of the chevron pattern were validated using differential interference contrast microscopy.

Similarly, using the same compression head paired, we register Raman spectra during compression at different point on the surface of the cartilage inside the area scanned by OCT. Analysis of these spectra will give us access to the dynamics of biochemical content.

In summary, our multimodal-imaging platform using compression-based depth-resolved PS-OCT and spectroscopy enhances our understanding of cartilage biomechanics and the impact of articular cartilage degeneration. It will allow to develop a comprehensive cartilage model and to pave the way for improved diagnostic strategies for cartilage-related conditions.

REFERENCES

- [1] A. Thambyah and N. Broom, "Micro-anatomical response of cartilage-on-bone to compression: mechanisms of deformation within and beyond the directly loaded matrix," *Journal of anatomy* 209(5), 611–622 (2006).
- [2] Q. Du, M. Gunzburger and L. Ju, "Advances in studies and applications of centroidal Voronoi tessellations," *Numerical Mathematics: Theory, Methods and Applications* 3(2), 119-142 (2010).

The Role of Red Blood Cells as Biomarkers in Human Aging and a Potential Route for Reverse-Aging

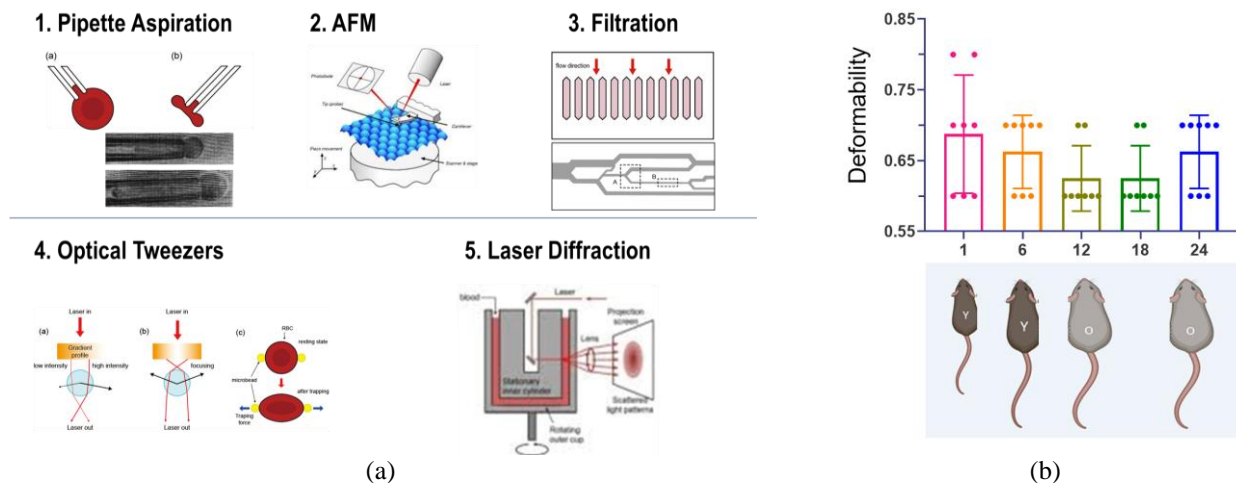
Sehyun Shin¹, Jihee You¹, Aekyung Kim² and Dobg-Ik Kim²

¹School of Mechanical Engineering, Korea University, Republic of Korea,
²Department of Internal Medicine, Sungkyunkwan University, Republic of Korea

lexerdshin@korea.ac.kr

ABSTRACT [HEADING 1 STYLE]

Red blood cells (RBCs) have emerged as significant biomarkers of the aging process, undergoing various changes associated with human aging and age-related diseases. A recent study performed a comprehensive literature search using online databases PubMed and ScienceDirect with the keywords “RBC as a biomarker of human aging”, “erythrocytes AND biomarkers AND human aging”, and “red blood cells”. There were a total of 474 relevant studies, which indicates that erythrocyte parameters, such as hemoglobin concentration, mean corpuscular volume, erythrocyte distribution width, erythrocyte membrane integrity, oxidative stress, and metabolism, undergo significant changes and are closely related to the aging process. Our research focused on the oxygen delivery capacity through capillary circulation, emphasizing that these functions are entirely dependent on the deformability of red blood cells. Therefore, the aim of our study is to explore the impact of human aging on RBC indices, particularly their correlation with erythrocyte deformability. Furthermore, we propose to pioneer new pathways for reversing aging by conducting comprehensive research on platelets and extracellular vesicles circulating in the blood, alongside improving the deformability of red blood cells.



Figures: (a) Techniques to measure RBC deformability, (c) Deformability variation with ages

Microcavity enhanced SERS biosensing

Chunxiang Xu

¹ School of Electronic Science and Engineering, Southeast University, Nanjing 210000, China

xcxseu@seu.edu.cn

ABSTRACT

Surface enhanced Raman scattering (SERS) has been widely investigated for sensitive bio-detection mainly based on the huge electromagnetic enhancement of localized surface plasmon resonance (LSPR). While whispering-gallery mode microcavity can also confine optical field near the cavity surface through totally inner wall reflection. It would be sufficiently enhanced the light-matter interaction through synergistically coupling of LSPR and WGM. In our researches, different metal nanoparticles, such as Au and Ag, were decorated on ZnO microrods or PS spheres to form complex microcavities as SERS substrates. Then the bio-sensors were constructed through further surface functional assembling of biomolecules. As results, high selective detection was carried out for various bio-targets, which include organic small molecules such as R6G, cardiac biomarkers such as cTnI, Alzheimer's biomarkers such as A β 1-42 and p-Tau181 protein, and so on. The limit of detection for most of the samples is as low as single molecular level. In addition, the sensors have also been utilized for living cell assaying in single cell level, such as *S. aureus*, *E. coli* and nasopharyngeal cancer cells. More importantly, it creates a platform in microfluidic chips for multi-samples real-time measuring synchronously.

Novel Raman approaches for the neurosurgical guidance

Daniel C. Côté^{1,2}

¹Department de physique, Génie Physique et Optique, Université Laval, Canada

²CERVO Brain Research Center, Canada

dccote@cervo.ulaval.ca

ABSTRACT

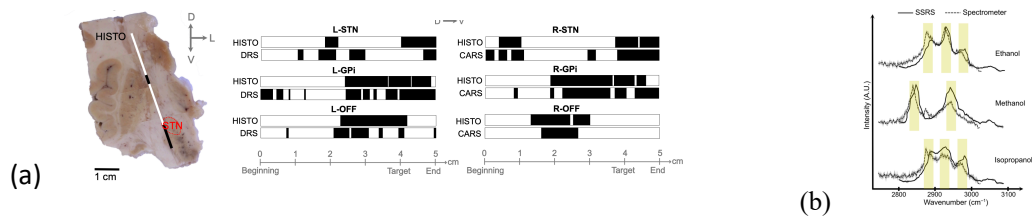
The limitations of conventional Raman spectroscopy are well known: its low efficiency due to scattering limits its applicability in highly scattering tissue. We show here that coherent Raman provides significant improvements in a clinical environment. We demonstrate in a Raman spectroscopy and optical techniques such as diffuse reflectance spectroscopy (DRS) and coherent anti-Stokes Raman scattering spectroscopy (CARS) are valuable for tissue identification, particularly in neurosurgical applications[1]. In addition to these results, we address the limitations of Raman spectroscopy by developing a wavelength-swept Raman spectroscopy approach that has the potential to be even more powerful than coherent Raman in tissue[2].

First, we demonstrate all the necessary elements for neurosurgical guidance. DRS and CARS spectra are acquired using a custom-built optical probe integrated into a commercial deep brain stimulation electrode. The hybrid probe is tested in a human cadaver by targeting specific brain regions and acquiring spectra at constant position increments during lead insertion. Spectra are analyzed to classify tissue composition and compared with histological classifications. We show how this can be used to locate the electrode, potentially in real-time. DRS and CARS spectra obtained during DBS lead insertion can identify white and gray matter, and DRS shows potential for detecting blood presence due to hemoglobin's strong optical absorption. PCA results support these findings.

Second, our wavelength-swept Raman spectroscopy configuration demonstrates a significantly stronger signal in simulations and a 200× improvement in photon detection experimentally compared to conventional spectroscopy setups. Data from a fixed monkey brain achieves 99% classification accuracy via k-nearest neighbor analysis.

Conclusions

Our work highlights the feasibility of using DRS and CARS for real-time neurosurgical guidance during DBS and showcases the potential of wavelength-swept Raman spectroscopy for tissue identification in highly scattering media, such as the brain. The developed techniques offer enhanced signal detection and tissue classification capabilities, paving the way for future in vivo applications and integration into standard clinical procedures. This could streamline DBS surgeries by potentially replacing microelectrode recordings (MERs) and reducing surgery time.



Figures: (a) Brain insertion tracts (left) and grey-white matter identification (right) along the tract. (b) Comparison of Swept-Source Raman Spectroscopy and Spectrometer-based Raman spectroscopy.

REFERENCES [HEADING 1 STYLE]

- [1] S. Jerczynski *et al.* Accepted for publication *SPIE J. Neurophotonics*, June 2024
- [2] E. Parham *et al.* Accepted for publication *SPIE J. Neurophotonics*, June 2024

Clinical translation of Low-cost Swept Source OCT - how low can you go?

Rainer Leitgeb^{1,2}, Milana Kendrisic^{1,2}, Stefan Georgiev³, Jonas Nienhaus¹, Matthias Salas^{1,2}, Clemens Vass⁴,
Oliver Findl³, Wolfgang Drexler¹, Tilman Schmoll⁵

¹Center for Medical Physics and Biomedical Engineering, Medical University of Vienna, Austria

²Christian Doppler Laboratory OPTRAMED, Medical University of Vienna

³Hanusch Hospital, VIROS, Austria

⁴University Clinics of Ophthalmology and Optometry, Medical University of Vienna, Austria

⁵Carl Zeiss Meditec, Germany

rainer.leitgeb@meduniwien.ac.at

ABSTRACT

Low-cost optical coherence tomography (OCT) has recently gained significant attention due to the increasing demand for OCT devices outside clinical settings as for example has been become evident during the recent pandemics. Among the different variants of OCT, swept source OCT combines the potential to be realized as compact system with the advantage of Fourier domain OCT regarding speed and sensitivity. A primary challenge in developing affordable swept-source OCT (SS-OCT) systems is the high cost of the laser. In this study, we examine the usability as well as the challenges of using a vertical-cavity surface-emitting laser (VCSEL) source at 850 nm. Such sources are used in billions in the automobile as well as cell phone and telecommunications industry and come therefore with a low price tag. Our work leverages on the strong dependence of the output wavelength of such sources on the temperature. The latter can be controlled through the driving current [1,2]. We discuss the impact of various tuning parameters of the driving current—such as frequency, duty cycle, modulation curve, and temperature—on the bandwidth VCSEL source. By optimizing these parameters, the laser achieves a tuning bandwidth of 10.2 nm at a 50 kHz A-scan rate. Utilizing deep-learning-based denoising significantly reduced noise in individual scans [3]. The question remains, whether the achieved axial resolution is of clinical value regarding diagnostics. We discuss different application settings in ophthalmology such as biometry, anterior eye, and posterior eye imaging. Finally, an outlook is given on potential improvements on the performance of VCSEL sources regarding OCT as well as OCT angiography.

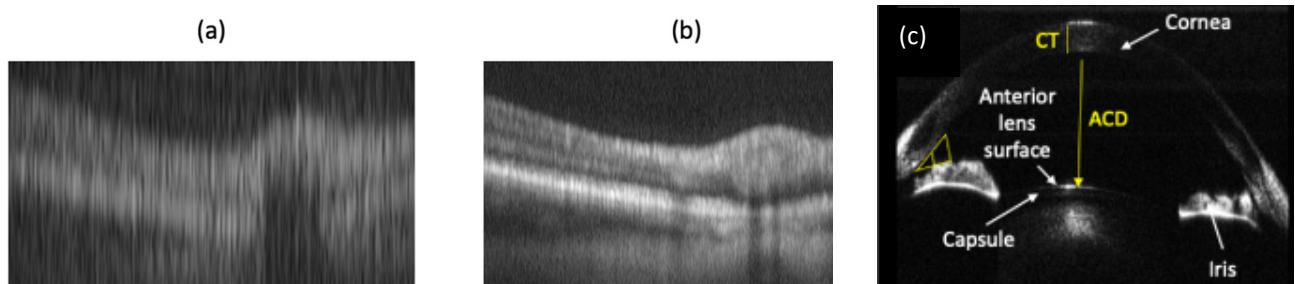


Figure: Impact of tuning range on potential diagnostic value (a) retinal imaging with 6nm tuning range (b) retinal imaging with 10nm tuning range (c) anterior chamber imaging with 9nm tuning range[3]

REFERENCES

- [1] M. Kendrisic et al, Opt. Lett. 48(11), 3079, 2023.
- [2] S. Moon and E. S. Choi, Biomed. Opt. Express 8(2), 1110, 2017.
- [3] M. Kendrisic et al, Biomed. Opt. Express 15, 4719-4736, 2024.

Applications and challenges of clinical adaptive optics optical coherence tomography

Michael Pircher

Center for Medical Physics and Biomedical Engineering, Medical University of Vienna, Austria

Michael.pircher@meduniwien.ac.at

ABSTRACT

Adaptive optics optical coherence tomography (AO-OCT) provides details on the cellular structure of retinal tissue. This includes visualization of various cell types such as photoreceptors, retinal pigment epithelium cells, ganglion cells and microglia. However, translation of this technology to a clinical setting is associated with various challenges and the clinical benefit in terms of diagnosis or treatment control is less clear. One of the challenges is associated with the limited field of view of AO-OCT volume recordings that typically cover only an area of $1^\circ \times 1^\circ$ ($300 \times 300 \mu\text{m}^2$). This prevents feasible imaging of larger areas in a clinical setting and greatly lowers the clinical attractiveness of this technology. With the Vienna AO-OCT instrument that supports a larger field of view of $4^\circ \times 4^\circ$, we demonstrate clinical imaging over this extended field of view in healthy volunteers and patients. Thereby, we specifically target the major vessel arc that can be covered in a few volume recordings (see. Fig. 1A). The entire examination time per subject (including alignment and imaging at various locations) could be kept below 20 minutes. By setting the focus of the system on the anterior retinal layers, details of retinal epi-vasculature structures including thickness of vessel walls could be revealed (cf. Fig. 1B to 1F). The system was used to image healthy volunteers and patients with different stages of diabetic retinopathy to investigate potential vascular changes that are caused by the disease. One additional asset of the system is the implementation of a pyramid wavefront sensor that allows for fast AO correction and detailed imaging of the pupil plane. Thereby, various conditions of the lens can be visualized including focal cataracts or artificial lenses (cf. Fig. 2).

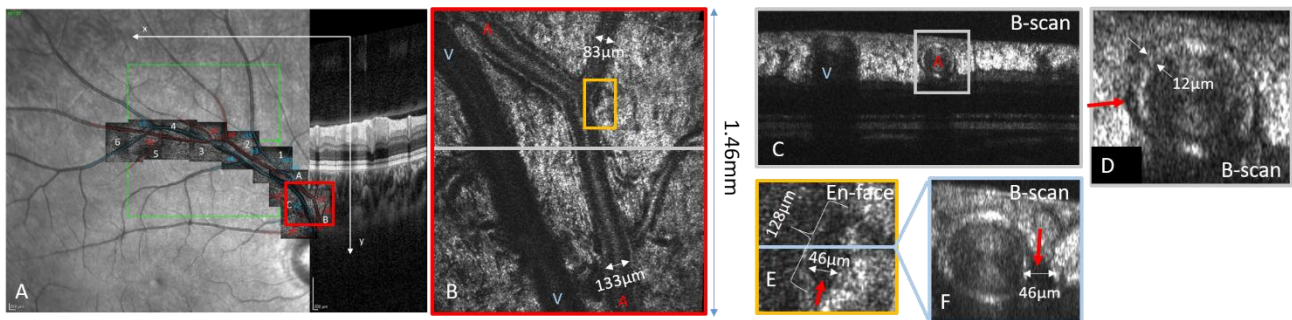


Fig.1. Representative AO-OCT image data along the major vessel arc of a healthy volunteer. A) Fundus image and overlaid the field of view that was covered by the AO-OCT, B) en-face image of a single location, C) B-scan at the location indicated in B, D) enlarged view of region of interest indicated in C, E) Enlarged view of region of interest in B, F) B-scan indicated in E. The red arrows point to hypo-reflective structures

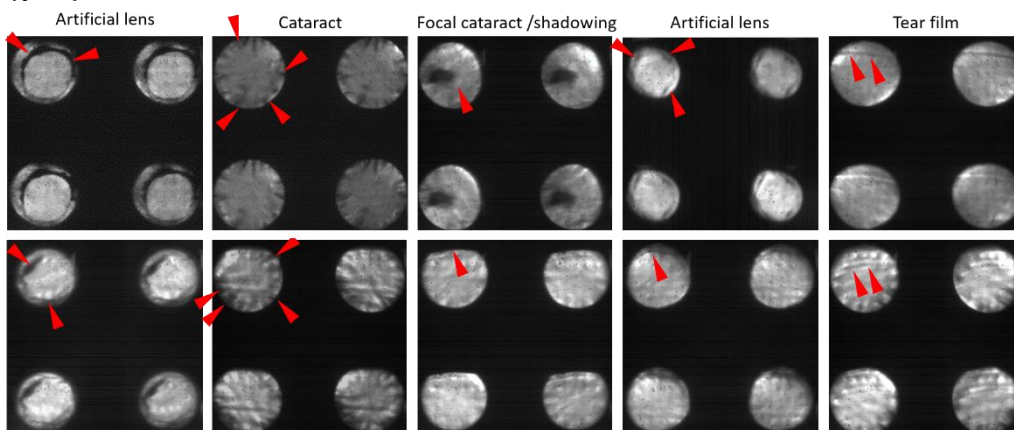


Fig.2. Representative pyramid wavefront sensor images recorded during AO-OCT imaging, illustrating various lens conditions in patients with diabetic retinopathy.

Non-Perturbative Optical Methods of Assessing Corneal Mechanical Properties

Brecken J BLACKBURN¹, John P MOGYORDY¹, Michael W JENKINS¹, William J DUPPS² and Andrew M ROLLINS¹

¹Biomedical Engineering, Case Western Reserve University, USA
²Ophthalmology, Cole Eye Institute, Cleveland Clinic, USA

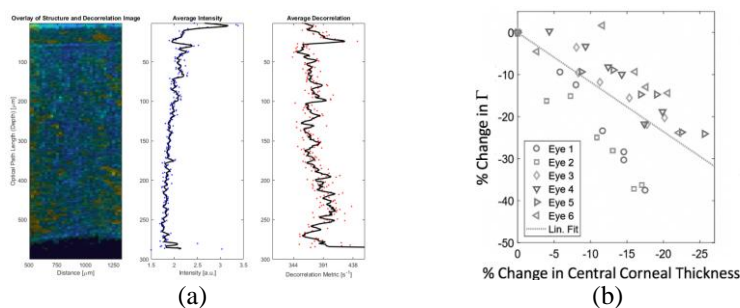
bjb125@case.edu

ABSTRACT

The mechanical properties of the cornea contribute significantly to the cornea's morphological response to refractive surgery, as well as ectatic disease states and corresponding treatment. Accordingly, there is growing interest in the measurement of cornea biomechanics in the clinic. Gaining insight into an individual patient's corneal biomechanics may improve risk assessment for refractive surgery, improve refractive surgery visual outcomes by allowing surgical plans to include individual corneal stiffness, and allow for earlier detection and monitoring of ectatic disease.

Many of these mechanical assessment modalities require a method of perturbing the cornea in order to observe its direct mechanical response. In practice, a non-perturbative technique may have advantages in terms of clinical adoption due to reduced hardware costs and lesser regulatory burden, especially if this approach may utilize existing imaging hardware. Non-perturbative techniques such as Brillouin spectroscopy[1], OCT image analysis (including temporal, dynamic, and spectral OCT techniques) have shown sensitivity to the mechanical state of the cornea without requiring external perturbation, even if conducted *in vivo* (see Fig 1 for an example of temporal decorrelation OCT analysis). However, each technique on its own may provide a limited amount of information about the mechanical state of the cornea and may be confounded by other factors that make direct mechanical interpretation (for instance, for use in surgical planning) difficult. Notably, the hydration state of the cornea dramatically influences mechanical properties and is variable over relatively short periods of time and between individuals.

The goal of this work is to demonstrate that by combining information across multiple non-perturbative OCT-based methods it is possible to separate mechanical properties which vary as a function of hydration from the contribution of the remaining protein components of the corneal stroma. In this work, the non-perturbative approaches implemented are OCT-based temporal (phase-decorrelation[2]), spatial, and spectral analysis. The methods of validation are benchtop elastography using a custom-built static compression elastography setup optimized for corneal tissue geometry and near-IR spectroscopy (NIRS). To demonstrate the approach, *ex vivo* corneas are imaged using OCT while their hydration state is varied. The same corneas are also assessed at the same range of hydration states using NIRS, which can accurately quantify water content[3], and benchtop elastography, which more accurately quantifies the viscoelastic response of the cornea. The resulting combination of PhD-OCT and NIRS data show that variable hydration content of the cornea can be disambiguated from the mechanical contribution of the rest of the corneal composition, which varies between individual corneas. Establishing in capability amongst non-perturbative methods of corneal biomechanical analysis is an important step in translating these methods to the clinic and delivering robust assessment which can be relied on for surgical planning.



Figures: (a) Temporal OCT signal correlation analysis (PhD-OCT) cross section of a cornea in vivo (b) Hydration changes (assessed by central corneal thickness) vary the dynamic mechanical properties measured by temporal decorrelation OCT.

REFERENCES

- [1] Zhang H, et al. Biomedical Optics Express. 2022 Dec 1;13(12):6196-210.
- [2] Blackburn BJ, et al. Investigative ophthalmology & visual science. 2019 Jan 2;60(1):41-51.
- [3] Qi P, et al. Journal of Biophotonics. 2019 Oct;12(10):e201800472.

Characterization of a combined fluorescence and spatial frequency domain imaging system to monitor photodynamic therapy dosimetry

Alec Walter¹ and E. Duco Jansen^{1,2}

¹*Department of Biomedical Engineering, Vanderbilt University, USA*

²*Department of Neurological Surgery, Vanderbilt University Medical Center, USA*

Duco.jansen@vanderbilt.edu

ABSTRACT

Current methods of measuring dosimetry for photodynamic therapy (PDT) have proven to be inadequate due to their inability to provide accurate, real-time, and spatially-resolved monitoring, unobtrusively, without interrupting the treatment. To address this need, we present a multi-modal approach and validate this combined treatment and dosimetry system capable of monitoring implicit and explicit dosimetry during PDT. By employing both fluorescence imaging and spatial frequency domain imaging (SFDI), the combined imaging system would be able to provide information on the spatial distributions of photosensitizer concentrations, tissue oxygenation, and delivered light dose, all while monitoring the photobleaching dynamics of the photosensitizer. While the concept behind the combined system is not specific to any one photosensitizer, this work focused on designing the system for the endogenous PDT of Gram-positive bacteria using coproporphyrin III. The overall performance of the system was assessed, with the accuracy, precision, and resolution of the SFDI-derived optical property maps being determined to fall within comparable ranges to other systems, despite the 1.0 mm⁻¹ spatial frequency utilized for the shorter wavelengths. After validating the ability of the system to correct for tissue-like optical properties, and thus produce accurate quantitative fluorescence images, a preliminary assessment of aPDT photobleaching dosimetry was performed, finding high correlation with treatment outcome. Overall, the developed imaging system showcases the potential to enable more thorough analysis of PDT dosimetry and the impact of different variables on treatment outcome.

Clinical implementation of near-infrared autofluorescence (NIRAF) for guiding endocrine neck surgery

Anita Mahadevan-Jansen^{1,2}, Alexandria Cousart¹, Giju Thomas¹, Parker Willmon¹, Colleen Kiernan², Carmen Solorzano²

¹*Department of Biomedical Engineering, Vanderbilt University, USA*

²*Department of Surgery, Vanderbilt University Medical Center, USA*

Anita.mahadevan-jansen@vanderbilt.edu

ABSTRACT

Thyroid and parathyroid diseases rely on surgery for definitive treatment. In these surgeries, parathyroid glands are difficult to distinguish from the thyroid and surrounding tissues in the neck, due to its small size and variability in position. Complications occur when the parathyroid is accidentally injured or removed during thyroidectomies. Hypoparathyroidism and hypocalcemia can occur, resulting in serious long term effects. The incidence of hypocalcemia is reported to occur in 9-21% of total thyroidectomies. In fact, hypocalcemia is the most common cause of malpractice litigation after endocrine surgery. Therefore, there is a critical need for a sensitive tool that can identify the parathyroid glands intraoperatively, regardless of disease state.

We have successfully developed near infrared autofluorescence for anatomical identification of the parathyroid gland regardless of its disease state with near 100% accuracy. The Food and Drug Administration has cleared an imaging as well as a probe based device based on NIRAF as an adjunct tool for label-free intraoperative parathyroid gland identification. A clinical trial was designed to determine the effect of using the probe based NIRAF system in terms of surgical effectiveness, surgeon effectiveness as well as patient outcome.

Here, we present our preliminary impressions from using the device as an adjunct to the surgeon's assessment of the parathyroid gland, as well as the results obtained when the probe based device is used by surgeons as part of the clinical work flow. Patients undergoing thyroidectomies and parathyroidectomies were recruited in a randomized clinical trial. Target tissues were intraoperatively assessed and the performance of probe based NIRAF was compared to the surgeon's visual assessment in parathyroid gland identification. A preliminary analysis of the results shows that probe based NIRAF yields an accuracy of 94.3% and increases the confidence of all participating surgeons in correctly identifying the parathyroid gland regardless of surgeons' experience.

Probe-based NIRAF detection has been repeatedly shown to be effective as an adjunct device to intraoperatively identify PGs for surgeons of varied training and experience.

Plasmonic materials based biomedical applications

Xiangwei Zhao^{1,2}

¹*State Key Laboratory of Digital Medical Engineering, School of Biological Science and Medical Engineering, Southeast University, China;*

²*Southeast University Shenzhen Research Institute, China*

xwzhao@seu.edu.cn

ABSTRACT

Surface plasmon (SP) derives from the interaction of light and matter at nanoscale accompanied by novel physical phenomena, which enables localized surface plasmon resonance, surface enhanced Raman spectrum and so on. In our study, we utilized plasmonic materials in biomedical applications like biosensing, bioimaging and biomanipulations. By engineering plasmonic materials and their nanostructure, as well as factors that affect the surface plasmon propagation, we showed that high sensitive biosensing of molecules and cells could be realized for convenient and rapid point of care testing (POCT) and single cell could be manipulated by SP as well. Also, SP could help gaining the molecule fingerprinting profiles of tissues in combination with spatial bio-omics data.

REFERENCES [HEADING 1 STYLE]

- [1] RP Chen et al, *Small*, 2002801, 20201996.
- [2] SY Kang et al, *Small Methods*, 2201379, 2023.
- [3] Y Lu et al, *Journal of Hazardous Materials*, 133763, 2024.

Structural and molecular imaging in vivo: PS-OCT and Immuno-OCT

Johannes F. de Boer¹

¹*Department of Physics and Astronomy, VU Amsterdam, The Netherlands
Laserlab Amsterdam, VU Amsterdam, The Netherlands*

j.f.de.boer@vu.nl

ABSTRACT

Optical Coherence Tomography provides high resolution cross sectional images of tissue in vivo. We provide two extensions to standard structural OCT imaging: Polarization sensitivity and molecular specific contrast (Immuno-OCT). Polarization sensitive OCT (PS-OCT) provides unique contrast in tissue for birefringent structures such as collagen, nerves and muscle. I will present endoscopic PS-OCT results in the human lung in vivo to diagnose airway smooth muscle thickness in healthy and Asthma patients, and the presence of fibrosis in the distal lung for improved diagnosis of Interstitial Lung Disease. For molecular contrast, Optical Coherence Tomography (OCT) was combined with Near Infrared Fluorescence (NIRF) imaging of fluorescently labelled monoclonal antibodies, to provide both structural information to a few millimeters in depth, *and* molecular contrast. This technique, Immuno-OCT, can be used to image the epithelia of hollow organs, and in particular the esophagus, where the monitoring of Barrett's esophagus (a metaplastic replacement of squamous tissue into columnar tissue) is crucial to the early-stage detection of esophageal adenocarcinoma (EAC). A motorized capsule endoscope was fitted with a double clad fiber for dual-modality OCT-NIRF imaging of the esophagus. We present the first *in vivo* imaging of Barrett's esophagus patients after intravenous administration of fluorescently labeled Bevacizumab-800CW, a targeted monoclonal antibody labelled with IRDye800-CW, which binds to vascular endothelial growth factor. To the date of submission, two patients have successfully undergone *in vivo* Immuno-OCT imaging. Resected samples from each patient were also imaged *ex vivo* using a galvanometer scanning system and full-field fluorescence scanning system.

Investigating the Mechanopathology of Soft Orthopedic Tissues in Degenerative Joint Disease

Seemantini K. Nadkarni^a

^aWellman Center for Photomedicine, Massachusetts General Hospital, Harvard Medical School, Boston, MA, USA

Osteoarthritis (OA) is a degenerative joint disease that affects millions of people worldwide and is a leading cause of disability, particularly among the aging population. While inflammation and cartilage degradation are widely studied in OA, increasing evidence suggests that mechanopathology, characterized by the role of mechanical behavior and its influence on tissue function, plays a crucial role in the initiation and progression of OA. The progression of OA is accompanied by the mechanical transformation of joint soft tissues, significantly contributing to functional deficits. In particular, orthopedic tissues rely on an intricate interplay between the solid matrix and interstitial fluid constituents to maintain normal function. Degenerative mechanopathological processes involve both the solid (elastic) and fluid (viscous) components to be compromised, severely impacting cellular and physiological function, ultimately resulting in progressive loss of joint function. Although reduction in elastic modulus associated with degradation of the solid matrix has long been investigated in orthopedic diseases, the contribution of viscous behavior and its role in governing tissue degeneration and repair remains largely unexplored. We implement *Speckle rHEologicAl micRoscopy (SHEAR)*, a novel optical imaging technique invented in the Nadkarni Lab, that maps the micromechanical landscape of tissue to investigate the viscoelastic behavior of healthy and injured soft orthopedic tissues of knee joints. SHEAR is based on natural thermal motion of native light scattering structures, enabling passive, noncontact measurement of tissue micromechanics. We conduct SHEAR measurements of shear elastic and viscous moduli in soft tissues and biofluids critical to the function of knee joint; our results demonstrate excellent correlation with conventional rheometry ($R=0.99$, $P<0.0001$). Furthermore, high-resolution SHEAR maps of both elastic and viscous behaviors unveil micromechanical features that are corroborated by Histology (Fig.1). We apply these capabilities to investigate micromechanical alterations that occur in orthopedic tissues as a result of injury and degenerative joint disease. Insights from such studies may greatly impact our understanding of the mechanopathology of joint disease and repair, and guide the development of tissue engineering and regenerative medicine approaches.

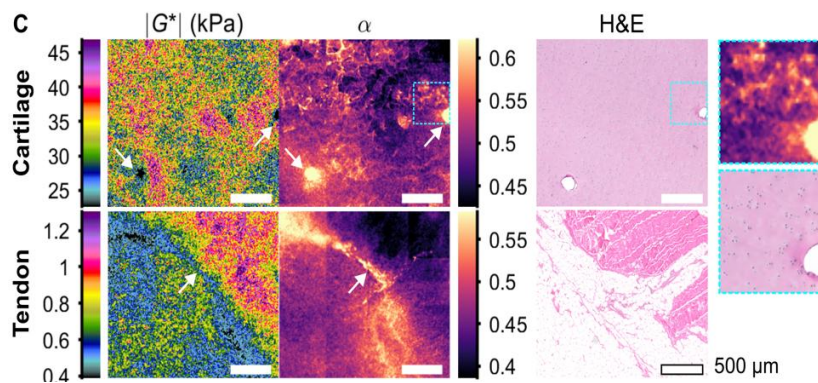


Figure 1. SHEAR mapping of viscoelastic moduli, G^* , and the accompanying viscoelastic index, α , in tissues of the knee joint with corresponding histology slides.

Research on some fundamental problems in classical optics

Xiaoyu WENG

College of Physics and Optoelectronic Engineering, Shenzhen University, China.

xiaoyu@szu.edu.cn

ABSTRACT

Throughout the development of optics, every breakthrough regarding new propagation behavior and special mechanism of light beam has not only deepened our knowledge but also opened a new era of optics, causing the field to flourish. Focusing on the properties of light beams, this report concentrates on three fundamental scientific problems in classical optics, including: (1) how to overcome the diffraction effect of light beams in free space[1]; (2) Property unification of inherent amplitude, phase and polarization within a light beam[2]; (3) Is there a stable vortex beam with non-integer topological charge in physics[3]? These three scientific problems mainly involve peculiar propagation behavior of non-diffractive light beams, new modulation principle of light field, and coupling of phase and polarization. We hope this report brings you different beauty of light beams.

REFERENCES

- [1] Xiaoyu Weng et al, Nat. Commun. 9, 5035, 2018.
- [2] Xiaoyu Weng et al, Fundam. Res. 1, 649–654, 2021.
- [3] Xiaoyu Weng et al, Adv. Photonics Res. 4, 2300152, 2023.

Laser Aggregometry of Red Blood Cells in a Microfluidic Channel Covered with Cultured Endothelial Cells

Andrei E. LUGOVTSOV¹, Petr B. ERMOLINSKY¹, Matvey K. MAKSIMOV¹,
Alexey N. SEMENOV², Olga N. SCHEGLOVITOVA³ and Alexander PRIEZZHEV¹

¹Physics Department, Lomonosov Moscow State University, Russia

²Dynamics of Fluids, Department of Experimental Physics, Saarland University, Germany

³N.F. Gamaleya National Research Center for Epidemiology and Microbiology, Russia

anlug@biomedphotonics.ru

ABSTRACT

Blood microbiology is essentially determined by the properties of blood plasma and the interaction between blood cells, i.e., the aggregation of red blood cells (RBCs), the interaction between different blood cells and endothelium, etc. Endothelial cells do not only act as an insulating layer between blood and tissues, but also play an important role in controlling the blood flow and influence blood cell properties, e.g., RBCs aggregation. RBCs can reversibly interact with each other under low shear stress forces forming linear and more complex structures. RBCs aggregation is mainly responsible for the non-Newtonian behavior of blood and regulates the microcirculation of blood in human body. Blood microrheology and its microcirculation are determined by the composition of blood plasma, deformability and interaction of blood cells, in particular, aggregation of RBCs and interaction between blood cells and endothelium. Endothelial cells (EC) covering the walls of blood vessels play an important role in regulating blood flow and also affect the properties of blood cells through the signaling molecules of gas transmitters secreted by them, in particular, nitric oxide (NO). The aim of the work is to measure the force of interaction between single RBC and EC at different concentrations of gas transmitter NO, as well as aggregation of RBCs in whole blood in microchannels covered by endothelium cells.

In the work, the ability of RBCs to aggregate in microchannels was measured using the laser aggregometry technique. The laser beam falls on a cuvette filled with whole blood, in the microchannel of which a flow is created. The intensity of backscattered light is detected. The smaller the size of the scattering particles (RBCs aggregates) and their number, the higher the detected signal. The pressure difference between the ends of the cuvette microchannel decreases monotonically over the measurement time (1-2 minutes), and at a certain point in time, a dynamic equilibrium is observed between the processes of aggregation and disaggregation of RBCs. The shear stress in the cuvette, calculated for this moment, is called the critical shear stress. This parameter characterizes the hydrodynamic strength of the RBCs aggregates. In the work, the laser tweezers were used, allowing manipulation of individual cells without mechanical contact, as well as measuring the interaction forces of RBCs and EC *in vitro*. ECs were obtained from the human umbilical vein (HUVEC) and grown at 37 degrees Celsius in a carbon dioxide environment on round glass slides to form a monolayer of cells. To stimulate NO production, EC were incubated with a solution of L-arginine in various concentrations of 0 - 1000 μM .

We demonstrated that hydrodynamic strength of erythrocyte aggregates (CSS) in whole blood of patients with arterial hypertension and in norm measured by laser aggregometry technique is lower in case of microfluidic channels covered by endothelial cells. This demonstrates the effect of the endothelial cells on the aggregation of RBCs. Also, it was shown that incubation of endothelial cells with L-arginine leads to a decrease in the forces of RBC aggregation at L-arginine concentrations up to 100 μM and its growth with a subsequent increase in concentration. The laser tweezers and laser aggregometry technique can be used to assess the interaction of RBCs and endothelial cells, as well as the aggregation properties of RBCs in microchannels with the endothelium. The presented results are important for understanding the influence of vascular endothelium on microrheology and blood microcirculation.

This research was funded by the Russian Science Foundation Grant No. 23-45-00027.

Detection of radiation-induced changes in the white matter of the rat brain based on attenuation coefficient estimation from optical coherence tomography data

Ksenia ACHKASOVA¹, Liudmila KUKHNINA¹, Alexander MOISEEV², Alexandra BOGOMOLOVA¹ and Natalia GLADKOVA¹

¹*Research Institute of Experimental Oncology and Biomedical Technologies, Privolzhsky Research Medical University, Russia*

²*Laboratory of Highly Sensitive Optical Measurements, Institute of Applied Physics of Russian Academy of Sciences, Russia*

achkasova.k@bk.ru

ABSTRACT

Radiation therapy is recommended in 95% of patients with glioblastoma (WHO Grade IV) after primary resection of the tumor focus, and is aimed at destroying the residual tumor cells in the tumor bed [1]. Unfortunately, despite active combined treatment, tumor recurrence occurs in nearly all patients, which requires repeated surgical intervention, the main purpose of which is to remove the tumor and surrounding damaged tissues while preventing damage to healthy tissues [2]. To accurately determine the boundaries of tumor resection it is necessary to analyze peritumoral white matter morphology. However, in the cases of repeated resections, the white matter morphology may be altered not only due to tumor growth, but also due to irradiation procedures. Thus, there is a need to develop new methods for diagnosing white matter changes that occur during radiation therapy that could be used during surgical intervention. In the consequence of optical coherence tomography (OCT) being a promising tool for brain tissue visualization, we decided to evaluate the effect of ionizing radiation on the scattering properties of the white matter of the brain using OCT.

The study was performed on Wistar rats (n=72 in total) divided into control and experimental groups. Animals from the experimental group undergone the brain irradiation procedure (once at a dose of 15 Gy per region of the right hemisphere of the brain). At 9 time points since the experiment had started (each 2 weeks until 14 weeks, at 6 and 7 months after irradiation), the animals were euthanized (5 rats from experimental group and 3 rats from the control group at each time point), followed by an OCT study and an immunohistochemical study of the frontal sections of the brain. Attenuation coefficient values were estimated from OCT data followed by building of en-face color-coded maps. The corpus callosum was chosen as the region of interest.

As a result, we discovered different stages of radiation-induced changes of the white matter. After 2 weeks from the irradiation procedure, we detected changes of attenuation coefficient values in the irradiated hemisphere, while at 6 and 12 weeks after the X-Rays exposure the attenuation coefficient values were decreased both in the irradiated and contralateral hemisphere. The detected changes were confirmed histologically: at the stage of 2 weeks after irradiation (acute phase of radiation-induced changes), a moderate edema occurred only in the area of the irradiated hemisphere, while at the stage of 6 and 12 weeks (early-delayed phase of changes) it was also found in the contralateral hemisphere and was characterized by significant severity, which indicates the spread of the process along the course of myelinated nerve fibers. At 6 and 7 months after irradiation procedure, we expected to detect the late phase of radiation-induced changes. However, the morphological changes of corpus callosum were not prominent in all cases, in particular, in 60% of cases, the development of mild or moderate edema, thickening of single myelin fibers, and the presence of fused fibers were observed, which was reflected in a statistically significant decrease in the attenuation coefficient. In cases where there was no development of edema and there were single changes in myelin fibers, the values of the attenuation coefficient remained unchanged.

Thus, in the course of this study, morphological changes in the corpus callosum resulting from exposure to ionizing radiation were recorded which were characterized by a decrease in its scattering properties, detected by OCT.

The study was financially supported by the Russian Science Foundation, grant No. 23-25-00118.

REFERENCES

- [1] A. Cabrera et al, *Pract. Radiat. Oncol* 6, 217, 2016.
- [2] J. Gerritsen et al, *Neurooncol. Pract* 9, 364, 2022.

Optical Criteria of the Pathological Liver during the Regeneration

Svetlana Rodimova¹, Vadim Elagin¹, Artem Mozherov¹, Maria Karabut¹, Alena Gavrina¹, Nikolay Bobrov², Vladimir Zagainov³, Elena Zagaynova^{1,4} and Daria Kuznetsova¹

¹Privolzhsky research medical university, Russia

²The Volga District Medical Centre of Federal Medical and Biological Agency, Russia

³Nizhny Novgorod Regional Clinical Oncologic Dispensary, Russia

⁴Lopukhin Federal Research and Clinical Center of Physical-Chemical Medicine of FMBA, Russia

srodimova123@gmail.com

ABSTRACT

Liver resection remains the most effective treatment of liver tumors [1]. However, in the presence of hepatic pathologies, the regenerative potential of the liver is significantly reduced [2]. Standard clinical methods do not allow assessing the condition of the liver intraoperatively and obtaining data on the metabolic state of hepatocytes. Modern label-free methods of multiphoton microscopy with second harmonic generation (SHG) and fluorescence lifetime imaging microscopy (FLIM) allow to determine the optical criteria of liver pathology and the degree of regenerative potential using bioimaging methods. To simplify the processing of FLIM data sets, we developed an automated approach based on convolutional neural networks.

Experiments were performed on Wistar rats. Liver fibrosis was induced by CCl₄ injections and steatosis was induced by 60% high-fat diet. At different stages of the pathology, we induced liver regeneration by 70% partial hepatectomy (PH). Using multiphoton microscopy, we analysed the structure of the liver tissue on 3rd and 7th day after PH, and also determined the intensity of NAD(P)H autofluorescence in the zones of low and high signal. Using FLIM, we determined the fluorescence lifetime contributions of the free and bound forms of NADH and NADPH. Standard morphological analysis and a standard biochemical blood test were performed as controls.

As a result, we revealed the characteristic optical criteria of hepatic state at different stages of liver regeneration with steatosis and fibrosis.

In the case of steatosis we identified: zones with a reduced signal of NAD(P)H fluorescence intensity, associated with lipid infiltration; the area of the zones increased with the development of pathology; few large areas of the second harmonic signal from foci of fibrosis; the absence of a sharp increase in a₂ and a₃ values on the 3rd day of regeneration for all stages of pathology. In the case of fibrosis we identified: zones with a reduced signal of NAD(P)H fluorescence intensity, associated with fibrous septa; the area of the zones increased with the development of pathology; multiple zones of second harmonic signal from fibrous septa; FLIM microscopy revealed the absence of a sharp increase in the values of a₂ and a₃ on the 3rd day of regeneration.

In the case of steatosis, the results obtained using the automatic approach are compared with the data obtained from the manual approach. In the case of fibrosis, the data from the two approaches differ, but the results from the automated approach are consistent with known metabolic changes characteristic of pathology.

With sufficient development of technology, all identified optical criteria can be used for intraoperative assessment of the liver condition and determination of the degree of pathology.

The work was supported by the Grant from the Russian Science Foundation No. 23-15-00421.

REFERENCES

- [1] E. Ramos et al, *Hpb*, 18, 389-396, 2016.
- [2] V.E. De Meijer, et al, *J Brit Surg*, 97, 1331-1339, 2010.

SIMULTANEOUS ASSESSMENT OF OXYGEN AND METABOLIC STATUS IN TUMOR MODELS USING FLIM AND PLIM TECHNOLOGIES

Anastasia KOMAROVA^{1,2}, Irina DRUZHKOVA², Leonid BOCHKAREV³, Artem MOZHEROV², Vladislav SHCHESLAVSKIY^{2,4} and Marina SHIRMANOVA²

¹Institute of Biology and Biomedicine, Lobachevsky State University of Nizhny Novgorod, Russia

²Institute of Experimental Oncology and Biomedical Technologies, Privolzhsky Research Medical University, Russia

³G. A. Razuvaev Institute of Organometallic Chemistry, Russian Academy of Science, Russia

⁴Becker&Hickl GmbH, Germany

komarova.anastasii@gmail.com

Tumor cells are well adapted to grow in conditions of variable oxygen supply and hypoxia by switching between different metabolic pathways. However, the regulatory effect of oxygen on metabolism and its contribution to the metabolic heterogeneity of tumors have not been fully explored. Time-resolved optical methods PLIM (Phosphorescence lifetime imaging) and FLIM (Fluorescence lifetime imaging) make it possible to non-invasively study the oxygen and metabolic status of tumors in real time. An urgent task is to combine these methods for simultaneous assessment of oxygenation and metabolism of tumors in *in vitro* and *in vivo* models.

The purpose of the work was to develop methodologies to assess oxygen and metabolic status using PLIM/FLIM microscopy in tumor models *in vitro* and *in vivo*.

Studies were carried out on CT26 mouse colorectal cancer cells in a cell monolayer model, 3D spheroids and *in vivo* tumors. Phosphorescent Ir(III)-based polymeric micelles were used as oxygen sensors [1]. Microscopic studies were carried out using a laser scanning microscope LSM 880 (Carl Zeiss, Germany) equipped with a TCSPC-based FLIM/PLIM module (Becker & Hickl GmbH, Germany). PIR3 phosphorescence was excited in a two-photon mode at a wavelength of 750 nm, and a signal was detected in the range of 600–740 nm. Metabolic status was assessed using the FLIM option by autofluorescence of the cofactor NAD(P)H: excitation at a wavelength of 750 nm and detection in the range of 450–490 nm. The laser excitation power on the sample was 6 mW, and the signal acquisition time was 120 s.

At the first stage of the work, the parameters for visualizing the phosphorescence of the PIR3 sensor on a laser scanning microscope in cancer cells were selected [1]. Next, a technique for simultaneous FLIM/PLIM was developed and tested on a monolayer of tumor cells, 3D tumor spheroids and mouse tumors [2]. Using the developed methodologies, it has been demonstrated that there is no heterogeneity of oxygen and metabolism in a monolayer of tumor cells (Fig. 1A). Under cell culture conditions, metabolic parameters highly correlated with oxygen level upon its variations ($r=0.73$). In spheroids, the inner layers of cells were more hypoxic compared to the outer layers. Metabolic differences were also observed between the outer and inner layers. *In vivo* mouse tumors had a high intratumoral and intertumoral heterogeneity in oxygen and metabolic statuses (Fig. 1B). In a tumor, the correlation between metabolic parameters and oxygen content was moderate, which indicated the contribution of factors other than oxygen to the regulation of cell metabolism.

Therefore, in this study we developed protocols for simultaneous imaging of oxygen and metabolism in *in vitro* and *in vivo* tumor models. The combination of PLIM and FLIM techniques presented here can be a valuable approach to better understand the fundamental features of tumor metabolism.

This work was partially supported by the Russian Science Foundation, project № 24-19-00618.

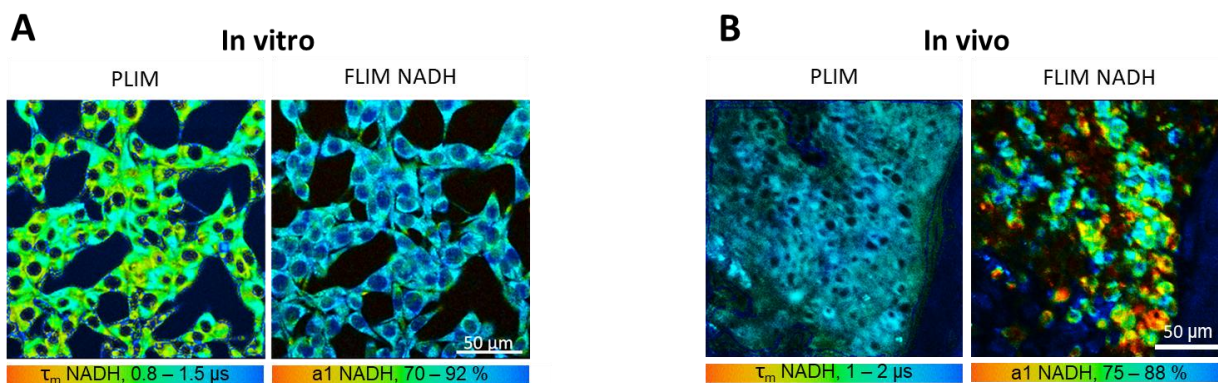


Figure 1: Simultaneous FLIM/PLIM imaging for assessing oxygen and metabolic status in monolayered cell *in vitro* (A) and in tumors *in vivo* (B).

REFERENCES

- [1] Y. Parshina et al, Int. J. Mol. Sci. 23, 10263, 2022.
- [2] A. Komarova et al, Methods Mol Biol. 2755, 91–105, 2024.

Laser-assisted drop-on-demand bioprinting for in-situ corneal repair

Hamid GOODARZI^{1,2,3}, Boda OM², Ahad MOHAMMADI^{1,2,3}, Jennyfer ZAPATA-FARFAN⁴, Michel MEUNIER⁴, May GRIFFITH^{1,2,3} and Christos BOUTOPOULOS^{1,2,3}

¹Department of Ophthalmology, Faculty of Medicine, University of Montreal, Canada

²Centre de Recherche Hôpital Maisonneuve-Rosemont, Montréal, Canada

³Institute of Biomedical Engineering, University of Montreal, Canada

⁴Engineering Physics Department, Polytechnique Montreal, Canada

christos.boutopoulos@umontreal.ca

ABSTRACT

Treating corneal wounds with corneal pro-regeneration biomaterials is an alternative to transplantation. The success of such treatment hinges on ensuring optical clarity and a smooth surface on the repaired cornea. Presently, the delivery methods for these biomaterials, typically employing conventional syringes, lack the precision required to restore the cornea's original topography. I will present a laser-based technology aiming to tackle this challenge. Our approach utilizes drop-on-demand (DOD) bioprinting, specifically laser-induced side transfer (LIST) [1-3], to deliver biomaterials to corneal wounds with precision.

By employing LIST, we successfully printed an acellular, medium viscosity, photo-crosslinkable ink based on Gelatin methacryloyl (GelMa), supporting the growth of human corneal epithelial cells (HCEC) and stromal cells in vitro (Fig. 1a). We established optimal printing conditions: a flow rate of 20 μL per minute, laser energy at 230 μJ , and a temperature of 37°C (Fig. 1b). Comparative analysis on printed and control samples revealed preserved optical and biomechanical properties, including optical transmission ($88\pm 2\%$ (printed) vs $90\pm 1\%$ (control)), diffuse reflectance ($1.0\pm 0.3\%$ vs $0.3\pm 0.1\%$), and storage modulus (1.9 ± 0.1 kPa vs 2.1 ± 0.1 kPa). Our in-situ repair workflow includes the use of optical coherence tomography (OCT) to characterize corneal wounds in cadaveric pig eyes (Fig. 1d-1e). We employed image processing to calculate the total volume of material required for wound filling and utilized LIST for precise delivery (Fig. 1f). Following UV crosslinking, we observed uniform wound filling, closely resembling the pre-wound corneal topography, with no trapped bubbles or off-target material deposition (Fig. 1g-1h). The sealed wound withstood pressure up to 38 ± 6 mm Hg, twice the average intraocular pressure (IOP).

Our ongoing research focuses on validating the printing workflow and assessing corneal wound healing capacity in vivo using a mouse model. In conclusion, our findings suggest that LIST printing effectively delivers corneal pro-regeneration biomaterials, achieving precise wound filling without compromising optical and biomechanical properties. With further refinement, this technology could emerge as a transplantation alternative for patients awaiting corneal grafts.

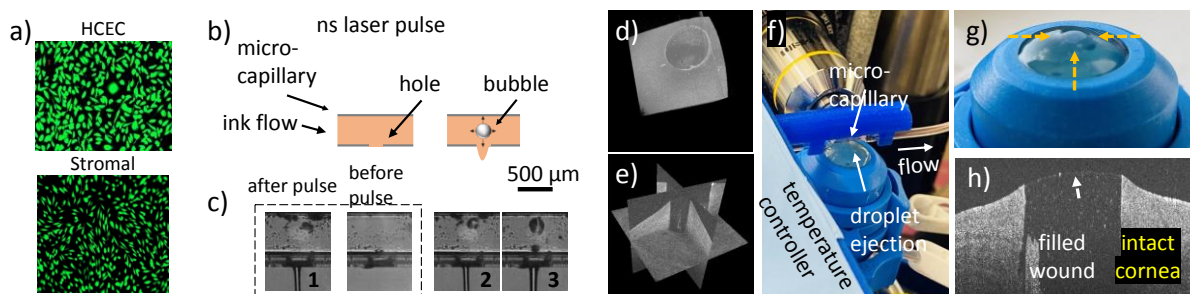


Figure 1: a) HCEC and stromal cell growth on GelMa-based sheets, b)-c) laser-assisted bioprinting, d-e) OCT mapping of corneal wounds, f) in-situ bioprinting, g)-h) images of a filled corneal wound.

REFERENCES

- [1] H Ebrahimi Orimi et al., Scientific Reports, 10(1), 9730 (2020)
- [2] K Roversi et al., BIO-PROTOCOL, 12(19), 1–12 (2022)
- [3] M Erfanian et al., IJB, in press (2024)

NIR photothermal immunotherapy of melanoma

Alissa Ramsey DORY^{1,2,3}, Ahad MOHAMMADI^{1,2}, Sebastien TALBOT^{4,5} and Christos BOUTOPOULOS^{1,2,3}

¹*Centre de Recherche Hôpital Maisonneuve-Rosemont, Montréal, Canada*

²*Institute of Biomedical Engineering, University of Montreal, Montreal, Quebec, Canada*

³*Department of Ophthalmology, Faculty of Medicine, University of Montreal, Montréal, Canada*

⁴*Department of Pharmacology and Physiology, Karolinska Institutet, Sweden*

⁵*Department of Biomedical and Molecular Sciences, Queen's University, Kingston, Canada*

christos.boutopoulos@umontreal.ca

ABSTRACT

Near-infrared (NIR) photothermal therapy (PTT) of solid tumors utilizes localized heat to induce immunogenic death of tumor cells. In melanoma tumors, PTT harnesses the absorptive capacity of melanin at NIR light to produce localized hyperthermia. Combination of PTT with checkpoint inhibitor therapy can further amplify the immune response and improve the therapeutic outcome in what is known as photothermal immunotherapy. Here we introduce a triple therapy where photothermal immunotherapy is further amplified by pharmacological silencing of tumor-infiltrating sensory neurons, an approach that was recently shown to affect tumor immunosurveillance as a standalone treatment [1].

For our model, B16F10-OVA (5×10^5) melanoma cells were injected subcutaneously in female mice aged 6 - 8 weeks. Once the tumors reached approximately 200 mm^3 , they were treated by NIR laser irradiation, local silencing of nociceptors with an idocaine derivative (QX-314), and immunotherapy alone (aPDL1) or in combination.

To establish NIR irradiation conditions, we employed mathematical modeling to predict heat distribution and necrotic tissue in mice bearing melanoma tumors. Our model utilized experimentally defined parameters, such as tissue thermal properties, tissue optical properties, tumor size, laser beam size and power, and irradiation time. The model was experimentally validated using data on tumor temperature increase acquired by a thermal camera. We found that the tumor size is a key determinant of temperature increase, which underscores the need for personalized treatment conditions for mice exhibiting even small tumor size variations. By aiming for complete ablation without carbonization, we determined optimal treatment conditions (808 nm, 0.3 W/cm^2 , 3 min) for mice bearing 200 mm^3 tumors.

Laser treatment was subsequently applied either alone (Laser+) or in combination with immunotherapy (aPDL1+) and neuronal silencing (QX-314+). When compared to control groups, the triple therapy (Laser+, QX-314+, and aPDL1+) significantly decreases tumor progression ($p=0.0003$) and increases survival time. Specifically, it resulted in complete ablation in 42% of the treated mice. Two months post-inoculation, treated mice were rechallenged with B16F10-OVA (5×10^5) cells. Tumor re-growth was observed in only 16% of the mice, suggesting an immune memory effect.

Our results indicated that triple treatment can lead to a significant reduction in tumor growth and complete tumor ablation in a significant fraction of the treated mice. Furthermore, the results underscore the importance of modeling in NIR treatment planning.

REFERENCES

[1] M. Balood et al., Nature 611, 405–412 (2022)

Advances in scanning optoacoustic angiography: leveraging highly sensitive wideband PVDF-TrFE piezopolymer detectors to enhancing tumor imaging

Alexey KURNIKOV¹, Anna GLYAVINA¹, Anna ORLOVA¹, Daniel RAZANSKY^{2,3} and Pavel SUBOCHEV¹

¹Department of Radiophysical Methods in Medicine, Institute of Applied Physics named after A.V. Gaponov-Grekhov of the Russian Academy of Sciences, Russia

²Institute of Pharmacology and Toxicology, Faculty of Medicine, UZH Zurich, Switzerland

³Institute for Biomedical Engineering, Department of Information Technology and Electrical Engineering, ETH Zurich, Switzerland

kurnikov.1997@mail.ru

ABSTRACT

Optoacoustic angiography is a non-invasive imaging technique currently actively employed for studying the growth of experimental tumors and their treatment methods. In this approach, biological tissue is exposed to short laser pulses, followed by the recording of ultrasonic signals using piezoelectric transducers. However, accurate and detailed visualization of tumor vasculature is often challenging due to limitations in angular coverage, reception bandwidth, and sensitivity of ultrasound detectors.

This work demonstrates advancements in the development of piezopolymer detectors based on PVDF-TrFE, significantly enhancing the quality of optoacoustic vascular images. The noise equivalent pressure of such detectors reaches 1.2 Pa in a frequency band of at least 30 MHz (from 0.1 to 30 MHz), and the numerical aperture of the focusing detectors reaches unity (angular coverage 180 degrees), surpassing standard piezoceramic detectors (Fig. 1a). Simulation results illustrate how these parameters impact the quality of optoacoustic images (Fig. 1b,c). Experimental in vivo data demonstrate excellent visualization quality of vessels in tumor nodes (Fig. 1e) within a volume of 10x10x2 mm³ [1].

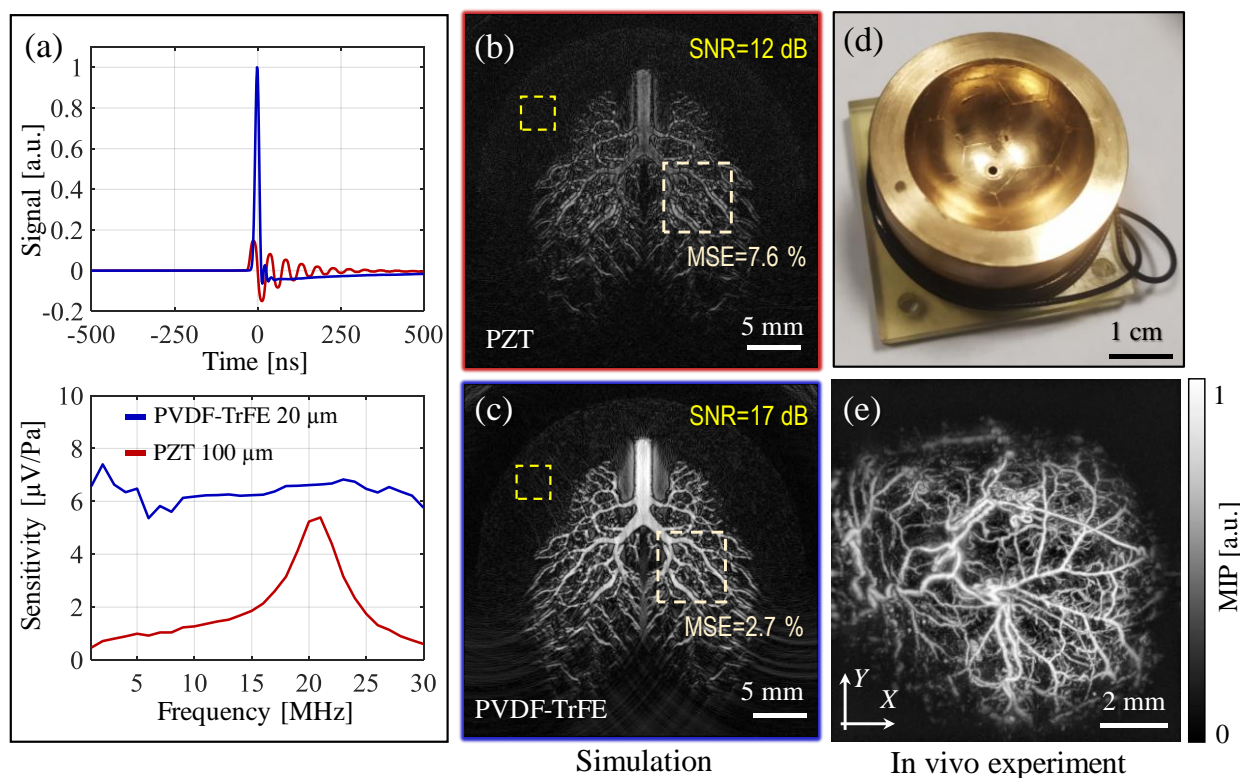


Figure 1: (a) Optoacoustic signal and sensitivity of the PVDF-TrFE detector (b,c) Simulations of tomography OA angiography performed by PZT and PVDF-TrFE detector arrays (d) A photo of the focusing PVDF-TrFE detector (e) Optoacoustic imaging of the experimental tumor vessels.

REFERENCES

[1] A. Kurnikov et al, Photoacoustics 31, 100507, 2023.

Avoiding overestimation in multivariate analysis of Raman spectra for biomedical applications

Lyudmila BRATCHENKO¹ and Ivan BRATCHENKO¹

¹*Department of Laser and Biotechnical Systems, Samara University, Russia*

shamina94@inbox.ru

ABSTRACT

Surface-enhanced Raman spectroscopy (SERS) in combination with multivariate analysis is a promising analytical tool for solving clinical practice tasks. However, there are numerical challenges between experimental studies and the implementation of SERS in practical applications, including multicollinearity in spectral data and the overestimation of complex models. To avoid such problems, one should correctly interpret the proposed classification and regression models. The goal of the current work is to interpret and overcome overfitting of models for analyzing SERS spectra of blood serum based on the adapted SHAP (SHapley Additive exPlanations) algorithm. SERS characteristics of the serum samples were obtained using an experimental stand consisting of a spectrometric system (EnSpectr R785, Spektr-M, Chernogolovka, Russia) and a microscope (ADF U300, ADF, China). The spectra were excited in the near-infrared range using a laser module with a central wavelength of 785 nm. A silver substrate based on a dried silver colloid with agglomerates of spherical silver particles with a size of about 200 nm was used as a substrate material to achieve surface enhancement of the Raman signal of the serum [1]. An important feature of the SERS configuration used is the insignificant spectral contribution of the silver substrate to the spectrum of the sample under study. An experimental database of spectral characteristics of blood serum of 400 patients with various diseases (chronic heart failure, chronic renal failure, chronic obstructive pulmonary disease, multiple myeloma) was formed. A comparative analysis of the multivariate approach (based on the method of projection to latent structures) and the approach involving deep learning (based on a convolutional neural network) for the recognition of SERS spectrum of serum was performed using the example of the discriminating the patients by disease and the tasks of regression of the content of proteins, urea [2,3]. When solving the problem of discriminating patients by pathology, the implementation of the chemometric method for analyzing experimental data and the method based on CNN identified the following spectral bands as the most informative: band 720-750 cm^{-1} with a peak maximum at 724 cm^{-1} (corresponding to hypoxanthine), band 990-1030 cm^{-1} with peak maximum at 1001 cm^{-1} (phenylalanine, $\nu(\text{CO})$, $\nu(\text{CC})$, $\delta(\text{OCH})$), band 1089-1110 cm^{-1} with peak maximum at 1095 cm^{-1} (carbohydrates), band 1220-1255 cm^{-1} with a peak maximum at 1238 cm^{-1} (lipids), band 1380-1415 cm^{-1} with a peak maximum at 1393 cm^{-1} (δCH_3). The band at 630-650 cm^{-1} with a peak maximum at 637 cm^{-1} (uric acid) is characterized by significant information content when constructing the PLS-DA model, while for the CNN model this band, although informative, is characterized by less relative information content for CNN classification. The accuracy of classification of spectral characteristics of serum according to pathologically associated characteristics was more than 85%. The application of the proposed algorithm for interpreting serum Raman analysis models based on the SHAP method demonstrated sensitivity to both model underfitting and overfitting.

REFERENCES

- [1] Sahar Z. Al-Sammarraie et al. Silver Nanoparticles-Based Substrate for Blood Serum Analysis under 785 nm Laser Excitation, *Journal of Biomedical Photonics & Engineering*, 8, 2022.
- [2] Sahar Z. Al-Sammarraie et al. Human blood plasma SERS analysis using silver nanoparticles for cardiovascular diseases detection, *Journal of Biomedical Photonics & Engineering*, 10, 2024.
- [3] L.A. Bratchenko et al. Analyzing the serum of hemodialysis patients with end-stage chronic kidney disease by means of the combination of SERS and machine learning, *Biomedical Optics Express*, 13, 4926-4938, 2022.

40 MHz time stretch Swept Source OCT imaging and Fast Measurements

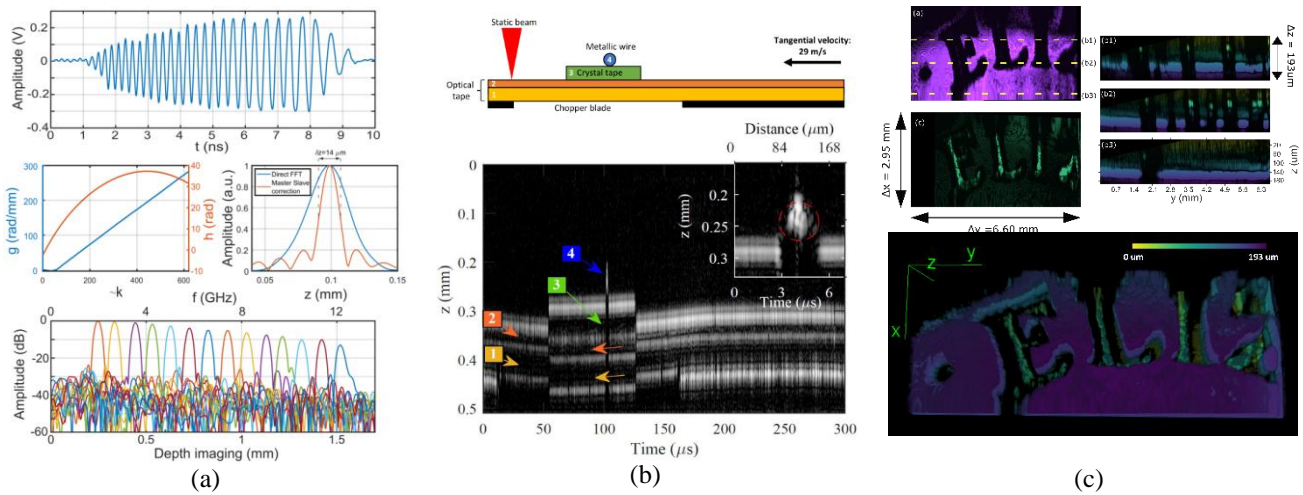
A. Martinez Jimenez¹, S. Grelet^{1,2}, P. Bowen², and A. Podoleanu¹
¹Applied Optics Group, University of Kent, United Kingdom
²NKT Photonics, Denmark
a.martinez-jimenez@kent.ac.uk

ABSTRACT

During the last decade, optical coherence tomography (OCT) has progressed considerably in the speed of acquisition, mainly due to advances in the swept source technology [1]. However, most of the sources available are based on mechanical movement parts of fast tuning spectral filters. Such sources might be able to reach a few-MHz tuning, with large coherence lengths but are unable to perform at multi-MHz speed. A promising akinetic technology for much faster tuning speed is the time-stretch, as demonstrated in 2006, where the mechanism of sweeping depends on the input pulse and the dispersion on the system [2] only.

Here, we explore time-stretch through a coherent supercontinuum mechanism [3,4]. Low-noise supercontinuum is achieved by pumping with a low-noise femtosecond pulse laser. Once the supercontinuum is generated, 2.7 km of fibre is used to stretch the pulse up to 12.5 ns, followed by a ytterbium amplifier, which amplifies the signal to compensate for the losses in the dispersive fibre. A high-speed swept source generates multi-GHz signals, and through a 20 GHz digital oscilloscope, the signal is captured and processed offline. We characterise the swept source parameters, such as coherence length, axial resolution, and relative intensity noise, as seen in Fig.1 (a).

Two applications are presented, fast imaging and fast measurements of a moving target. First, we demonstrate the image of a custom-made phantom with several layers. The phantom is attached to a chopper rotating at 3 kHz, where it is finally imaged, as shown in Fig. 1 (b). For fast imaging, a polarisation sensitive interferometer is assembled incorporating a fast deflector in its sample arm. This is able to match the speed of the source [5], based on an electro-optic modulator, KTN, driven with a sinusoidal pattern at 100 kHz. A galvanometer scanner is used to complete 2D ratsres, making it possible to produce volumes at 400 Hz. As a demonstration, the volume of a coin is presented in Fig. 1(c).



Figures: (a) Swept source characterisation, channel spectrum, dispersion, and nonlinearities of the source, point spread function, and sensitivity roll-off profile. (b) Sketch of the phantom used, and M-Scan of the sample. (c) En-face images at two different depths with B-Scans at the dashed yellow lines, volume of the sample.

REFERENCES

- [1] T. Klein et al, BOE, 8(2), 825-859, 2017.
- [2] S. Moon et al, OE, 14(24), 11575-11584, 2006.
- [3] E. Genier et al, OL, 46(8), 1820-1823, 2021.
- [4] S. Grelet et al, IEEE PJ, 14(6), 1-6, 2022.
- [5] A. Martinez Jimenez et al, IEEE PTL, 34(23), 1277-1280, 2022.

Tissue Composition Analysis: An Intuitive Application for the Broadband Absorption Spectra Reconstruction

Maria PINHEIRO^{1,2}, Maria CARVALHO^{1,2}, Valery TUCHIN^{3,4,5}, and Luís OLIVEIRA^{1,6}

¹Centre of Telecommunications and Multimedia, Institute for Systems and Computer Engineering, Technology and Science, Porto, Portugal

²Department of Electrical and Computer Engineering, Faculty of Engineering of Porto University, Porto, Portugal

³Institute of Physics and Science Medical Center, Saratov State University, Saratov, Russian Federation

⁴Laboratory of Laser Diagnostics of Technical and Living Systems, Institute of Precision Mechanics and Control of the FRC “Saratov Scientific Centre of the Russian Academy of Sciences”, Saratov, Russian Federation

⁵Laboratory of Laser Molecular Imaging and Machine Learning, Tomsk State University, Tomsk, Russian Federation

⁶Physics Department, Polytechnic of Porto – School of Engineering, Portugal

maria.r.pinho@inesctec.pt

ABSTRACT

The determination of tissue optical properties in a broad spectral range holds major relevance for the development of optical technologies in healthcare. Such properties quantify the mechanisms of light interaction with tissue components and may provide information to enable the differentiation of pathologies [1]. Biological tissues contain various components, such as water, DNA, oxy- and deoxy-hemoglobin, lipids, proteins, and pigments, including melanin and lipofuscin [1]. Among all the optical properties of tissues, the broadband spectrum of the absorption coefficient, $\mu_a(\lambda)$, is possibly the most important, since it clearly presents the absorption bands that correspond to the main tissue components, and allows for their immediate identification and possible evaluation of their contents in the tissue.

The $\mu_a(\lambda)$ of a tissue can be obtained through inverse simulations, or through direct calculations, which are based on the photon diffusion approximation [2,3]. The reconstruction of the $\mu_a(\lambda)$ of a tissue as a weighted sum of the absorption spectra of tissue components has been recently demonstrated to be a new method for the estimation of the components concentrations [4]. Recent studies showed that the reconstruction of the $\mu_a(\lambda)$ can provide differentiated concentrations for some tissue components between healthy and pathological tissues [5,6].

The present work was developed to simplify the process of such reconstruction of the $\mu_a(\lambda)$, through the creation of a user-friendly application, where the selection of the spectrum of each tissue component is possible and iterative. Using this application, the user can evaluate which weight for each tissue component enables a better fitting between the experimental and the reconstructed μ_a spectra. In cases where the experimental $\mu_a(\lambda)$ presents a broadband exponential-decreasing baseline, the application also allows to reconstruct such baseline through a weighted sum of the absorption spectra of pigments. After obtaining an optimized reconstruction, the weights used for the tissue components can be converted into concentration values, allowing for a numerical evaluation of the components contents in the tissue.

The developed application was tested through the reconstruction of the $\mu_a(\lambda)$ of cardiac muscle from 200 to 1000 nm, obtaining a correlation of 99.99% between the experimental and the reconstructed spectra. Assuming a water concentration of 77.9 % in the heart [7], the concentration of the remaining components was calculated by the application. The results show that oxy-hemoglobin, DNA, proteins, and pigments are the components with higher concentrations in the cardiac muscle. It was verified that deoxy-hemoglobin and lipids are also present in the cardiac muscle, but in much smaller contents. Future features and methods can be added to the application to support optical technology for diagnostic and treatment purposes.

REFERENCES

- [1] I. S. Martins et al, Opt. Express 14, 249, 2023.
- [2] V. V. Tuchin, Tissue Optics: Light Scattering Methods and Instruments for Medical Diagnosis, 3rd Edition (SPIE Press), (2015).
- [3] T. M. Gonçalves et al, Photochem 1, 190, 2021.
- [4] S. L. Jacques, Phys. Med. Biol. 58, R37, 2013.
- [5] M. R. Pinheiro et al, J. Biophotonics, e202300494, 2024.
- [6] M. R. Pinheiro et al, J. Biophotonics, e202300466, 2024.
- [7] R. F. Reinoso et al, J. Pharmacol. Toxicol. Methods 38, 87, 1997.

Optical methods for detecting single biomolecules: visualization, sensing, sequencing of DNA molecules

Aleksei KALMYKOV¹, Anton GRITCHENKO¹, Pavel MELENTIEV¹, Victor BALYKIN¹, Anton BUKATIN², Anatoly EVSTRAPOV² and Yakov ALEXEEV³

¹*Institute of Spectroscopy RAS, Russia*

²*Institute for Analytical Instrumentation RAS, Russia*

³*Sintol Ltd., Russia*

kalmykov_100@mail.ru

ABSTRACT

The development of methods for the effective detection, visualization and determination of the optical, chemical and physical properties of single molecules is an important fundamental task in the field of microscopy and nanophotonics. Recently, these methods have found numerous socially significant applications for the optical detection of biomolecules: (1) determination of ultra-low concentrations using single molecule counting methods, SMCM [1], (2) detection and determination of parameters of virus particles [2], (3) sequencing of DNA molecules [3].

This work shows that the use of modern (state-of-the-art) methods of nanophotonics and nanotechnologies for the optical detection of single molecules can significantly increase the accuracy of registration of single biomolecules, shorten the time for determining the concentration of the analyte, determine the degree of virulence of individual virus particles and perform molecular sequencing of DNA with a high degree of confidence.

The use of SMCM to determine the concentration of troponin molecules in human blood has been demonstrated. The determination of troponin concentration is a direct way to detect severe cardiovascular diseases. The developed method [4] enables the determination of the concentration of troponin T molecules in the patient's blood serum with a minimum concentration determination of 1 pg/ml and a measurement time of about 5 minutes. The concentration determination achieved is sufficient for the early diagnosis of cardiovascular diseases in humans.

Another socially important task that requires the use of SMCM methods is the rapid determination of the concentration and degree of virulence of virus particles [2]. Using the SARS-CoV-2 virus as an example, we recently succeeded in solving this problem using SMCM methods for the first time. The optical diagnostics of the SARS-CoV-2 virus was realized with fluorescent nanoprobe in the form of core-shell nanoparticles. Such nanoparticles are characterized by a bright and stable fluorescence, which is suitable for the detection of a single virus. Such fluorescent markers were used to label monoclonal antibodies against the SARS-CoV-2 S protein. A developed method for the detection of active SARS-CoV-2 virions enables the determination of the concentration of virus particles in a sample. The detection limit of the developed method is around 800 virions/ml. We have shown that it is possible to determine the virulence of coronavirus particles based on the brightness of a nanolocalized light source, as the brightness is proportional to the number of spikes on the lipid envelope.

The development of methods for the detection of biological single molecules has enabled optical single-molecule sequencing of DNA molecules. Single-molecule real-time optical DNA sequencing (SMRT) [3] is a modern method that can determine the nucleotide sequence of a single DNA molecule with an accuracy of over 99%. Sequencing is performed by synthesizing a complementary DNA sequence using DNA polymerase, which completes the DNA with four fluorescently labeled nucleotides. Sequence determination is based on recording the signals of the individual fluorophores and determining their spectrum. To solve this problem, the following were developed: (1) optical acquisition scheme, (2) sequencing reaction cells, (3) reagents and polymerase, (4) sample preparation procedures. During the work, the nucleotide sequences of the synthesized oligonucleotides were recovered.

The study was supported by a grant Russian Science Foundation No. 23-42-00049, <https://rscf.ru/project/23-42-00049/>.

REFERENCES

- [1] Ma, F., Li, Y., Tang, B., & Zhang, C. Y. (2016). Fluorescent biosensors based on single-molecule counting. *Accounts of chemical research*, 49(9), 1722-1730.
- [2] Bhat, T., Cao, A., & Yin, J. (2022). Virus-like particles: Measures and biological functions. *Viruses*, 14(2), 383.
- [3] Eid, J., Fehr, A., Gray, J., Luong, K., Lyle, J., Otto, G., ... & Turner, S. (2009). Real-time DNA sequencing from single polymerase molecules. *Science*, 323(5910), 133-138.
- [4] Melentiev, P. N., Son, L. V., Kudryavtsev, D. S., Kasheverov, I. E., Tsetlin, V. I., Esenaliev, R. O., & Balykin, V. I. (2020). Ultrafast, ultrasensitive detection and imaging of single cardiac troponin-T molecules. *ACS sensors*, 5(11), 3576-3583.

Wearable laser Doppler flowmetry for the study of blood microcirculation peculiarities in the forehead skin in patients in the remote post-COVID period

Elena ZHARKIKH¹, Yulia LOKTIONOVA¹, Andrey FEDOROVICH^{1,2} and Andrey DUNAEV¹

¹Research and Development Center of Biomedical Photonics, Orel State University, Russian Federation

²National Medical Research Center for Therapy and Preventive Medicine of the Ministry of Healthcare of the Russian Federation

ev.zharkikh@gmail.com

ABSTRACT

Cognitive disorders are one of the most common manifestations of long COVID syndrome. From 27 to 44% of those who recovered from COVID-19 report impaired concentration, memory loss, and the onset or increased frequency of headaches. It is currently believed that disorders of blood microcirculation and endothelial damage is one of the potential causes of long COVID syndrome [1,2]. Therefore, the aim of the present study was to analyse the features of blood microcirculation in rest and during cognitive test in patients in the remote post-COVID period.

Fifty patients who had previously suffered from COVID-19 participated in the experimental study. According to the results of the questionnaire about the presence and duration of symptoms of long COVID syndrome, the subjects were divided into 3 groups: with mild, moderate and severe course of long COVID syndrome. To measure the parameters of the blood microcirculatory system, the wearable devices "LAZMA PF" (SPE "LAZMA", Moscow) were used, implementing the method of laser Doppler flowmetry for non-invasive diagnostics of the microcirculatory bed [3,4], and the values of the index of blood microcirculation (I_m , p.u.) and amplitudes of blood flow oscillations in endothelial (A_E), neurogenic (A_N), myogenic (A_M), respiratory (A_R) and cardiac (A_C) ranges reflecting the regulation of the blood microcirculation system were calculated and analysed. Symmetrical forehead skin areas in the region of supraorbital artery basins were chosen as the measurement area. The study included registration of parameters in the state of physical and psychological rest (baseline test, BT) for 10 min, as well as during and after the cognitive test (CT). The Schulte test was chosen as the cognitive test, which is a psychodiagnostic test to investigate the properties of attention.

The results of the study indicate that patients with a more pronounced course of long COVID syndrome are characterised by a decrease in I_m values compared to the group with a mild course (30% decrease), as well as a decrease in the amplitudes of all active blood flow oscillations. The implementation of the cognitive test leads to an increase in the perfusion of the forehead skin of patients and an increase in the activity of myogenic oscillations. These changes are most pronounced in groups with moderate and severe course of long COVID syndrome, which may be associated with the development of cognitive disorders in patients. It was noted that in all groups of subjects, CT causes a shift of the peak of the dominant active amplitude of blood flow oscillations to a higher frequency region (during BT the peak of active regulation falls on oscillations with a frequency of 0.11 Hz; during CT – 0.16 Hz), which may indicate the activation of cholinergic parasympathetic regulation. At the recovery stage (after CT) there is an increase in neurogenic regulation of blood flow.

Thus, with the use of wearable laser Doppler flowmetry devices, the peculiarities of forehead skin microcirculation in patients with different severity of the long COVID syndrome were investigated, and the influence of cognitive load on changes in skin perfusion was assessed. The results obtained are of interest for their further application in assessing the effectiveness of therapy and rehabilitation measures.

The study was supported by the Russian Science Foundation grant № 23-25-00522.

REFERENCES

- [1] E.V. Zharkikh et al., *Diagnostics* 13(5), 920, 2023.
- [2] E. Zharkikh et al., *Proc. SPIE* 12627, 126272, 2023.
- [3] A. Dunaev, *Journal of Biomedical Photonics & Engineering* 9(2), 1-10, 2023.
- [4] E. Zharkikh, A. Dunaev, *Biomedical Engineering*, 58(7), 2024.

Complex application of fluorescence imaging and digital diaphanoscopy methods for screening pathological conditions of the oral mucosa and the maxillary sinus tissues

Ekaterina BRYANSKAYA¹, Viktor DREMIN¹, Andrey VINOKUROV¹, Andrey DUNAEV¹ and Andrey ABRAMOV^{1,2}

¹Research and Development Center of Biomedical Photonics, Orel State University, Russia

²Department of Clinical and Movement Neurosciences, UCL Queen Square Institute of Neurology, UK

bryanskayae@mail.ru

ABSTRACT

Worldwide, 600 thousand cases of malignant neoplasms of the oral mucosa (for example, squamous cell carcinoma) are observed annually, which develop due to untimely diagnosis of potentially malignant diseases (precancerous). There is a high correlation between the development of oral mucosa and maxillary sinus pathologies due to the close proximity of tissues.

It is known that the development of oral mucosa lesions is characterized by changes in the endogenous fluorophores' concentration [1]. Preliminary experimental studies have shown that the FAD signal makes the greatest contribution to the formation of the high level of autofluorescence intensity observed in pathology in the blue-green spectrum [2]. At the same time, for diagnostic purposes, it is very important to know which flavin proteins format such a signal. For this purpose, we performed studies on human skin fibroblasts, as well as primary neuron-glia culture using a Zeiss LSM 900 laser scanning confocal microscope (excitation wavelength – 488 nm, autofluorescence registration – 505-550 nm). It was revealed that cell cultures with metabolic disorders had a high intensity of FAD autofluorescence compared with healthy cells due to overactivation of complex II of mitochondrial ETC and the activity of monoamine oxidase. At the same time, death of high-intensity cells was observed only after 24 hours. The results obtained showed the prospects of using the fluorescence imaging method to diagnose oral mucosa pathologies. In this connection, the high level intensity of FAD can be a marker of a precancerous condition, and the low level intensity of FAD – a marker of the beginning of the process of cell degeneration into tumor (malignancy process) [3].

To diagnose the condition of maxillary sinus tissues, a digital diaphanoscopy technology was previously developed, including an LED applicator for probing maxillary sinus tissues (650 and 850 nm), a CMOS camera for recording diaphanograms and software. The software based on the classification model allows to detect the presence of pathology with sensitivity of 0.88 and specificity of 0.98 [4,5]. An upgrade of the digital diaphanoscopy device with the addition of fluorescent imaging channel is proposed. That channel includes microLEDs in the blue spectrum (450 nm, 0.5 mW) to excite FAD in the oral mucosa and a microcamera for autofluorescence visualization. The use of convolutional neural networks will allow binary classification of the oral mucosa condition into classes of presence or absence of pathology, and differentiate various maxillary sinus pathologies. Thus, the probability of a false negative diagnosis will be reduced and diagnostic effectiveness will be increased.

This work was supported by Russian Science Foundation under the project no. 24-75-00144 and by the grant of the Russian Federation Government no. 075-15-2024-621.

REFERENCES

1. A. Sah et al., J. Fluorescence 33, 1375-1383 (2023).
2. E. Bryanskaya et al., Biochim. Biophys. Acta, Gen. Subj. 1868, 1, 2023.
3. D. Elvers et al., British Journal of Oral and Maxillofacial Surgery 2(53), 164-169 (2015).
4. E. Bryanskaya et al., Diagnostics 11, 1, 2021.
5. E. Bryanskaya et al., J. Biophotonics 16, 9, 2023.

Optical Methods in Elastography of Ocular Tissues

Salavat AGLYAMOV¹ and Kirill LARIN²

¹*Department of Mechanical Engineering, University of Houston, USA*

²*Department of Biomedical Engineering, University of Houston, USA*

saglyamo@central.uh.edu

ABSTRACT

Microscopic changes in biological tissues leading to pathologies often result in macroscopic changes in tissue biomechanical properties, such as tissue elasticity. It is known, that the biomechanical characteristics of ocular tissues have a profound influence on the health, structural integrity, and normal function of the human eye. Such conditions as presbyopia, corneal ectasia and keratoconus correlate with stiffness of the ocular tissues.

Optical Coherence Elastography (OCE) utilizes Optical Coherence Tomography (OCT) to remotely assess the biomechanical properties of tissues. By measuring tissue motion in response to external stimuli, OCE enables the evaluation of tissue elasticity. Our team has pioneered several OCE techniques that assess the elastic properties of ocular tissues using diverse excitation methods. The evaluation of biomechanical properties is based on a mathematical model that characterizes the dynamic deformation of the viscoelastic medium. This methodology has been successfully validated through studies with phantoms, ex vivo and in vivo animal experiments, and human studies.

We developed several methods to evaluate eye biomechanics by measuring elastic wave propagation in eye tissues using a phase-sensitive OCT imaging system. This was done after stimulating the eye with air-puff pulses, acoustic radiation force, and a piezoelectric actuator. We examined different ocular tissues, including the anterior parts, such as the cornea and sclera, as well as internal parts, like the crystalline lens and iris. For the cornea, we utilized noncontact approaches with air-puff and air-coupled acoustic stimuli. We measured elastic wave propagation to quantify corneal biomechanics in animal eyes, both before and after corneal crosslinking (CXL), in the whole eye-globe configuration. The biomechanical properties of untreated and CXL-treated eyes were assessed at various intraocular pressures (IOPs). Our findings indicated that corneal stiffness increased post-CXL and that corneal stiffness was nearly linearly correlated with IOP. Additionally, we investigated how corneal thickness and curvature influenced the propagation of elastic waves.

We developed an approach using acoustic radiation force to assess the biomechanical properties of the crystalline lens. This method was applied to measure the biomechanical properties of lenses in intact animal eyes in situ, considering different ages and intraocular pressures (IOPs). Acoustic waves remotely disturbed the anterior surface of the lenses through the cornea and aqueous humor. The results showed significant differences in the elastic properties between young and mature lenses. Additionally, the safety of using acoustic radiation force was evaluated in animal studies.

In summary, optical coherence elastography has shown to be a promising tool for the noninvasive assessment of ocular tissue biomechanical properties.

This study was supported by the National Institute of Health grants EY022362, EY030063, and EY033978.

Moisture quantification of allogeneic tissues by fiber-optic NIR spectroscopy

Anastasiia SURKOVA¹, Dmitrii SINITSYN², Nikolay RYABOV³, Artem VOLOV³, Larisa VOLOVA³, Jelena MUNCAN⁴ and Anna ORLOVA¹

¹International Laboratory “Hybrid Nanostructures for Biomedicine”, ITMO University, Russia

²Department of Analytical and Physical Chemistry, Samara State Technical University, Russia

³Research Institute of Biotechnology “BioTech”, Samara State Medical University of the Ministry of Health of the Russian Federation, Russia

⁴Aquaphotomics Research Field, Graduate School of Agricultural Sciences, Kobe University, Japan

melenteva-anastasija@rambler.ru

ABSTRACT

Lyophilized allogeneic biomaterials are effectively used in the modern medicine to compensate various defects of supporting and connective tissues [1]. These biomaterials should be thoroughly tested and standardized before being used for clinical purposes, as well as at the stages of their production in tissue banks. One of the important criteria for evaluation of allomaterials in the process of their production is the determination of residual moisture content in dry and lyophilized products. The moisture content strongly influences the shelf life of biologically active substances in samples. If the required moisture content is maintained, the samples can be stored at room temperature and easily transported.

One of the most common tools for moisture control is thermogravimetric analysis. Despite the fact that the device allows to determine moisture content with a sufficiently high accuracy, its use is associated with the destruction of the analyzed sample and the drying process generally takes a long time [2]. Therefore, a new method is needed that allows rapid and non-invasive control of moisture content in allogeneic biomaterials, preferably through the protective film used as packaging.

Near infrared (NIR) spectroscopy is well established method in various fields of science, technology, and industry due to its ability to perform fast, non-invasive, non-destructive, and inexpensive analysis. In recent years, NIR spectroscopy has been increasingly used in pharmaceuticals [3] and drug manufacturing for non-destructive drug testing [4]. NIR absorption spectra contain rich information about the structure of water, especially in the first overtone region of the OH stretching band (1300–1600 nm), where many absorption bands are recognized. In this regard, NIR spectroscopy can be an effective tool for estimating the moisture content of various products [5–7].

This study evaluated the performance of fiber-optic NIR spectroscopy in determining the moisture content of allogeneic human bone tissue bioimplants processed according to the original patented technology “Lioplast”® (Research Institute of Biotechnology “BioTech”, Samara State Medical University, Samara, Russia) [8]. The “Lioplast”® bioimplants have unique features due to biocompatibility, biodegradability, low antigenicity, and the ability to replace by their own organotypic tissue.

At the first stage, lyophilized and non-lyophilized (dry) samples of human bone tissue bioimplants were studied. The classification model built using partial least squares discriminant analysis (PLS-DA) demonstrated good separation between dry and lyophilized samples. Further, NIR spectra of samples were acquired during the drying process and PLS regression models were constructed to quantify the moisture in the samples. In addition, the structure of water in bioimplants during the drying process was studied using aquaphotomics [9] – a novel approach in the field of NIR spectroscopy which utilizes the water absorbance spectral features for a characterization of the samples.

The obtained results demonstrated the high prospectively of NIR spectroscopy for estimating the moisture content of bioimplants. The application of NIR spectroscopy will be especially effective for moisture assessment of both serial and individual bioimplants, i.e. it will allow to monitoring the quality of each sample without destroying it.

This work was financially supported by the ITMO Fellowship Program and by the Ministry of Education and Science of the Russian Federation, State assignment, Passport 2019-1080 (Goszadanie 2019-1080).

REFERENCES

- [1] A. Nather et al, World Scientific: Singapore, 565p, 2010.
- [2] Y. Pomeranz et al. Food Analysis. Springer, Boston, MA, 1994.
- [3] B.F. MacDonald et al, J Pharm Biomed Anal. 11(11-12),1077-1085,1993.
- [4] O.Ye. Rodionova et al, Talanta 195, 662–667, 2019.
- [5] R. Kapoor et al, LWT 154, 112602, 2022.
- [6] P. Mishra et al, Talanta 223, 121733, 2021.
- [7] H. Trnka et al, J Pharm Sci. 103(9), 2839–2846, 2014.
- [8] I.L. Tsiklin et al, Polymers 14, 941, 2022.
- [9] R. Tsenkova, J. Near Infrared Spectrosc. 17, 303–313, 2009.

In vivo study of vascularization and oxygenation of tumor xenografts under the influence of the antiangiogenic drug axitinib

Anna Glyavina¹, Ksenia Akhmedzhanova¹, Alexey Kurnikov¹, Yulia Khochenkova²,
Dmitry Khochenkov², Ilya Turchin¹, Pavel Subochev¹ and Anna Orlova¹

1- Department of Radiophysical Methods in Medicine, Institute of Applied Physics Russian Academy of Sciences, Russia

2- Laboratory of Biomarkers and mechanisms of tumor angiogenesis, N.N. Blokhin National Medical Research Center of Oncology, Russia

annaglyavina@gmail.com

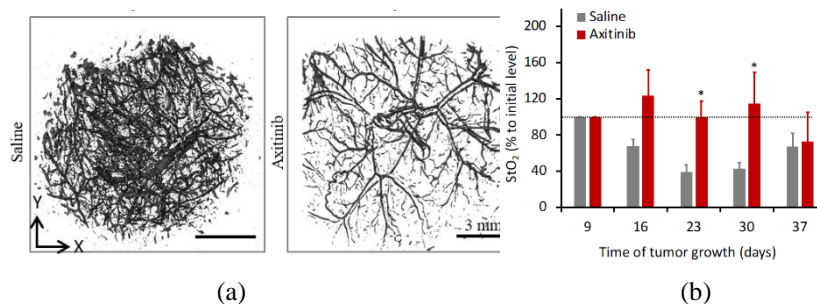
ABSTRACT

Axitinib is an inhibitor of tyrosine kinase receptors of vascular endothelial growth factor involved in the mechanisms of pathological angiogenesis, growth and metastasis of malignant neoplasms. To study the effects of Axitinib on vascular structure and oxygenation of experimental tumors the combination of optoacoustic (OA) microscopy and diffuse optical spectroscopy (DOS) was used. To verify the DOS data, an immunohistochemical (IHC) analysis of tumor tissues with the hypoxia marker pimonidazole (PM) was carried out.

The study was conducted on female Balb/c-nude mice with subcutaneously inoculated tumors based on human colon carcinoma Colo320 cell line. Axitinib was administered *per os* from days 9 to 37 of tumor growth every five days a week at a dose of 50 mg/kg. Tumor volume was measured every 4 - 7 days. OA and DOS studies were carried out starting from the 9th day of tumor growth with an interval of 7 days until the 37th day.

For OA and DOS studies, animals under isoflurane anesthesia were fixed in a position on their side on a portable support plate with an opening for the study area above the OA sensor of the microscope. Two facilities (IAP RAS) were used for experiments: OA system with the 532 nm laser source with a repetition frequency and pulse duration of 2 kHz and 1 ns and wideband ultrasound PWDF detector [1]; DOS system with optical probe made of four fibers, broadband LED as a light source and a spectrometer as a detector [2]. The vessel fraction, as a percentage of the volume of vessels to the volume of the tumor, the number of branchpoints, as well as the total vessel length, normalized to tumor volume were calculated from the OA images. According to DOS data, blood oxygen saturation (StO_2) was determined as the percentage of oxyhemoglobin in the total blood pool. For IHC, after administration of PM, tumors were extracted and cryopresections were made, which were stained using mouse fluorescently labeled antibodies to PM. The relative hypoxic fraction was calculated as a percentage of the area of PM-positive zones from the total area of the sample.

The work showed that tumors treated with Axitinib had a volume 5 times less than in the control group. The tumor growth inhibition rate was more than 80%. OA imaging shows the absence of a regular structure of the vasculature (Fig. 1a). Fraction of vessels, the number of branch points, as well as the total length of the vessels reduced under the Axitinib action. Differences between groups in all studied parameters were revealed starting from 23-30 days of tumor growth. The DOS method showed that in untreated tumors there was a rapid decrease in StO_2 levels during the first 14 days of the experiment (Fig. 1b). When exposed to Axitinib on days 20-30, StO_2 was 2 times higher than the control. IHC analysis showed higher RHF values after exposure to Axitinib compared to controls, demonstrating an increase in the area of hypoxic zones.



Figures 1: (a) Examples of OA images of Colo320 vasculature without and after treatment with axitinib on the 37th day of growth (b) Blood oxygen saturation level (StO_2) $M \pm SEM$. * - statistically significant differences between the treatment groups

The work was supported by the Center of Excellence "Center of Photonics" funded by the Ministry of Science and Higher Education of the Russian Federation, Contract No. 075-15-2022-316.

REFERENCES

- [1] M.S Kleshnin, et al, Quantum Electronics 49(7), 628-632, 2019
- [2] P. Subochev, Optics letters 41(5), 1006-1009, 2016

Laser generation of reactive oxygen and nitrogen species to influence physiological and metabolic parameters of human blood in vitro

Roman KORNEV¹, Andrey BULANOV¹, Artur ERMAKOV¹, Vladimir SHKRUNIN¹,
Andrew MARTUSEVICH², Vladimir NAZAROV²

¹ PECVD Department, G.G. Devyatykh Institute of Chemistry of High-Purity Substances of RAS, Russia

²Laboratory of Medical Biophysics, Privolzhsky Research Medical University, Russia

romanakornev@gmail.com

ABSTRACT

Under plasma conditions induced by laser optical breakdown using a pulsed Nd:YAG laser at a wavelength of 1.064 μm , the formation of reactive oxygen and nitrogen species NO, NO₂ and O₃ in various mixtures with inert gases Ar, He, Kr and Xe was studied. The most probable reactions for the formation of intermediate active particles are proposed. The mechanisms of formation of NO, NO₂ and O₃ are discussed.

One of the promising discharges capable of generating ozone, NO, NO₂ and singlet oxygen is a gas discharge induced by an optical breakdown of a high-power laser (Laser-induced dielectric breakdown (LIDB)). It allows you to localize the plasma region and generate high-purity reactive forms of oxygen and nitrogen for their subsequent impact on the physiological and metabolic parameters of human blood.

The characteristics of laser breakdown in pure gases N₂ and O₂ at a wavelength of 1.064 μm using a pulsed Nd:YAG laser with a duration of 10 ns in the pressure range from 1 to 50 atm were studied in [1]. In [2], dielectric breakdown of a near-IR laser with a power of 85 J and a pulse duration of 450 ps was realized in gas mixtures of the composition CO-N₂-H₂O. After irradiation, the appearance of N₂O, CO₂, ethane, acetylene, ethylene and acetone was recorded in the mixture. In [3], under conditions of laser dielectric breakdown of an Nd:YAG laser, the formation of ozone and nitrogen oxides was studied during repeated laser breakdown of oxygen-nitrogen mixtures at atmospheric pressure.

The purpose of this work is to study the possibility of generating active forms of NO, NO₂ and O₃ in LIDB plasma in a mixture of air with Ar, He, Kr and Xe.

The experimental setup is described in detail in [4]. It allows you to study plasma generated by LIDB in various gas mixtures using OES, IR spectroscopy, UV spectrophotometry and mass spectrometry.

The formation of molecules in LIDB plasma can be summarized as follows.

1. The formation of NO and NO₂ in LIDB plasma significantly depends on the type of inert gas.
2. An increase in the concentration of NO and NO₂ is affected by the complication of the electronic configuration of the inert gas, as well as a decrease in its ionization potential.
3. Complication of the electronic configuration of an inert gas, as well as a decrease in its ionization potential leads to suppression of the lines of nitrogen and oxygen ions. Thus, it can be assumed that the main mechanism influencing the chemical transformations in these mixtures and, in particular, the formation of NO and NO₂, is atomic.
4. Ozone formation occurs outside the gas-discharge zone through the photolysis reaction.
5. It has been established that the equilibrium concentration of NO in pure air and in mixtures of air with inert gases is at the same level and does not depend on the choice of inert gas. The equilibrium concentration of the NO⁺ ion in clean air is maximum and decreases in mixtures of air with inert gases. Moreover, the more complex the electronic configuration of the inert gas, the lower the concentration of NO⁺.

The work was supported by the state task of the Ministry of Science and Higher Education of the Russian Federation, topic No. 0095-2019-0008.

REFERENCES

- [1] J. Stricker, Journal of Applied Physics. 53, 851, 1982
- [2] S.Civiš et al, Journal of Physical Chemistry A. 112, 7162, 2008
- [3] I. B. Gornushkin et al, Appl. Spect. 57, 1442, 2003
- [4] A. Martusevich, R. Kornev et al, Sensors. 23, 932 2023

Automated system for analyzing the effectiveness of photobiomodulation of lymphatic removal of beta-amyloid from tissues of the aging brain

Anastasiia SEMIACHKINA-GLUSHKOVSKAYA¹, Viktoria ADUSHKINA¹, Daria ZLATOGORSKAYA¹, Dmitry MYAGKOV¹, Dmitry TUKTAROV¹, Sergey POPOV¹, Timopheyy INOZEMCEV¹, Ivan FEDOSOV¹, and Oxana SEMYACHKINA-GLUSHKOVSKAYA¹

Saratov State University, scientific medical center, laboratory "Smart Sleep", Saratov, Russia

nastyia.glushkovskaya04@mail.ru

ABSTRACT

Age is a natural factor for the accumulation of a toxic neuronal metabolite, such as the amyloid beta (A β), in brain tissues. This is accompanied by a decrease in cognitive function, as well as sleep deficiency. Recent discoveries show that the meningeal lymphatic vessels play an important role in removing toxins from brain tissues. Our research group has developed a technology for photobiomodulation (PBM) of lymphatic drainage processes in the mouse brain. Our results have been shown effective photo-treatment of mice with Alzheimer's disease, including the removal of A β from the brain [1, 2]. Based on our previous results, this study examined the effects of PBM on a large group of mice to correct age-related accumulation of A β in brain tissues and improve their cognitive function using a developed automated system for analyzing memory and motor activity of mice.

In the experiments, we used the PBM technology (a course of 10 days daily, 1050 nm, 30 J/cm², pulsed mode) in male mice of different ages: 6 months, 12 months, 24 months, and studied the A β content in brain tissues using the enzyme immunoassay method and confocal microscopy. To study the cognitive functions of mice, tests of novel object recognition, open field and operant behavior were used. Software has been developed based on the cv2, numpy, datetime libraries for automatic analysis of the cognitive functions of mice.

Our results have shown that with age, there is a progressive accumulation of A β in brain tissues of mice, which is accompanied by a decrease in cognitive functions (development of conditioned reflexes). The use of a course of PBM significantly reduced the level of A β in the brain tissues of mice aged 12 months, but not 24 months, bringing their values closer to 6 month-old mice. This was also accompanied by an increase in the effectiveness of development of conditioned reflexes that was most pronounced in mice 6 and 12, but not 24 months old.

Overall, the results showed that PBM may be an effective method for preventing both age-related accumulation of A β in brain tissues and the development of cognitive deficits in aging, but not in old, mice. This is consistent with the results of other studies indicating reversible processes of mild dementia, including that observed with age [3]. Based on preclinical studies, we have developed the PBM technology for therapy of elderly people experiencing sleep deficiency and cognitive impairment.

The research was supported by the Russian Science Foundation grant No. 24-75-10047.

REFERENCES

- [1] O. Semyachkina-Glushkovskaya et al. *Front. Optoelectron.* 16, 22, 2023.
- [2] O. Semyachkina-Glushkovskaya O. *Biomed. Opt. Express* 15, 44-58, 2024.
- [3] J. Fessel et al. *Clin. Med.* 12, 4873, 2023.

Mouse phenotyping technology to evaluate the effectiveness of phototherapy in mice with Alzheimer's disease

Dmitry MYAGKOV¹, Dmitry TUKTAROV¹, Sergey POPOV¹, Timopheyy INOZEMCEV¹, Viktoria ADUSHKINA¹, Daria ZLATOGORSKAYA¹, Anastasiia SEMIACHKINA-GLUSHKOVSKAYA¹, Ivan FEDOSOV¹, and Oxana SEMYACHKINA-GLUSHKOVSKAYA¹

Saratov State University, scientific medical center, laboratory "Smart Sleep", Saratov, Russia

dmyagk0v@yandex.ru

ABSTRACT

The use of phenotyping systems is one of the main methods for assessing the cognitive abilities of experimental animals during preclinical research. This method is the main one for assessing the state of the brain in various neurodegenerative diseases, such as dementia and Alzheimer's disease [1, 2]. Despite the widespread demand for the use of installations for complex phenotyping, not every laboratory has the opportunity to use existing commercial versions (the TSE Systems) of these installations due to their high cost. In addition, the phenotyping systems produced by companies do not allow for networking of facilities to track large numbers of laboratory animals. Combining the setup with various sensors will improve the phenotyping system, giving laboratories the ability to customize the flexibility of the experiment, as well as easy replacement of components.

This work presents a technology for phenotyping laboratory animals in a home cage for pharmacological and preclinical medical research, including the construction of a network of devices. The device is a device measuring 210x200 mm, height 110 mm, which contains 2 optical sensors for mouse detection and a feeder for stimulation. The front wall is made of steel, which prevents the mouse from damaging the device. The sensors are located inside a sealed shell made of PLA. The feeder is located inside, is modular and controlled by a programmable stepper motor. The system is controlled by an STM32 based microcontroller. On the outer surface of the case there is a push-button switch and an LED indicator of the device's operating mode.

The developed phenotyping system can be used in medical companies and scientific laboratories that evaluate treatments for a large number of laboratory mice, including the analysis of phototherapy for Alzheimer's disease and cognitive function in mice [3]. Using this technology, we found that photobiomodulation of lymphatic clearance of beta-amyloid during sleep, compared to wakefulness, was significantly more effective in improving the cognitive abilities of mice with Alzheimer's disease.

The research was supported by the Russian Science Foundation grant No. 23–75–30001.

REFERENCES

- [1] M. Shakir et al. *Journal of Neuropathology & Experimental Neurology*, 1, 2–15, 2022.
- [2] O. Silva et al. *Sensors*, 23, 288, 2023.
- [3] O. Semyachkina-Glushkovskaya O. *Biomed. Opt. Express* 15, 44-58, 2024.

Diffuse Reflectance Spectra Changes After Photodynamic Therapy of Rat Model Tumors with and Without Optical Clearing

Vadim GENIN^{1,2}, Alla BUCHARSKAYA^{1,2,3}, Elina GENINA^{1,2}, Nikita NAVOLOKIN^{1,3} and Valery TUCHIN^{1,2,4}

¹Department of Optics and Biophotonics, Saratov State University, Russia

²Laboratory of Laser Molecular Imaging and Machine Learning, Tomsk State University, Russia

³Department of Pathological Anatomy, Saratov State Medical University, Russia

⁴Institute of Precision Mechanics and Control Problems of the Russian Academy of Sciences, Federal Research Center "Saratov Scientific Center of the RAS", Russia

versetty2005@yandex.ru

ABSTRACT

The relevance of the development of innovative methods of therapy in oncology based on the combined technologies of photodynamic therapy (PDT) and optical clearing (OC) is due to the insufficient effectiveness of standard therapies for the treatment of tumors of hard-to-reach localizations. Optical clearing is a method of immersing tissue with an optical clearing agent (OCA) that matches the refractive indices of tissue structural components and interstitial fluid to reduce tissue scattering. This matching effect can reduce skin damage when irradiating subcutaneous tumors.

The aim of the study was to investigate diffuse reflectance spectra changes in the tumor region after the PDT with and without optical clearing in rats with transplanted cholangiocarcinoma of the PC-1 line.

For PDT, a solution of the photosensitizer indocyanine green (ICG) in polyethylene glycol (PEG-300) with concentration of 1 mg/100 μ l was used. The maximum absorption of the solution was observed near 790 nm. A mixture of 70% glycerol, 5% DMSO, 25% water was used as OCA.

When the tumor volume reached 3 ± 0.3 cm³, the rats were intratumorally injected with an ICG solution at a dose of 2 mg/kg of rat body (approximately 200 μ l of solution). Then rats were divided into three groups. The rats in the first group (PDT group) were exposed to PDT only: an hour after the ICG injection, the tumors were irradiated percutaneously with an 808 nm diode infrared laser at a power density of 2.3 W/cm² for 15 min. The rats in the second group (PDT+OC group) were exposed to PDT during OC and irradiated percutaneously with the same laser at a power density of 1.1 W/cm² for 10 min. The rats in the third group (PDT+OC+PDT group) were exposed to PDT in two stages: during OC with the same laser at a power density of 1.1 W/cm² for 10 min at the first stage, and after OCA removing at a power density of 2.3 W/cm² for 15 min at the second stage. The temperature of local heating of the tumor was measured with a thermal imager. Diffuse reflectance spectra in the tumor region were measured at different stages of the experiment using a fiber spectrometer in the spectral range of 400-2100 nm and analyzed.

Animals were removed from the experiment 72 hours and 21 days after therapy. Morphological studies of the tumor were performed on sections stained with standard and immunohistochemical methods.

The work was supported by RSF grant 23-14-00287.

Excited-states relaxation in FAD excited states: the role of conformations

Denis VOLKOV¹, Ioanna GORBUNOVA¹, Dmitrii YASHKOV¹, Maxim SASIN¹, Maria KHRENOVA² and Oleg VASYUTINSKII¹

¹ Ioffe Institute, Russian Academy of Sciences, Russia

² Department of Chemistry, Lomonosov Moscow State University, Russia

olegvasyutinskii@gmail.com

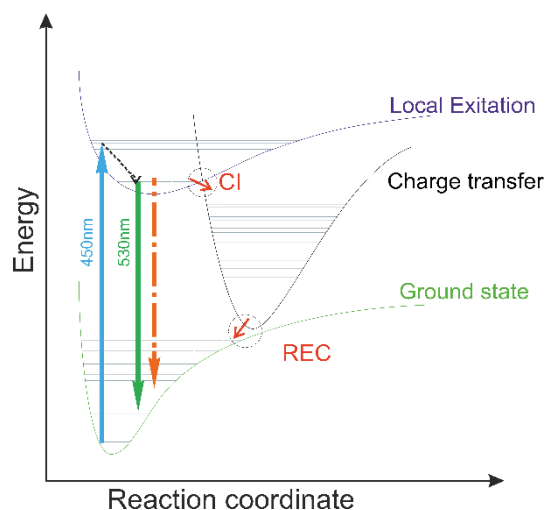
ABSTRACT

Flavine adenine dinucleotide (FAD) is an important endogenous fluorophore that is actively used nowadays for monitoring living cells metabolism using Fluorescence Lifetime Imaging Microscopy (FLIM). The fluorescence dynamics of FAD excited states manifests multiexponential decay, with decay times ranging from a few picoseconds to several nanoseconds [1]. Despite intensive studies, the nature of undergoing relaxation processes is still not clear enough. We present the investigation of relationship between the fluorescence decay times in FAD in water-methanol mixtures and the related conformation dynamics by means of a number of experimental and theoretical approaches: time-resolved fluorescence spectroscopy, quantum mechanical/molecular mechanical (QM/MM) computations, and classical molecular dynamics (MD) simulations.

The fluorescence decay signals in FAD in water-methanol solutions were recorded under excitation at 450 nm using time-correlated single-photon counting (TCSPC) method. It was found that in pure water FAD exhibited four fluorescence decay times of $\tau_1 = 0.02$ ns, $\tau_2 = 0.21$ ns, $\tau_3 = 2.7$ ns, and $\tau_4 = 3.85$ ns with the major contribution from τ_1 of 0.50. In 90% of methanol solution, only two fluorescence decay times, τ_2 and τ_4 , were observed with the major contribution from τ_4 of 0.78. For interpretation of the experimental results obtained, QM/MM and MD simulations were carried out by using NAMD 3.0 and Gromacs software, respectively. The MD simulations have allowed to separate three different conformations: (1) Stack I where the adenine (Ad) ring is parallel to the isoalloxazine (Iso) ring taking a position above the pyrimidine and pyrazine moieties, (2) Stack III where the Ad ring is parallel to the Iso ring taking a position above the xylene moiety, (3) Unfolded where Ad is located far away from Iso. A new model was developed for elucidation of relaxation channels in FAD excited states. The schematic of optical excitation in FAD and following relaxation pathways are shown in Scheme.

According to the model, two main picosecond nonradiative relaxation processes occur after local excitation (LE) by a laser pulse with electron density redistribution from N1 to N5 atoms within the Iso ring. These are: vibrational relaxation within the LE electronic state and charge transfer transition through a conical intersection (CI) with electron density redistribution from Ad to Iso rings. The latter process occurs mostly in Stack III and Stack I conformations due to π -stacking interaction and relates to sub-nanosecond fluorescence decay times of $\tau_1 = 0.02$ ns and $\tau_2 = 0.21$ ns, respectively that were observed in experiment. The Unfolded conformation does not undergo charge transfer relaxation transition and relate to the fluorescence decay time of $\tau_4 = 3.85$ ns. Red down arrow in Scheme indicates relatively slow nanosecond nonradiative relaxation processes. The MD simulations performed have demonstrated that conformational equilibrium is very sensitive to alcohol concentration in solutions: the fractional concentration of the Stack III conformation decreased dramatically with methanol concentration, while that of the Stack I conformation remained practically the same. At the same time the fractional concentration of Unfolded conformations increased with methanol concentration from 0.16 in pure aqueous solution to 0.73 in 90% of methanol solution. The changes in weighting coefficients in water-methanol mixtures reflected conformation changes in FAD. Understanding of the nature of these fluorescence lifetimes and dynamics processes in FAD can be used in cellular research using FLIM.

The research was funded by Russian Science Foundation, grant number 23-22-00230.



Scheme: Optical excitation of FAD via the first excited state and relaxation pathways.

REFERENCES

- [1] A. Heikal et al, Biomarkers Med. 4, 241–263, 2010.
- [2] I. Gorbunova et al, J. Phys. Chem. B 124, 10682-10697, 2020.

Overcome cross-border barriers to health data integration, access, FAIRification, and pre-processing

Sergei G. Sokolovski¹ & Matteo Bregonzio²

¹ Aston Institute of Photonics Technologies, Aston University, Birmingham, UK

² DATRIX Group Ltd, Milano, Italy

In recent years, data-driven medicine has gained increasing importance in terms of diagnosis, treatment, and research due to the exponential growth of healthcare data. The linkage of health data from various sources, including genomics, and analysis via innovative approaches based on artificial intelligence (AI) advanced the understanding of risk factors, causes, and development of optimal treatment in different disease areas. Furthermore, it contributed to the development of a high-quality accessible health care system. However, medical study results often depend on the amount of available patient data, crucially when it comes to rare diseases this dependency is accentuated. The reuse of patient data for medical research is often limited to data sets available at a single medical centre. The most imminent reasons why medical data is not heavily shared for research across institutional borders rely on *ethical, legal, and privacy aspects and rules*. Data protection regulations prohibit data centralisation for analysis purposes because of privacy risks like the accidental disclosure of personal data to third parties. Therefore, in order to (1) enable health data sharing across national borders, (2) fully comply with present GDPR privacy guidelines and (3) innovate by pushing research beyond the state of the art, this project proposes a robust decentralised infrastructure which will empower researchers, innovators and healthcare professionals to exploit the full potential of larger sets of multi-source health data via tailored made AI tools useful to compare, integrate, and analyse in a secure, cost-effective fashion; with the very final aim of supporting improvement of citizen's health outcomes. In detail, this interdisciplinary project proposes 3 use cases involving 7 medical centres located in the EU and beyond, where sensitive patient data, including genomics, are made available and analysed in a GDPR compliant mechanism via a Distributed Analytics (DA) paradigm called the Personal Health Train (PHT). The main principle of the PHT is that the analytical task is brought to the data provider (medical centre) and the data instances remain in their original location. For this project, two mature implementations of the PHT called PADME (Platform for Analytics and Distributed Machine Learning for Enterprises, padme-analytics.de) and Vantage6 (priVAcY preserviNg federaTed leArninG infrastruCTurE for Secure Insight eXchange, distributedlearning.ai) will be fused and adopted as building blocks for the proposed BETTER platform. This work shows that federated learning in the healthcare domain is technically feasible.

We focused on clinical use case Inherited Retinal Dystrophies (IRD). The medical centres diagnosing and treating IRD will be guided in collecting patients' data following a common schema in order to promote interoperability and re-use of datasets in scope. This includes legal, ethical and data protection authorisations, and data documentation, cataloguing, mapping to well-established and therefore widely understood ontologies. Attention will be devoted to the FAIRification of the framework and integration of external sources such as, but not limited to, public health registries, European Health Data Space (EHDS), the 1+Million Genomes initiative (1+MG).

Table of contents

Ultrafast optoacoustic imaging in biology and the clinics, Razansky Daniel	1
Multimodal optical endoscopy, Drexler Wolfgang	2
Fluorescence Lifetime Imaging in Clinical Interventions, Marcu Laura	3
Axial tomography in live cell microscopy, Schneckenburger Herbert	4
Combined Photodynamic/Photothermal Therapy of Model Cholangiocarcinoma Using Indocyanine Green and Gold Nanorods, Genina Elina [et al.]	5
Application of NIR microsecond laser pulses for tissue coagulation and resection. Current results and perspectives, Dolganova Irina [et al.]	6
Terahertz-wave – turbid tissue interactions, Zaytsev Kirill [et al.]	7
Characterization of UV transparency windows in tissues as a function of glycerol osmolarity, Oliveira Luís	8
Phase transition monitoring in adipose tissue by multimodal approach, Yanina Irina [et al.]	9
Computational augmentation of optical coherence tomography contrasts for label-free tissue dynamics and property imaging, Yasuno Yoshiaki	10
Raman spectroscopy and machine learning in the prognosis of patients with coronary heart disease complicated by chronic heart failure, Bratchenko Ivan	11

Non-contact biomechanical imaging of cell and tissue using optical Brillouin microscopy, Zhang Jitao	12
Biophotonics methods for study the functional state of microcirculatory-tissue systems during long-term isolation in the ground model of a space station and in space flight conditions, Dunaev Andrey	13
Master Slave Optical Coherence Tomography for ultra Fast Swept Sources, Podoleanu Adrian	14
Qualitative and quantitative analysis of gas samples THz and IR absorption spectra for medical and ecological applications, Kistenev Yury	15
Revolutionizing Vascular Diagnostics: the Role of Wideband Ultrasound Detectors in Laser Optoacoustic Angiography, Subochev Pavel	16
Development of FF-SS-OCT systems for structural and bleach-induced functional retinal imaging., Zawadzki Robert [et al.]	17
Multimodal nonlinear microscopy of ratiometric fluorescent sensor-proteins in vivo, Chebotarev Artem [et al.]	18
Photon Time-of-Flight Sensing for Color-Bias-Free Pulse Oxymetry, Anderson Engels Stefan [et al.]	19
Photodynamics of Molecular Probes in Solutions, Cells, and on Organic Surfaces, Vasyutinskii Oleg	20
Nanostructures for Multi-response Selective Volatile Organic Compound Sensing, Orlova Anna	21
Hyperspectral imaging of intestinal ischemia supported by machine learning, Dremine Viktor	22
Optical monitoring of intrafollicular drug delivery by means of vaterite carriers, Svenskaya Yulia [et al.]	23
Pulsed Laser Trigger Released of Gene and Drug from Lipid Nanoparti-	

cles, Meunier Michel	24
NIR-II fluorescence functional imaging of immune cells in cancer immunotherapy, Liu Xiaolong	25
Tissue optical clearing imaging: from in vitro to in vivo, Zhu Dan	26
Terahertz Spectroscopy of Body Fluids for Cancer Diagnosis, Cherkasova Olga [et al.]	27
Photonic 3D printing of human tissue models for disease research and treatment, Rafailov Edik [et al.]	28
Advanced Fiber Spectroscopy for Life Science Applications, Artyushenko Viacheslav	29
Clinically translatable molecular photoacoustic imaging, Sokolov Konstantin	30
Non-invasive in vivo imaging of the multi-colored tattoo inks in the skin using two-photon excited fluorescence lifetime imaging, Darvin Maxim	31
Imaging, spectroscopy and therapy enhanced by tissue optical clearing, Tuchin Valery	32
Advanced Image-Based Techniques in Miniaturized Devices for Biosensing Applications, Tekin H. Cumhuri	33
Where does photonics meet acoustics and nanostructured materials for biomedical applications?, Gorin Dmitry	34
Novel Photo-Activated Treatments in Ophthalmology, Marcos Susana	35
Surgery guidance with optical spectroscopy: from bench to bedside, Shirshin Evgeny	36
Breaking the Speed Barrier: High-Speed Light-Field Microscopy for Kilo-hertz to Terahertz 3D Imaging, Gao Liang	37

Engineering Biomedical Sensing Technologies to Advance Human Health, Ceylan Koydemir Hatice	38
Multi-modal, label-free, optical imaging of metabolic function: From mitochondria to humans, Georgakoudi Irene [et al.]	39
Portable fNIRS for measuring brain activity anytime, anywhere, Bowden Audrey [et al.]	40
Non-obvious features imaging in OCT, Gelikonov Grigory	42
Pre-clinical and clinical investigations on Hyperspectral-Imaging, Rühm Adrian [et al.]	43
Ultracompact multimodal femtosecond fiber multiphoton tomograph, Koenig Karsten	44
Multispectral Light Scattering Imaging for Precancer Detection and Cell Analysis, Perelman Lev	45
Dynamic imaging and optogenetic control of mammalian embryonic cardiogenesis, Mccown Michaela [et al.]	46
Photoacoustic tracking of stem cells, Leahy Martin	47
tSNIP Transient Selective Neural Inhibition via Photobiomodulation, Moffitt Michael [et al.]	48
AI Assisted Rapid Quantitative Optical Cytopathology of Cancer, Yaroslavsky Anna	49
Revealing the Micro-Scale Mechanics of Cancer Using Optical Coherence Elastography, Kennedy Brendan	50
Milling Microscopy: A Platform for Large-Scale Sub-Cellular 3D Histology, Guo Jiaming [et al.]	51

Mueller matrix microscopy for digital pathology, Ma Hui	52
Correlation of endothelium function with optically measured blood microcirculation parameters in healthy volunteers and patients suffering from cardiac diseases, Priezzhev Alexander [et al.]	53
Explainable AI (XAI) Applied to Laser Applications in Life Sciences, Conde Olga M. [et al.]	54
Fractional Laser Treatment of Cartilage: Review of Recent Ex Vivo and Clinical Data, Yaroslavsky Ilya	55
Progress on imaging neurovascular coupling in the retina, Bizheva Kostadinka	56
Multimodal imaging platform to study cartilage degeneration using compression-based depth-resolved polarisation-sensitive optical coherence tomography and vibrational spectroscopy, Vanholsbeeck Frederique [et al.]	57
The Role of Red Blood Cells as Biomarkers in Human Aging and a Potential Route for Reverse-Aging, Shin Sehyun	58
Microcavity-enhanced SERS biosensing, Xu Chunxiang	59
Novel Raman approaches for the neurosurgical guidance, Côté Daniel	60
Clinical translation of Low-cost Swept Source OCT - how low can you go?, Leitgeb Rainer	61
Applications and challenges of clinical adaptive optics optical coherence tomography, Pircher Michael	62
Non-Perturbative Optical Methods of Assessing Corneal Mechanical Properties, Blackburn Brecken [et al.]	63
Characterization of a combined fluorescence and spatial frequency domain imaging system to monitor photodynamic therapy dosimetry, Jansen E. Duco	64

Clinical implementation of near-infrared autofluorescence (NIRAF) for guiding endocrine neck surgery, Mahadevan-Jansen Anita	65
Plasmonic materials based biomedical applications, Zhao Xiangwei	66
Structural and molecular imaging in vivo: PS-OCT and Immuno-OCT, De Boer Johannes	67
Investigating the mechanopathology of soft orthopedic tissues in degenerative joint disease, Nadkarni Seemantini	68
Research on some fundamental problems in classical optics, Weng Xiaoyu	69
Laser Aggregometry of Red Blood Cells in a Microfluidic Channel Covered with Cultured Endothelial Cells, Lugovtsov Andrei [et al.]	70
Detection of radiation-induced changes in the white matter of the rat brain based on attenuation coefficient estimation from optical coherence tomography data, Achkasova Ksenia [et al.]	71
Optical Criteria of the Pathological Liver during the Regeneration, Rodimova Svetlana [et al.]	72
SIMULTANEOUS ASSESSMENT OF OXYGEN AND METABOLIC STATUS IN TUMOR MODELS USING FLIM AND PLIM TECHNOLOGIES, Komarova Anastasia [et al.]	73
Laser-assisted drop-on-demand bioprinting for in-situ corneal repair, Goodarzi Hamid [et al.]	74
NIR photothermal immunotherapy of melanoma, Dory Alissa [et al.]	75
Advances in scanning optoacoustic angiography: leveraging highly sensitive wideband PVDF-TrFE piezopolymer detectors to enhancing tumor imaging, Kurnikov Alexey [et al.]	76
Avoiding overestimation in multivariate analysis of Raman spectra for biomedical applications, Bratchenko Lyudmila [et al.]	77

40 MHz time stretch Swept Source OCT imaging and Fast Measurements, Martinez Alejandro [et al.]	78
Tissue Composition Analysis: An Intuitive Application for the Broadband Absorption Spectra Reconstruction, Santos Pinheiro Maria Do Rosário [et al.]	79
Optical methods for detecting single biomolecules: visualization, sensing, sequencing of DNA molecules, Kalmykov Aleksei [et al.]	80
Wearable laser Doppler flowmetry for the study of blood microcirculation peculiarities in the forehead skin in patients in the remote post-COVID period, Zharkikh Elena [et al.]	81
Complex application of fluorescence imaging and digital diaphanoscopy methods for screening pathological conditions of the oral mucosa and the maxillary sinus tissues, Bryanskaya Ekaterina [et al.]	82
Optical Methods in Elastography of Ocular Tissues, Aglyamov Salavat [et al.]	83
Moisture quantification of allogeneic tissues by fiber-optic NIR spectroscopy, Surkova Anastasiia [et al.]	84
In vivo study of vascularization and oxygenation of tumor xenografts under the influence of the antiangiogenic drug axitinib, Glyavina Anna [et al.]	85
Laser generation of reactive oxygen and nitrogen species to influence physiological and metabolic parameters of human blood in vitro, Kornev Roman [et al.]	86
Automated system for analyzing the effectiveness of photobiomodulation of lymphatic removal of beta-amyloid from tissues of the aging brain, Semyachkina-Glushkovskaya Anastasya [et al.]	87
Mouse phenotyping technology to evaluate the effectiveness of phototherapy in mice with Alzheimer's disease, Myagkov Dmitry [et al.]	88
Diffuse Reflectance Spectra Changes After Photodynamic Therapy of Rat Model Tumors With and Without Optical Clearing, Genin Vadim D. [et al.]	89

Excited-states relaxation in FAD excited states: the role of conformations, Vasyutinskii Oleg [et al.]	90
Overcome cross-border barriers to health data integration, access, FAIRification, and pre-processing, Sokolovski Sergei [et al.]	91
Author Index	100

Author Index

- Abramov Andrey, 82
Achkasova Ksenia, 71
Adushkina Viktoria, 87, 88
Aglyamov Salavat, 83
Akhmedzhanova Ksenia, 85
Aleksandrova Polina, 6
Alekseev Yakov, 80
Alekseeva Anna, 6
Andersson Engels Stefan, 19
Artyushenko Viacheslav, 29
Aumiller Maximilian, 43
- Balykin Victor, 80
Belousov Vsevolod, 18
Bilan Dmitry, 18
Bizheva Kostadinka, 56
Blackburn Brecken, 63
Bluhm Maximillian, 51
Bobrov Nikolay, 72
Bochkarev Leonid, 73
Bogomolova Alexandra, 71
Bonesi Marco, 57
Boutopoulos Christos, 74
Bowden Audrey, 40, 41
Bratchenko Ivan, 11, 77
Bratchenko Lyudmila, 77
Bregonzio Matteo, 91
Bryanskaya Ekaterina, 82
Bucharskaya Alla, 5, 89
Bukatin Anton, 80
Bulanov Andrey, 86
Buzza Andrew, 48
- Carvalho Maria, 79
Ceylan Koydemir Hatice, 38
Chebotarev Artem, 18
Cherkasova Olga, 27
Chernomyrdin Nikita, 7
Christos Boutopoulos, 75
Conde Olga M., 54
Crawford Seth, 40, 41
Côté Daniel, 60
- Dabot Pierre, 57
Darvin Maxim, 31
- De Boer Johannes, 67
Doble Nathan, 17
Dolganova Irina, 6, 7
Dory Alissa, 75
Dremin Viktor, 22, 82
Drexler Wolfgang, 2
Druzhkova Irina, 73
Dunaev Andrey, 13, 81, 82
Dupps William, 63
- Elagin Vadim, 72
Eriksen Jason, 51
Ermakov Artur, 86
Ermolinskiy Petr, 53, 70
Everett Daniel, 57
Evstrapov Anatoly, 80
- Fedorovich Andrey, 81
Fedosov Ivan, 87
Fedotov Andrei, 18
Felicio-Briegel Axelle, 43
Frey Müller Christian, 43
Fu Yuhang, 39
- Gao Liang, 37
Gavrina Alena, 72
Gelikonov Grigory, 42
Genin Vadim, 5
Genin Vadim D., 89
Genina Elina, 5, 89
Georgakoudi Irene, 39
Gladkova Natalia, 71
Glyavina Anna, 76, 85
Gnanatheepam Einstein, 39
Goodarzi Hamid, 74
Goodwin Matthew, 57
Gorbunova Ioanna, 90
Gorin Dmitry, 34
Grelet Sacha, 78
Griffith May, 74
Gritchenko Anton, 80
Guo Jiaming, 51
Gurfinkel Yuri, 53
Gutierrez-Gutiérrez José A., 54

Happach Daniel, 43
 Inozemcev Timopheyy, 87, 88
 Jansen E. Duco, 64
 Jenkins Michael, 48, 63
 Jonnal Ravi, 17
 Kalmykov Aleksei, 80
 Karabut Maria, 72
 Kennedy Brendan, 50
 Khlebtsov Boris, 5
 Khlebtsov Nikolai, 5
 Khochenkov Dmitry, 85
 Khochenkova Yulia, 85
 Khrenova Maria, 90
 Kistenev Yury, 9, 15
 Kochiev David, 6
 Kochubey Vyacheslav, 9
 Koenig Karsten, 44
 Komarova Anastasia, 73
 Kornev Roman, 86
 Kucheryavenko Anna, 7
 Kukhnina Liudmila, 71
 Kumar Kothuri Suraj, 19
 Kurlov Vladimir, 6
 Kurnikov Alexey, 76, 85
 Kuznetsova Daria, 72
 Lanin Aleksandr, 18
 Lanka Pranav, 19
 Larin Kirill, 83
 Larina Irina, 46
 Le Tiffany-Chau, 40, 41
 Leahy Martin, 47
 Lee Soohyun, 17
 Leitgeb Rainer, 61
 Lindley Matthew, 39
 Linek Matthäus, 43
 Liu Daniel, 40, 41
 Liu Xiaolong, 25
 Loktionova Yulia, 81
 Lugovtsov Andrei, 53, 70
 Ma Hui, 19, 52
 Mahadevan-Jansen Anita, 65
 Maksimov Matvey, 70
 Marcos Susana, 35
 Marcu Laura, 3
 Martinez Alejandro, 78
 Martusevich Andrew, 86
 Maslyakova Galina, 5
 Mayerich David, 51
 Mccown Michaela, 46
 Mcglashan Sue, 57
 MCGoverin Cushla, 57
 Melentiev Pavel, 80
 Meleppat Ratheesh, 17
 Meunier Michel, 24, 74
 Mieites Veronica, 54
 Mirchandani Prishita, 43
 Moffitt Michael, 48
 Mogyordy John, 63
 Mohammadi Ahad, 74, 75
 Moiseev Alexander, 71
 Montague Patrick, 78
 Moree Wilna, 51
 Mozherov Artem, 73
 Mudrak Dmitry, 5
 Munćan Jelena, 84
 Musina Guzel, 46
 Myagkov Dmitry, 87, 88
 Nadkarni Seemantini, 68
 Najafi Ghalehlou Nima, 39
 Navolokin Nikita, 5, 89
 Nazarov Vladimir, 86
 Niger Meher, 51
 Nikolaev Nazar, 27
 Nikolaev Viktor, 9
 Nunzia Guadagno Claudia, 19
 Oliveira Luíś, 8, 79
 Om Boda, 74
 Orlova Anna, 21, 76, 84, 85
 Pachyn Esther, 43
 Perelman Lev, 45
 Pijewska Ewelina, 17
 Pircher Michael, 62
 Podoleanu Adrian, 14, 78
 Polleys Christopher, 39
 Popov Sergey, 87, 88
 Potekhina Ekaterina, 18
 Priezhev Alexander, 53, 70
 Rafailov Edik, 28
 Razansky Daniel, 1, 76
 Rekha Gautam, 19
 Rodimova Svetlana, 72
 Rollins Andrew, 63
 Ryabov Nikolay, 84
 Rühm Adrian, 43
 Santos Pinheiro Maria Do Rosário, 79
 Sasin Maxim, 90

Savvidou Maria, 39
 Scheglovitova Olga, 70
 Schneckenburger Herbert, 4
 Seeber Marco, 43
 Sekar Sanathana Konugolu Venkata, 19
 Semenov Alexey, 70
 Semyachkina-Glushkovskaya Anastasya, 87
 Semyachkina-Glushkovskaya Oxana, 87
 Shcheslavskiy Vladislav, 73
 Shin Sehyun, 58
 Shirmanova Marina, 73
 Shirshin Evgeny, 36
 Shkrinin Vladimir, 86
 Shokhina Arina, 18
 Sinitsyn Dmitrii, 84
 Skubal Aaron, 48
 Sokolov Konstantin, 30
 Sokolovski Sergei, 28, 91
 Sroka Ronald, 43
 Stadler Ina, 43
 Subochev Pavel, 16, 76, 85
 Surkova Anastasiia, 84
 Svenskaya Yulia, 23

 Talbot Sebastien, 75
 Tekin H. Cumhur, 33
 Thambyah Ashvin, 57
 Tharan Darven, 57
 Tuchin Valery, 5, 7, 9, 23, 32, 79, 89
 Tuktarov Dmitry, 87, 88
 Turchin Ilya, 85

 Valente Denise, 17
 Vanholsbeeck Frederique, 57
 Vasyutinskii Oleg, 20, 90
 Vinokurov Andrey, 82
 Volgger Veronika, 43
 Volkov Denis, 90
 Volov Artem, 84
 Volova Larisa, 84
 Vrazhnov Denis, 9

 Weng Xiaoyu, 69

 Xu Chunxiang, 59

 Yakovlev Egor, 6
 Yanina Irina, 9
 Yaroslavsky Anna, 49
 Yaroslavsky Ilya, 55
 Yashkov Dmitrii, 90
 Yasuno Yoshiaki, 10

 Zagainov Vladimir, 72
 Zagaynova Elena, 72
 Zapata-Farfan Jennyfer, 74
 Zawadzki Robert, 17
 Zaytsev Kirill, 6, 7
 Zhang Jitao, 12
 Zhang Yang, 39
 Zhao Xiangwei, 66
 Zharkikh Elena, 81
 Zhu Dan, 26
 Zlatogorskaya Daria, 87
 Zotov Arsen, 6